Title
Searching for RNAP II on the Compact HSV-1 Genome

Author
Ou, Mark

Publication Date
2014

Peer reviewed|Thesis/dissertation

UNIVERSITY OF CALIFOANIA,
IRVINE

Searching for RNAP II on the Compact HSV-1 Genome

DISSERTATION

submitted in partial satisfaction of the requirements
for the degree of

DOCTOR OF PHILOSOPHY

in Biomedical Sciences

by

Mark Ou

Dissertation Committee:
Professor Rozanne M. Sandri-Goldin, Chair
Professor Kyoko Yokomori
Professor Marian L. Waterman
Associate Professor. Yongsheng Shi

2014

Table of Contents

List of Figures

List of Tables

Acknowledgments

It has been eight years since I entered this graduate program in 2006 and it has been a defining time for me on every imaginable level. Scientifically I went from a trained lab monkey to somebody who can design simple experiments and troubleshoot procedures methodically. Professionally, I went from an inept speaker who rambles and stutters every other sentences to somebody who is able to think on his feet and answers questions logically. Personally, I went from a lone wolf to somebody who appreciates family and friend above all else. The steps in all of these transformations were small and I was lucky that I had many, many people who took the journey with me. Without these people, I would have been the same lab monkey, stutter, and lone wolf that I was eight years ago. To all my family and friends who were with me, either in person or in spirit, I dedicate this work to you.

This body of work would not have been possible without the kind and generous support of the faculties, post-doc's, graduate students, and support staff of the MMG department. As a department, we have the reputation of taking forever to graduate, but I would like to think that is in part due to the fact that this department is so supportive of its members that we are not all in a hurry to get out. When experiments don't work, there is always somebody who can give your technical advices or offer an alternative strategy. Namely, I thank Ling Li, Jenny Dai-Ju, Stuart Souki, and Felicia Hernandez for their training and feed backs during their time in the Sandri-Goldin lab. Michele Wu, our lab manager was an angel who took care of us, be it be ordering lab supplies or food. We never had to worry about the lab as long as Michele wasn't on vacation! I'd also like to thank Becky Tsai for her help on IP experiments, Andrea Cathcart and Bei-Bei Wu for thier expertise in transfection protocols, Serena Chan for her help on plasmid construction, Will Muller for his suggestions on designing qPCR primers, and Brian Tanaka for his helping hand on all things mechanical. Another group that deserves thanks is the MMG office staff who took care of all the administrative paperwork for me! Char Anderson and Mike Vo, our grad coordinators were two of the kindest and most welcoming people I have the pleasure of meeting, and they are like family. I also

had the pleasure of working with Linda Pawloski, Kimberly Smith-Lyons, Nashaunda Williams, Darlene Arrowood, Lisa Rapp, and Anna Chang, and I thank them for their dedication to their work. Last but least, my thesis committee members most definitively deserve my deepest gratitude. I thank Yongsheng Shi an Kyoko Yokomori for their insightful critiques and suggestions as well as encouragements. I am grateful to Marian Waterman for spending time sitting down with me troubleshooting whatever difficulty I brought to her door step. Of course, I am indebted to my mentor, Roz Sandri-Goldin for taking me under her wings and supporting me through this entire journey. Roz was patient and supportive like a mom but she also gave me enough independence to learn on my own. To say Roz was generous would be an understatement. She supported me in attending international conferences, never asked me to support myself through TAship, and stood behind me when I decided to pursuit teaching as my career. Words alone cannot express my gratitude for Roz.

I can't say that public speaking is one of my favorite things to do, and I have never imagined that I'll be doing just that professionally. I am glad that the MMG department places a great emphasis on the grad student to present our ideas and findings clearly to our audiences. I have always imagined Tamkin Hall as a medieval court room of sorts, with us down in the pit, arguing for our cases to an audience of lords and ladies. This of course, is frighteningly intimidating to say the least, but it does become a bit easier as you hone your skills. I would like to thank Rani Najdi for giving the great advice that helped me to survive my first departmental seminar. Without his sage advice, I probably would still be an rambling idiot when I teach classes today. Diane O'Dowd also deserve thanks for showing me her passion for teaching and inventive deliveries. I would also like to thank my CCCIP mentor, Patty Oertel for giving the opportunities to learn and grow as a classroom instructor. Patty has been so supportive and encouraging, and I am truly lucky to have a mentor like Patty.

I am blessed to be born with good senses when it comes with numbers. It also helped that my dad had been checking my homework every night since 4th grade. He has taught me the power of careful

observations and logical thinking growing up. He was also the person who believed in that I could get into an UC if I tried, and he was right. My mom also nurtured my sense of curiosity since I could read. The first present that I could remember was a set of 200 books on history, sciences, and technology that came with its own bookshelf. I spent countless hours lost in wonders found in these books. Though later I found that that they weren't always right, but my parents have always given me an answer to my bazillion questions. More remarkably, they have never discouraged me from asking questions. I would not be a scientist today if my parents did not foster and help grow my curiosity all these years. It also helped that they have never asked me about when am I going to be finished with grad school. Instead, they tried to understand what is it that I am actually doing, despite not having been a modern biology class ever themselves. Thank you mom and dad!

The grad students in the department have been more than just colleagues, they have been my comrades and dear friends. We share a bound that is rooted in our hearts and souls as each of us try to forge a path for ourselves and hold one another up. Without them, I would have given up a long time ago. Without them, there would have been no joy in my work. To Heather Swesey and Andrea Cathcart, I am ever grateful that you were there to see me through all of the ups and downs. You are true and honest; I can ask nothing more of you. To Polen Sean, I thank you for extending a friendly hand that summer I came to Irvine. To Will Muller, I thank you for your always cheerful remarks and I will always be looking forward to fist bumping you, wherever you are. To Kate Ball, I thank you for all of our invigorating discussions about science and faith and I believe that your passion for both will win any student of yours over. To Brian Tanaka and Eric Cheng, I thank you for inviting me to your brewery crawls and really showing me some good local bear! To Stephanie Sprowl, I thank you for sharing all of your wedding ideas, especially in the search for an engagement diamond! To Becky Tsai, I thank you for all of your witty banters and photo bombing.

In December 2010, I met Mabel Perez, who I tied the knot with on July 3rd 2013 in stunning Palos Verdes Estate. Mabel has been my anchor to the real world. Before I met her, I was drifting in this world, with no real roots anywhere. Sure, I have family and friends that I care deeply about, but I did not have a home. Mabel put up with my silliness and deadpan humor and showed me that there is more to me that I have ever known myself. She accepted and loved me for who and what I am, as rough around the edges as I was. I cannot thank this amazing woman enough and she changed my life forever. For evolving me to the next level, I promise that I will always keep a Disneyland Annual Pass! This work would not have been possible without your loving support and understanding.

Curriculum Vitae

Mark Ou

University of California, Irvine
School of Medicine
Department of Microbiology and Molecular Genetics
Medical Sciences I B280
Irvine, CA 92697
949-824-7086
oum@uci.edu

EDUCATION

University of California, Irvine 2014
Doctor of Philosophy Candidate
Dissertation: Searching for RNAP II on the Compact HSV-1 Genome

University of California, Davis 2002
Bachelor of Science - Genetics

RESEARCH AND PROFESSIONAL EXPERIENCE

Graduate student with Professor Rozanne M. Sandri-Goldin 2006 – present
Department of Microbiology and Molecular Genetics
University of California, Irvine, CA

Research Assistant for Professor Peggy Lemaux 2005-2006
Department of Plant and Microbial Biology
University of California Berkeley, Berkeley, CA

Undergraduate Researcher with Professor Neelima Sinha 2000-2002
Section of Plant Biology
UC Davis, Davis, CA

Publication

Ou, M. and R. M. Sandri-Goldin. 2013. Inhibition of cdk9 during herpes simplex virus 1 infection impedes viral transcription. PLoS.One. **8**:e79007. doi:10.1371/journal.pone.0079007 [doi];PONE-D-13-28584 [pii].

AWARDS AND HONORS

University of California, Irvine Howard Hughes Medical Institute Graduate Fellow 2011

Departmental Seminar Speaker Search Committee Member, Department of Microbiology and Molecular Genetics, University of California, Irvine 2010

Outstanding Senior, University of California, Davis, College of Letters and Science 2002

University of California, Davis, Plant Biology Training Fellowship 2000

TEACHING EXPERIENCE

Instructor - laboratory in microbiology; Division of Math and Sciences Santa Ana College	2013-2014
Instructor - laboratory in introductory biology; Division of Math and Sciences Santa Ana College	2013-2014
Instructor - laboratory in biology for non-majors; Division of Math and Sciences Santa Ana College	2012-2014
Teach assistant - lecture in genetics; School of Biological Sciences University of California, Irvine	2012
Discussion leader – lecture in introductory biology; School of Biological Sciences University of California, Irvine	2010
Instructor - laboratory in molecular biology; School of Biological Sciences University of California, Irvine	2007
Teaching assistant - laboratory in genetics; School of Letters and Sciences University of California, Davis	2002

Abstract of the Thesis

Searching for RNAP II on the Compact HSV-1 Genome

By

Mark Ou

Doctor of Philosophy in Medical Biosciences

University of California, Irvine, 2014

Professor Sandri-Goldin, Chair

Herpes Simplex Virus type-1 (HSV-1) is one of the eight human herpes viruses and it causes cold sores in infected individuals. HSV-1 infects epithelial cells, then travels to the trigeminal ganglion through retrograde transport in the peripheral neurons. During the initial lytic infection in the epithelial host cell, HSV-1 hijacks cellular RNA polymerase II (RNAP II) to sites of viral transcription for viral gene expression. Previous studies have found an intermediately phosphorylated form of RNAP II in HSV-1 infected cells starting approximately 5 hours post infection (133,134,155). This intermediately phosphorylated form of RNAP II appeared to be different from the usual hypo- and hyperphosphorylated forms of RNAP II normally found in uninfected cells. Subsequent studies had revealed that at late time in HSV-1 infection, elongating RNAP II, marked by phosphorylated serine 2 residues at the C-terminal domain (CTD), was degraded in infected cells, and this degradation could be prevented by inhibiting transcription (37). The loss of elongating RNAP II was in contrast to the high levels of viral transcription that occurs during late phase of HSV-1 replication cycle. We have previously proposed a collision model where the compact viral genome becomes overburdened by the high transcriptional activities at late time in HSV-1 infection, leading to arrested RNAP II complexes that then in turn, trigger a proteasome-mediated proteolysis of the polymerase to resolve stalled transcription. In this body of work, we first attempted to determine the if HSV-1 transcription is more similar to cellular transcription in that it requires phosphoserine-2 form of

RNAP II and found that when we inhibited cdk9, the kinase responsible for phosphorylating serine 2 residues of the RNAP II CTD, viral transcription was also inhibited. Viral yield under cdk9 inhibition was also dramatically reduced, supporting the idea that like cellular transcription, HSV-1 transcription requires phosphoserine-2 form of RNAP II. We also attempted to substantiate our RNAP II collision model by assessing RNAP II occupancy on the HSV-1 genome using chromatin immunoprecipitation (ChIP) quantitative polymerase chain reaction (qPCR) analysis. In our ChIP qPCR analysis of an Early HSV-1 gene cluster, we found that though ChIP signals from one of the antibodies were consistent with known expression patterns of the genes, we were unable to validate the results with phosphoform-specific ChIP results due to the high noise levels of these phosphoform-specific antibodies. When analyzing a Late HSV-1 gene cluster, we were unable to achieve satisfactory signal-to-noise ratios regardless of the antibody used. Therefore we were unsuccessful to support or refute our collision model at this time. Lastly, we investigated a possible link between HSV-1 induced RNAP II degradation and the cellular transcription-coupled nucleotide excision repair (TC-NER) pathway by examining the role of a general transcription factor TFIIS, a factor known to stimulate transcription after RNAP II becomes stalled, in HSV-1 transcription. Our initial immunofluorescence studies had shown that one of the isoforms of TFIIS (TCEA2) appeared to re-localize to HSV-1 transcription replicative compartments in infected cells. Subsequent confocal microscopy co-location studies however, showed a rather inconsistent localization patterns among the isoforms of TFIIS. When attempting to perform functional knock-down experiments of each of the TFIIS isoforms, we found that the antibodies we were using exhibited cross-reactivity to unknown antigens in Western blot analysis. More importantly, these antibodies failed to recognize FLAG-tagged TFIIS transiently expressed in HeLa cells, thereby overturning our initial re-localization results. At this time, we do not have evidence that support a functional involvement of TFIIS in HSV-1 transcription. We believe that further experimentation would be required to support our colliding RNAP II model during HSV-1 lytic infection.

Chapter 1
Eukaryotic mRNA transcription by RNA Polymerase II and Herpes Simplex Virus type-1 Transcription

The first step of gene expression is transcription, and in mammalian cells, protein-encoding genes are transcribed by RNA polymerase II (RNAP II) into messenger RNAs (mRNAs). RNAP II is a large complex greater than 500 kDa and made of more than ten polypeptides. Early *in vitro* studies have demonstrated that RNAP II can synthesize RNA in a template-dependent manner without additional factors if provided with a RNA primer in the reaction (reviewed in (142)). *In vivo* however, RNAP II transcription requires both general transcription factors (GTF) and gene-specific transcription factors, and occurs in three major phases: initiation, elongation, and termination. Each of the major phases involves multiple processes, and is regulated by the cell to ensure proper expression of the gene products.

The first phase of RNAP II transcription is initiation, and it starts with the assembly of the pre-initiation complex (PIC) at the promoter region of the gene. In addition to RNAP II, the PIC includes GTFs IID, IIB, IIE, IIF, and IIH, as well as other factors that might be gene-specific. The GTFs IIE and IIH in the PIC melt the DNA template in an ATP-dependent manner and establish an open complex. To engage in transcription, two nucleoside triphosphates directed by the DNA template are joined in a phosphodiester bond. The next step in initiation is promoter clearance, a critical step prior to transcription elongation. After the formation of the first phosphodiester bond, the PIC pauses at the promoter region and produces short (8-9nt) RNAs in the absence of positive regulatory signals. Two proteins are thought to induce RNAP II pausing at the promoter: DRB sensitivity inducing factor (DSIF) and negative elongation factor (NELF) (168,177,178). Recent crystal structure studies on DSIF subunits suggested that together with NELF, these proteins might bind to the Clamp domain of RNAP II that holds the DNA-RNA hybrid, and thereby influence processivity of the polymerase (26,119,171). Biochemical and genetic studies however, have shown both DSIF and NELF can affect transcription either negatively or positively depending on the system studied

(68,138,160,168). At the current time, there is no clear consensus as to the underlying mechanism by which DSIF and NELF suppress RNAP II transcription elongation.

Transitioning from promoter clearance to productive elongation appears to be triggered by the action of the positive transcription elongation factor b (P-TEFb), composed of cyclin T1 and the kinase CDK9. P-TEFb was first identified in *Drosophila* as a factor that stimulated transcription elongation in a DRB sensitive fashion (97-99). P-TEFb phosphorylates both DSIF and NELF and thereby releases NELF from the polymerase. DSIF remains in contact with RNAP II, but without NELF, it no longer suppresses transcription elongation (55,132,175). The polymerase can now transcribe beyond the promoter region of the gene.

Promoter clearance marks the start of transcription elongation, and the nascent transcript is capped with a 7-methylguanosine at the 5' end as it emerges from the exit site of the polymerase by the capping complex. Many of the transcription factors that were in the PIC are now exchanged for another set of protein complexes that regulate elongation. Members of the ELL and Elongin families have been demonstrated to interact with RNAP II and to stimulate transcription elongation in early *in vitro* studies (147,148,165). Mutations in ELL subsequently have been shown to reduce transcript levels of several large genes (46). Elongin proteins appeared to aid elongation by maintaining the proper alignment of the 3' hydroxyl group of the nascent RNA chain with the catalytic active site of the polymerase, thereby suppressing RNAP II pausing (63,161). In addition to transcription factors that directly bind to RNAP II during transcription, chromatin remodeling proteins also stimulate elongation by modification or removal of histone proteins of the chromatin template (reviewed in (144,149)).

The final phase of RNAP II transcription is 3' end processing and termination. As RNAP II continues to transcribe the chromatin template, it changes its associations with various protein complexes that are involved in RNA synthesis for a set of protein factors required for 3' end processing. (145). The cleavage

and polyadenylation specificity factor (CPSF) and the cleavage stimulation factor (CstF) associated with the elongating RNAP II recognize and bind to AAUAAA and a U/GU-rich sequence respectively at the 3' end of the nascent RNA. The 73 kDa subunit of CPSF is thought to be responsible for carrying out the endonuclease cleavage of the nascent transcript at approximately 10-30 nt downstream of the AAUAAA sequence (96). Following cleavage, poly(A) polymerase (PAP) is recruited to the transcript and polyadenylates it. RNAP II, after depositing CPSF and CstF onto the nascent transcript, continues to transcribe on the template chromatin. To terminate transcription, exonucleases such as 5'-3' exoribonuclease 2 (XRN2) are recruited to the RNA that is downstream of the polyadenylation site and to degrade it. When XRN2 "catches up" to the polymerase, it releases RNAP II from the template and terminates transcription (173).

RNA polymerase subunit B1 (RPB1), the largest subunit is the catalytic subunit of RNAP II. The carboxyl terminal domain (CTD) of RPB1 is composed of multiple (up to 52 in mammals) heptapeptide tandem repeats with the consensus sequence of YSPTSPS (reviewed in (43,72,124)). Multiple studies have shown that deletions of the RPB1 CTD are lethal in yeast, *Drosophila*, and mice, indicating its critical functions (4,116,183). *In vitro* results found that RPB1 lacking the CTD altogether could support a basal level of transcription (24,102). Truncation of the CTD appeared to be tolerated in cell culture systems if the deletion was less than ~50% of the natural number of repeats, suggesting a minimal length requirement for proper function . Work done in the Bentley lab and others provided evidence that the CTD is involved in 5' capping, splicing, and 3' end processing by demonstrating that cells expressing RPB1 lacking CTD exhibited abnormalities in all these processes (16,50,51,101-103).

The serine residues of each YSPTSPS heptad repeat are sites of reversible phosphorylation and the pattern in which they are phosphorylated influences the activity of RNAP II. Unphosphorylated RNAP II, is thought to be the only phospho-form that is capable of forming PIC in the pioneering round of transcription (86). RNAP II found in PICs is primarily phosphorylated at ser-5 (S5p) residues by the CDK7

component of GTF TFIIH. Akoulitchev *et al.* found that reconstituted *in vitro* transcription assays were unable to proceed when activity of CDK7 and its cyclin partner, cyclin H, was absent (2,3). Subsequent studies have shown that mutations in CDK7 resulted in a decreased level of S5 phosphorylation at the promoter regions (86,135). Chromatin immunoprecipitation (ChIP) data added support in that TFIIH was co-occupied with RNAP II near the 5' end of genes (60,86). In addition to the ser-5 in the CTD, CDK7 also phosphorylates DSIF and NELF, two proteins that regulate promoter clearance during the transcription cycle. TFIIH continues to associate with RNAP II after promoter clearance and phosphorylates ser-5. As the polymerase continues to transcribe the DNA, small CTD phosphatase (SCP1-3) dephosphorylates S5p, resulting in a decrease in S5p toward the 3' end of the gene (180,184).

Another modification that affects RNAP II activity is phosphorylation at ser-2 (S2p) residues of the CTD. In addition to promoting the transition from initiation to elongation by phosphorylating negative regulators DSIF and NELF, P-TEFb also phosphorylates ser-2 in the CTD during elongation (22,126,176). Studies have shown that inhibition of transcription by blocking P-TEFb coincided with a drastic decrease in phosphorylation of RNAP II *in vivo* (19,95,123,181). A recent genome-wide ChIP analysis by Mayer *et al.* found that S2p levels gradually increased after the transcription start site (TSS), peaking at approximately 600 nt downstream of the TSS, and then decreased significantly at about 100 nt 3' of the polyadenylation site. The highest level of phosphorylation on the CTD occurred at around 450 nt downstream of the TSS, where both ser-5 and ser-2 were phosphorylated (100). This general model of RNAP II CTD phosphorylation was less consistent among the shorter genes examined however, and the authors found that shorter genes showed higher S5p levels than S2p levels. Similar to dephosphorylation of S5p by SCP, S2p is dephosphorylated by a CTD specific phosphatase, TFIIF-associated CTD phosphatase 1 (FCP1). FCP1 phosphatase activity has been demonstrated to be essential in recycling RNAP II PIC assembly so the polymerase may initiate transcription again. Cells depleted of FCP1 accumulated high levels of S2p RNAP II and showed little or no transcriptional activity (12,29,30).

In 2007, Chapman *et al*. found that transcribing RNAP II was phosphorylated at ser-7 (S7p) residues in the CTD *in vivo*, and a companion report demonstrated that S7p facilitated interaction between RNAP II and the Integrator complex in expression of snRNA genes (25,44). CDK7 has been found to be responsible for phosphorylating ser-7 *in vivo*, in support of the finding that S7p and S5p patterns appeared to overlap somewhat. S7p patterns showed more variability compared to S5p and S2p patterns. The initial report found enrichment of S7p at the 3' coding region of the genes, while Kim *et al*. subsequently reported enrichment at 5' and/or 3' ends of the genes (58,82,84). In 2012, Bataille *et al*. found that S7p levels were uniform along the genes in a ChIP analysis (12). At this time, the significance of ser-7 phosphorylation in the CTD and its role in RNAP II transcription is yet unclear. It is clear however, that there appears to be a "CTD code" made up of combinations of phosphorylated serines in RPB1. The dynamic switching of this CTD code, governed by the multiple kinases and phosphatases involved, in turn influences RNAP II transcription and mRNA processing.

Herpes Simplex Virus type-1 (HSV-1) is an enveloped DNA virus that establishes a life-long infection in neuronal cells. HSV-1 infects epithelial cells, then peripheral neurons and travels to the trigeminal ganglion, where the virus becomes latent. Sporadically, the latent virus reactivates and produces progeny virus that travel down the same axon and replicate at or near the site of the initial infection. In healthy individuals, HSV-1 reactivation causes cold sores that can be treated with drugs such as acyclovir and valacyclovir that target viral DNA replication. More serious infections can occur such as HSV-1 keratitis, which can result in blindness and herpes encephalitis, which results in significant morbidity and mortality.

The HSV-1 genome is 152 kb in length and encodes more than eighty open-reading frames (ORFs). The ORFs are expressed in a temporal cascade during lytic infection. The immediate-early (IE) genes are expressed first and four of the IE gene products act as regulators that alter cellular processes and recruit host cell machineries to viral sites of transcription and replication. The early (E) gene products are

responsible for viral DNA replication and their expression is triggered by expression of IE gene products in the infected cell. Early gene products can be detected by Western blot analysis at about four hours post-infection. The late (L) genes encode capsid, envelope glycoproteins, and tegument proteins of the virus and their expression follows replication of viral DNA, at approximately five to six hours post-infection. Viral genomes are packaged into capsids inside the nuclei of infected cells. Capsids acquire a glycoprotein studded envelope in the Golgi and endoplasmic reticulum and enveloped virion particles egress by budding out of the host cells at around 12-16 hours post-infection in cell culture systems.

HSV-1 hijacks cellular RNAP II to viral sites of transcription-replication through the action of an IE gene product called infected cell proteins 27 (ICP27) (37). ICP27 is a multifunctional protein that has been demonstrated to be involved in various aspects of viral RNA metabolism. It disrupts host cell splicing by mediating aberrant phosphorylation of host splicing proteins. It also facilitates viral mRNA export to the cytoplasm through its interactions with host mRNA transport adaptor proteins and the TAP/NXF export receptor protein. Experimental data have also suggested that cytoplasmic ICP27 stimulates translation of some viral L genes (reviewed in (141)). ICP27 was first found to interact with RNAP II in association with another viral protein ICP8, and subsequent studies have shown that ICP27 alone is sufficient to bind to CTD of RNAP II *in vitro* (37,185). Furthermore, the interaction between ICP27 and RNAP II is critical for recruitment of RNAP II to viral sites of transcription, as RNAP II did not co-localize with ICP4, the major trans-activator of viral transcription in cells infected with d27lacZ, a HSV-1 ICP27-null mutant virus. Rice *et al.* demonstrated that HSV-1 infected cells exhibited a form of RNAP II that migrated between the hypo-phosphorylated and the hyper-phosphorylated forms of RNAP II on Western blots, starting at about five hours post-infection (134). These authors subsequently observed this intermediately phosphorylated RNAP II in cells transiently expressing another HSV-1 IE gene product, ICP22, and there appeared to be a loss of S2p RNAP II (54,133). As the study was not done in the context of HSV-1 infection, and ICP22-null

mutant virus exhibits no significant defect in viral replication in cell culture systems, the significance of these findings is unclear at this time.

Dia-Ju and colleagues found that the overall level of RNAP II in wild type HSV-1 KOS infected cells dropped significantly at late times in infection, and it was primarily the S2p form, and not the S5p form of RNAP II that was decreasing in infected cells. Decreases in RNAP II levels could be prevented by inhibiting transcription with actinomyocin D, or by inhibiting proteasomal degradation using MG132 or Lactocystin in HSV-1 infected cells (37). These data suggested that the decrease in RNAP II required viral transcription and was carried out by the proteasome degradation pathway. Interestingly, cells infected with HSV-1 exhibited a lower viral yield when they were treated with MG132 to prevent proteasomal degradation. This suggested that degradation of RNAP II in infected cells might actually be beneficial to HSV-1 replication. These findings were paradoxical to the fact that viral transcription levels are high at late times in infection. If transcribing RNAP II is degraded by the proteasomes in HSV-1 infected cells, why does viral transcription remain high? One might postulate that preventing proteasomal degradation of elongating RNAP II should be beneficial to viral replication, but that appeared not to be case. Dai-Ju *et al*. proposed that at late times in infection when viral transcriptional activity is high, the compact HSV-1 genome might be over burdened by transcribing RNAP II complexes and some of the RNAP II complexes might collide with other transcribing RNAP II complexes on the viral genome and become stalled. Arrested RNAP II has been shown to trigger transcription-coupled DNA repair response (152,158,159,174) in which elongating RNAP II is poly-ubiquitinated and undergoes proteasomal degradation to ensure that at least some of the transcripts can be completed by RNAP II. This collision model is supported by earlier studies showing that HSV-1 infected cells appear to have many incomplete viral transcripts.

Eukaryotic cells can experience pausing or stalling of RNAP II in absence of a viral infection. For example, promoter clearance of the polymerase during transcription initiation is a kind of pausing itself. RNAP II may also pause on the chromatin template due to secondary DNA structure and/or nucleosome

occupancy. RNAP II pausing directly affects transcription kinetics and thereby can influence splice site and polyadenylation site choices. During pausing, RNAP II has been found to backtrack approximately 7-9 nt on the DNA template before attempting to go forward again (49,63). The protein transcription elongation factor A (TCEA1-3), also known as TFIIS, helps the polymerase to reestablish proper alignment of the DNA-RNA hybrid by cleavage of the RNA at the active site of RNAP II thereby promoting fidelity of the transcript (81,131). If resolution of the paused RNAP II is achieved, transcription continues, but if resolution is impossible, then the polymerase becomes arrested on the chromatin template.

Arrested RNAP II is often associated with DNA damage induced by UV irradiation and/or crosslinking agents such as cisplatin. When transcribing RNAP II encounters such DNA lesions, it will attempt to resolve the block and read through, but if it cannot it becomes arrested. If the DNA lesions are left unrepaired, transcription will eventually shut down completely (108). The cell recognizes arrested RNAP II as a signal of potential DNA damage and activates the transcription-coupled nucleotide excision repair (TC-NER) pathway to correct the damage at the site of the arrested RNAP II. The TC-NER pathway relies on active transcription and studies have found that the rate of repair was higher at expressing genes than non-expressing genes (104-106). Cockayne syndrome proteins (CSA & CSB) appeared to play a major role in the initial step in TC-NER by binding to arrested RNAP II and subsequently recruiting TC-NER factors (90,166,167). The TC-NER complex assembles around the arrested RNAP II and opens up the DNA-RNA-RNAP II ternary complex to make the lesion available to the DNA repair machinery in the cell. The opening of the transcription apparatus destabilizes the interactions between the DNA, RNA, and the polymerase, ultimately loosening the RNAP II from the chromatin. While in contact with the TC-NER complex, arrested RNAP II is ubiquitinated at lysine residue 63 (K63u) of RPB1 possibly by the E3 ubiquitin ligase, neural precursor cell expressed, developmentally down-regulated 4 (NEDD4). NEDD4 appeared to ubiquitinate S2p RPB1 *in vitro*, suggesting specificity for previously elongating RNAP II (5,67). IF the K63u modification remains on RPB1 after partially disassociating from the chromatin template, RPB1 becomes

polyubiquitinated at lysine 48 (K48u) by the Elongin A/B/C heterotrimer complex. Independent studies have found that Elongin A/B/C polyubiquitination of RPB1 required NEDD4 activity as reduced NEDD4 protein levels lead to an overall reduction in RPB1 ubiquitination and degradation. In 2004, Gillette *et al*. demonstrated that the 26S proteasome was recruited to elongating RNAP II during transcription, and inhibition of the proteasome resulted in an increase in read-through by the polymerase (57). Currently the 26S proteasome is believed to degrade polyubiquitinated RPB1 on the chromatin template in the TC-NER pathway.

While many aspects of HSV-1 gene expression have been worked out, including the temporal programing and mechanistic details of how the virus acquires some host cell protein complexes for mRNA synthesis and export during lytic infection (reviewed in (170)), there remains the paradox of diminishing RNAP II levels at a time when viral transcription is robust. Currently there are two models that attempt to reconcile contradictory data. The Rice group, the first to observe the intermediately phosphorylated RNAP II in wild type (WT) HSV-1 infected cells, proposed that perhaps unlike host cell transcription, viral transcription does not require the hyper-phosphorylated form of RNAP II, and this intermediately phosphorylated RNAP II is sufficient to carry out viral transcription elongation. In this model, the viral protein ICP22 and its viral kinase partner UL13 alter CTD phosphorylation and somehow induce a decrease of S2p RNAP II in HSV-1 infected cells, and this in turn promotes viral transcription over cellular transcription. The second model put forward by our lab, proposes that transcription complexes may collide or pile up in areas of the genome with many overlapping transcripts at later times during infection when viral transcription is very high. This could result in stalling of RNAP II complexes and the subsequent observed loss of S2p RNAP II to clear arrested RNAP II by proteasomal degradation. The data on inhibiting proteasome degradation resulting in lower viral progeny yield support this model (37)). Given the complexity of the RNAP II transcription cycle and the regulatory nature of the CTD code, it is difficult to believe that alterations proposed by the Rice group would have little to no negative effect on the well-

conserved transcriptional processes that HSV-1 exploits for its replication. At the heart is the question, "how different is HSV-1 transcription compared to its host cell?" In **Chapter 2**, we examined the requirement of serine-2 phosphorylation on HSV-1 transcription during lytic infection. We found that inhibition of CDK9, the kinase responsible for S2p modification of the CTD, lead to a significant global reduction in viral RNA synthesis and viral replication. Data on overexpression of a kinase-dead CDK9 or hexamethylene bis-acetamide inducible protein 1 (HEXIM1), a negative regulator or CDK9, showed a similar, though weaker effect on HSV-1 transcription. In **Chapter 3**, we attempted to substantiate the RNAP II collision model by examining the RNAP II occupancy on the HSV-1 genome by ChIP analysis using antibodies recognizing RNAP II in its various phospho-states. Of the antibodies we used, only 4H8, a pan-RNAP II antibody generated strong ChIP signals, while the H14 and H5 antibodies, recognizing S5p and S2p CTD respectively, produced ChIP signals equivalent to normal mouse IgM controls. The 4H8 ChIP data was insufficient due to lack of genome coverage in the current experimental design. A somewhat surprising finding of this work was that viral DNA replication appeared to outpace viral transcription, suggesting that perhaps newly replicated viral genomes were not available to serve as templates for viral transcription. To complement our ChIP analysis, we investigated possible involvement of TFIIS in resolving arrested RNAP II complexes predicted by the collision model. In **Chapter 4**, Preliminary evidence suggested that TCEA2, one of the isoforms of TFIIS, might be relocalized to the nuclei of HSV-1 infected cells. Subsequent co-localization studies suggested that all three isoforms of TFIIS might co-localized with ICP4 during infection. The western blot analysis however, revealed that the TFIIS antibodies used in these studies did not show discreet bands in the expected molecular weight range of TFIIS isoforms but instead, several bands of both higher and lower molecular weight were seen. This non-specific binding cast doubt on which proteins were stained and relocalized in the immunofluorescence experiments. Currently, we cannot provide direct experimental evidence in support of the colliding RNAP II model during HSV-1 lytic infection. In **Chapter 5**, we discuss potential improvements in experimental design and other avenues of research

that might shed light on these questions. Overall, this thesis demonstrates progress toward a more detailed understanding of HSV-1 transcription.

Chapter 2
Inhibition of CDK9 during Herpes Simplex Virus 1 Infection Impedes Viral Transcription

Summary

During herpes simplex virus 1 (HSV-1) infection there is a loss of the serine-2 phosphorylated (S2p) form of RNA polymerase II (RNAP II) found in elongation complexes. This occurs in part because RNAP II undergoes ubiquitination and proteasomal degradation during times of highly active viral transcription, which may result from stalled elongating complexes. In addition, a viral protein, ICP22, was reported to trigger a loss of S2p RNAP II. These findings have led to some speculation that the S2p form of RNAP II may not be required for HSV-1 transcription, although this form is required for cellular transcription elongation and RNA processing. Cellular kinase CDK9 phosphorylates serine-2 in the C-terminal domain (CTD) of RNAP II. To determine if S2p RNAP II is required for HSV-1 transcription, we inhibited CDK9 during HSV-1 infection and measured viral gene expression. Inhibition was achieved by adding CDK9 inhibitors 5,6-dichlorobenzimidazone-1-β-D- ribofuranoside (DRB) or flavopiridol (FVP) or by expression of a dominant–negative CDK9 or HEXIM1, which in conjunction with 7SK snRNA inhibits CDK9 in complex with cyclin T1. Here we report that inhibition of CDK9 resulted in decreased viral yields and levels of late proteins, poor formation of viral transcription-replication compartments, reduced levels of poly(A)+ mRNA and decreased RNA synthesis as measured by uptake of 5-bromouridine into nascent RNA. Importantly, a global reduction in viral mRNAs was seen as determined by microarray analysis. We conclude that serine-2 phosphorylation of the CTD of RNAP II is required for HSV-1 transcription.

Introduction

The largest subunit of RNA polymerase II (RNAP II) in eukaryotes contains a highly conserved C-terminal domain that consists of tandem repeats of the heptapeptide YSPTSPS, which is repeated 52 times in humans. Serine residues at positions 2 and 5 are reversibly phosphorylated during transcription (36). While unphosphorylated RNAP II is recruited to promoters, after assembly of the pre-initiation complex, serine-5 becomes phosphorylated (S5p) during initiation, primarily by the kinase CDK7, which is associated with the general transcription factor TFIIH (36,86). Capping of the 5' end of the nascent RNA is associated with initiation and serine-5 phosphorylation (36,56,86,126). Transition into the elongation phase of RNAP II transcription requires phosphorylation of serine-2 (S2p) by the kinase CDK9, which acts in conjunction with cyclin 1 in mammalian cells and the complex is referred to as P-TEFb for positive transcription elongation factor (86,126). Following initiation, transcription is paused by the repressors DSIF and the negative elongation factor, NELF resulting in short transcripts that require the recruitment of CDK9 (14,56,126). DSIF and NELF are phosphorylated by CDK9, relieving the transcriptional pause and CDK9 also then phosphorylates serine-2 of the CTD of RNAP II (50,70,110,114,126,130,164,168,178). Phosphorylation of CTD serine-2 has also been shown to be required for co-transcriptional mRNA processing including splicing and polyadenylation (1,16,32,62,86,93).

During herpes simplex virus 1 (HSV-1) infection, it has been reported that RNAP II phosphorylation patterns are altered compared to uninfected cells, resulting in an intermediate form of RNAP II that migrates more slowly than the hypophosphorylated form but faster than the hyperphosphorylated form (134). It was subsequently shown that the viral immediate early protein ICP22 and a viral kinase U_L13 are required for this intermediate form of RNAP II (11,133). The actual CTD phosphorylation sites for U_L13 have not been identified, nor has the role that this intermediately phosphorylated form plays during viral infection been elucidated. It has also been shown that ICP22 associates with CDK9 and co-localizes with CDK9 and RNAP II (41,42). Paradoxically, HSV-1 infection leads to a loss of RNAP II CTD S2p (37,53,54). This

occurs during times of highly active transcription of early and late genes during infection and in fact, there is a measurable decrease in total RNAP II levels at later times of HSV-1 infection (37,92). We showed that this resulted from proteasomal degradation of RNAP II and could be prevented using proteasome inhibitors MG132 or lactacystin or the transcription elongation inhibitor actinomycin D (37). We postulated that because the HSV-1 genome is transcribed from both DNA strands and it contains several regions where transcripts from different genes overlap, during highly active viral transcription, RNAP II elongating complexes might collide or pile up resulting in stalled complexes. Proteasomal degradation of stalled complexes would allow re-initiation and elongation through the former site of the stalled complex. Loss of S2p has also been shown to occur in cells that were transfected with a plasmid expressing HSV-1 protein ICP22, and this did not require any other viral factors or viral transcription (54). Because it was shown that ICP22 binds CDK9 and that both can be found co-localized with RNAP II (42), it is possible that ICP22 may modulate CDK9 activity in some manner although how this might occur has not been demonstrated.

Because of the decrease in S2p during HSV-1 infection, it has been proposed that S2p RNAP II may not be required for HSV-1 transcription elongation. To determine whether S2p RNAP II is required during HSV-1 replication, we inhibited CDK9 and observed decreased viral yields and reduced viral transcription, indicating that serine-2 phosphorylation of RNAP II CTD is required during HSV-1 replication.

Results

RNAP II levels are reduced during HSV-1 infection

We showed previously that during wild type HSV-1 KOS infection, levels of S2p RNAP II were significantly reduced, and in fact, levels of total RNAP II, both hyperphosphorylated and hypophosphorylated were decreased by around 5 hours post infection when HSV-1 transcription and DNA replication are highly active (37). This decrease in total RNAP II levels can be seen in Figure 2-1, which shows a western blot analysis of whole cell lysates from cells that were mock infected or were infected

with HSV-1 ICP27 null mutant 27- GFP or WT KOS for 1, 3, 5, 7 and 9 hours. Blots were probed with antibody N20, a polyclonal antibody that recognizes an epitope in the N-terminus of the large subunit of RNAP II and therefore, which recognizes all forms of RNAP II (Table 2-1). By 5 hour post infection, there was a decrease in both hyperphosphorylated and hypophosphorylated RNAP II in KOS infected cells and this decrease was even more pronounced at 7 and 9 hours post infection when viral transcription is highly robust (Figure 2-1). In contrast, as we reported previously, when ICP27 was not expressed during infection, there was little decrease in RNAP II levels (Figure 2-1). We inferred that this is because ICP27 is required to relocalize RNAP II to viral transcription-replication sites (37,134) and during 27-GFP infection, viral transcription of early and late genes is greatly reduced (37,92). These results led us to postulate that during highly robust viral transcription in WT KOS infected cells, elongating transcription complexes might collide or pile up and become arrested. We further showed that RNAP II becomes ubiquitinated during KOS infection and that proteasome inhibitors were able to prevent the decrease in RNAP II levels, indicating that stalled RNAP II complexes were likely being degraded by the proteasome (37). Thus, the decrease in RNAP II levels and particularly in S2p levels may be attributed to proteasomal degradation of arrested elongating RNAP II transcription complexes during highly active transcription in WT HSV-1 infections.

Effects of DRB and FVP on RNAP II and HSV-1 protein levels

Because the S2p form of RNAP II CTD is decreased during HSV-1 KOS infection as we (37) and Fraser and Rice showed (53), we wanted to address the importance of the Sp2 RNAP II to viral gene expression during HSV-1 infection. In mammalian cells, serine-2 phosphorylation of RNAP II CTD is required for transcription elongation as well as for RNA processing (1,16,50,62,70,114). RNAP II CTD is phosphorylated on serine-2 by kinase CDK9, which acts in conjunction with cyclin T1 in mammalian cells and the complex is referred to as P-TEFb for positive transcription elongation factor (86,126). DRB is an adenosine analogue that is a specific inhibitor of CDK9. Although DRB can also affect the activity of other

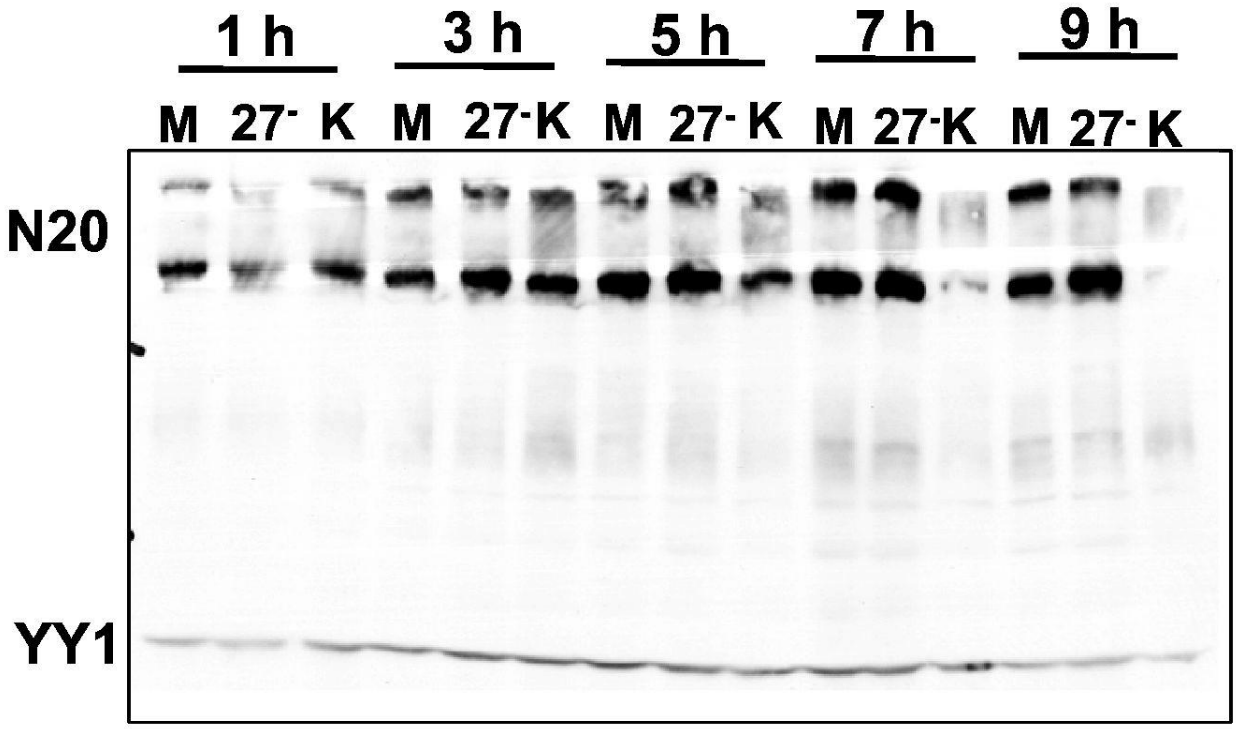

Figure 2-1: Total RNAP II levels decrease during WT HSV-1 KOS infection.
HeLa cells were either mock infected or infected with WT HSV-1 KOS or with an ICP27 null mutant, 27-GFP in which the ICP27 coding sequence was replaced with GFP. Cells lysates were prepared at 1, 3, 5, 7 and 9 hours post infection and separated on a 5-15% gradient SDS-polyacrylamide gel. Western blots were probed with polyclonal antibody N20, which detects all forms of RNAP II The cellular protein YY1 served as the loading control.

kinases, its affinity for CDK9 at IC_{50} μM ranges from 3 fold greater than its affinity for CDK7 to more than 10 fold higher for CDK9 compared to CKII and PKA (95). Analysis of the crystal structure of CDK9 in complex with DRB showed that DRB chlorine atoms form halogen bonds with oxygen in the CDK9 hinge region and that is the basis for its specificity (14). We first determined the effect of different concentrations of DRB on the phosphorylated forms of RNAP II in mock-infected cells compared to HSV-1 KOS infected cells. Increasing concentrations of DRB were added at 1, 3 and 5 hours post infection and whole cell lysates were isolated at 8 hours post infection and western blot analysis was performed (Figure 2-2). In mock infected cells, addition of 50 or 100 μM DRB resulted in a loss of the more slowly migrating hyperphosphorylated form of RNAP II detected by antibody N20 with a shift to the faster migrating hypophosphorylated form (Figure 2-2). In HSV-1 KOS infected cells, the results were more complex. When DRB was added at 1 and 3 hours post infection, hypophosphorylated RNAP II was seen with antibody N20 at both concentrations of DRB with little of the hyperphosphorylated form visible (Figure 2-2). In the samples to which dimethyl formamide (DMF) alone or no DRB were added, there was a pronounced decrease in both forms of RNAP II in KOS infected cells. We interpret this result to mean that in the absence of the inhibitor, robust HSV-1 transcription transpired during the 8-hour infection, which would result in arrested elongation complexes and proteasomal degradation of RNAP II as described earlier and shown in Figure 2-1. When DRB was added at 5 hours post infection, very low levels of RNAP II were detected in the presence or absence of DRB. This finding suggests that by 5 hours post infection, proteasomal degradation of RNAP II is already occurring as shown in Figure 2-1, and addition of DRB would further reduce the hyperphosphorylated form by blocking CDK9 activity (Figure 2-2).

In looking specifically at the S2p RNAP II, as detected with antibody H5, the addition of 100 μM DRB was more effective than 50 μM in reducing S2p in mock infected cells, as were longer incubation times with DRB present (Figure 2-2). In HSV-1 KOS infected cells, there was a significant reduction in S2p RNAP II in the DMF vehicle alone or no DRB samples. This in accordance with previous results that

demonstrated that the S2p RNAP II is degraded during HSV-1 infection, which proceeded for 8 hours with no drugs in these control samples (37). Treatment with 100 μM DRB reduced S2p to an even greater extent compared to 50 μM DRB. That DRB was specific for CDK9 at the concentrations used in these studies was shown by probing the blots with antibody H14, which recognizes phophoserine-5 (S5p) (Table 2-1). Serine-5 is phosphorylated by CDK7. S5p levels were largely unaffected by DRB in mock or KOS infected cells regardless of the DRB concentration or time of addition (Figure 2-2) These results demonstrate that the addition of 100 μM DRB is more effective in reducing serine-2 phosphorylation of RNAP II CTD by CDK9.

To determine what effect reducing S2p RNAP II levels would have on HSV-1 immediate early (IE) and late protein levels, we analyzed the expression of IE proteins ICP4 and ICP27 and late proteins glycoprotein B (gB) and glycoprotein D (gD) in the presence and absence of DRB. ICP4 levels were only slightly decreased when 100 μM DRB was added 1 hour post infection, and were not appreciably affected by 50 μM DRB or when DRB was present for shorter times during infection (Figure 2-2). A similar result for ICP4 was reported by Durand and Roizman (42) who monitored ICP4 expression in cells treated with 50 μM DRB for 8 hours beginning 2 hours post infection. ICP27 levels were significantly reduced by the addition of 50 and 100 μM DRB when added 1 hour post infection but were unaffected when DRB was added at later times (Figure 2-2). Levels of late proteins gB and gD were significantly decreased when DRB was added at 1 and 3 hours post infection but were not visibly affected by DRB addition at 5 hour.

Next, we probed the importance of S2p RNAP II during HSV-1 infection by using another inhibitor of CDK9, namely flavopiridol (FVP), which has been used extensively to study the role of P-TEFb on transcription elongation (10,95,107,109,123,126,186). FVP binds to the ATP site of CDK9 through ATP-like hydrogen bond interactions that induce structural changes in CDK9 (15). FVP inhibits CDK9 activity specifically. First we tested different concentrations of FVP (Figure 2-3). Dimethyl sulfoxide (DMSO) vehicle alone or increasing concentrations of FVP were added to mock and HSV-1 KOS infected cells at 1 hour post infection and whole cell lysates were prepared at 8 hours post infection. In mock infected cells,

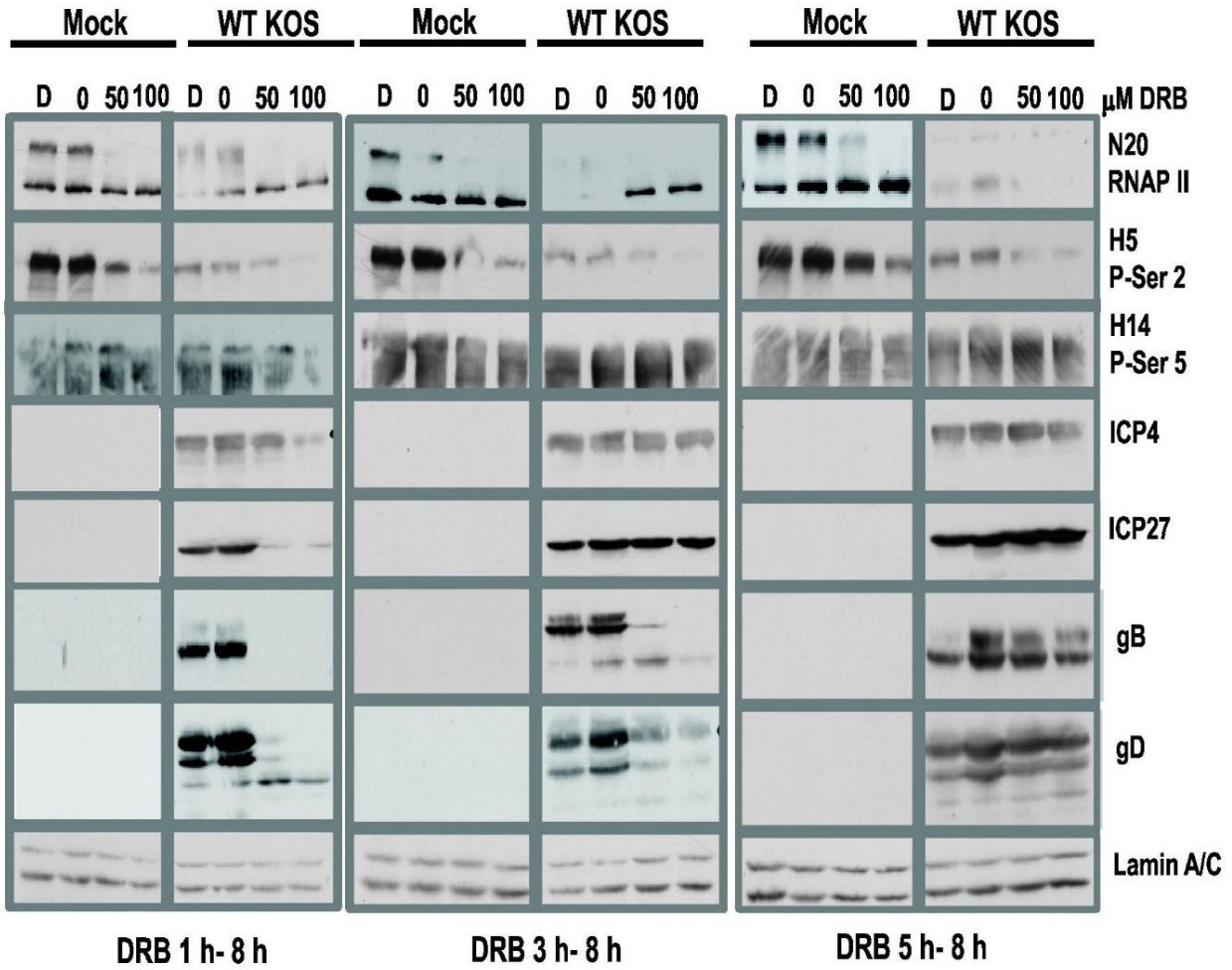

Figure 2-2: RNAP II CTD phosphoserine-2 levels decreased with increasing amounts of DRB.
HeLa cells were mock infected or infected with WT HSV-1 KOS at an MOI of 10. DRB stocks were prepared in dimethyl formaldehyde (DMF). At 1, 3 and 5 hours post infection, DMF alone (D) or increasing amounts of DRB from 0 to 100 μM were added to cell monolayers. At 8 hours post infection, whole cell lysates were prepared and separated on 5-15% gradient SDS-polyacrylamide gels. Western blots were probed with polyclonal antibody N20, which detects all forms of RNAP II; monoclonal antibody H5, which detects S2p CTD, and monoclonal antibody H14, which detects S5p CTD. For HSV-1 proteins, antibody P1011 was used to detect IE protein ICP4, P1119 for ICP27, P1123 for gB and P1103 for gD. Lamin A/C served as a sample loading control.

Table 2-1: Specificity of antibodies against RNA polymerase II.

Antibody	RNAP II form	Epitope
ARNA3 (mouse monoclonal IgG)	All forms; unphosphorylated, Initiating, and elongating	N-terminal epitope in largest subunit of RNAP II holoenzyme
N-20 (rabbit polyclonal)	All forms; unphosphorylated, Initiating, and elongating	N-terminal epitope in largest subunit of RNAP II holoenzyme
H14 (mouse monoclonal IgM)	RNAP II initiating complex	Ser-5-phosphorylated (S5p) CTD
H5 (mouse monoclonal IgM)	RNAP II elongating complex	Ser-2-phosphorylated (S2p) CTD

300 and 450 nM concentrations of FVP were effective in shifting hyperphosphorylated RNAP II to the hypophosphorylated form as detected by antibody N20 (Figure 2-3A). A similar result was seen in KOS infected cells (Figure 2-3A). Here again, in the absence of FVP, total levels of RNAP II detected by N20 were greatly reduced in accord with proteasomal degradation of RNAP II during the 8-hour HSV-1 infection. A concentration of 450 nM FVP was more effective in reducing S2p RNAP II as detected by antibody H5 for both mock and KOS infected cells (Figure 2-3A), and no significant effect was seen in S5p RNAP II levels detected by antibody H14. In contrast to the results that we observed with DRB, addition of FVP at either concentration at 1 hour post infection diminished ICP4, ICP27, gB and gD levels (Figure 2-3A). To determine how the time of treatment with FVP would affect RNAP II and HSV-1 proteins, 450 nM FVP was added to mock and KOS infected cells at 1, 3 and 5 hours post infection and cell lysates were harvested at 8 hours post infection (Figure 2-3B). Total RNAP II levels as detected by N20 were significantly decreased in KOS infected cells, reflecting both a reduction in hyperphosphorylated RNAP II by addition of FVP early in infection and proteasomal degradation of elongating complexes when FVP was added at later times of infection. S2p RNAP II was significantly and specifically decreased by FVP as seen in the H5 panels for both mock and KOS infected cells compared to the H14 samples, showing that S5p was generally unaffected. The time of addition of FVP was important for HSV-1 protein expression. Addition of FVP at 1 and 3 hours post infection significantly affected ICP4 and ICP27 protein levels, whereas there was a marginal effect when FVP was added at 5 hours (Figure 2-3B). Late proteins gB and gD were more adversely affected when FVP was added at 1 and 3 hours post infection but addition at 5 hours also resulted in lower levels of these late proteins.

The results with DRB and FVP demonstrate that S2p RNAP II levels were specifically reduced in both mock and KOS infected cells and that expression of IE proteins ICP4 and ICP27 was affected more adversely when FVP was added at earlier times. Levels of late proteins gB and gD were reduced when

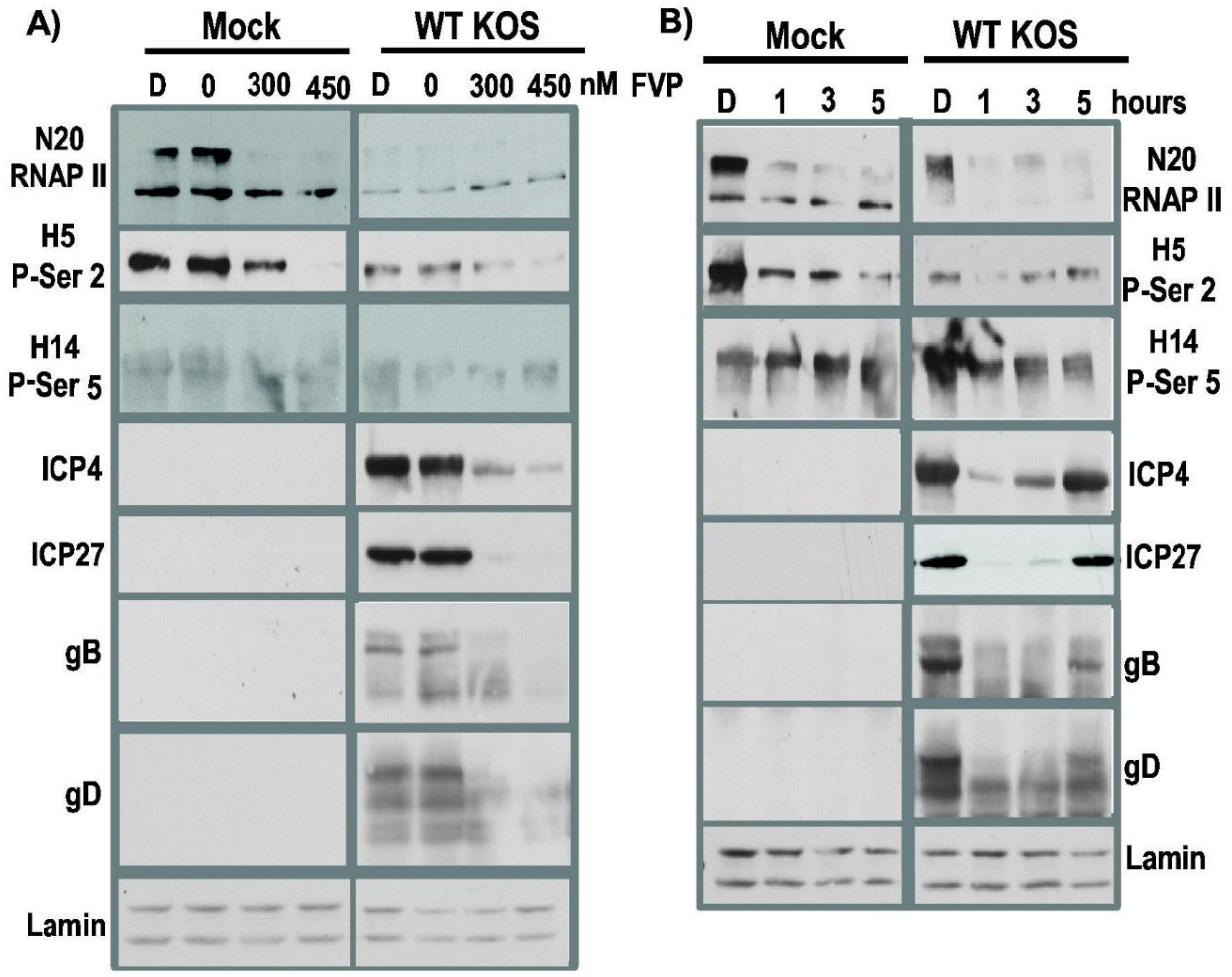

Figure 2-3: Addition of FVP reduced S2p RNAP II levels and levels of HSV-1 IE proteins ICP4 and ICP27 and late proteins gB and gD were also reduced.

A) HeLa cells were mock infected or infected with WT HSV-1 KOS at MOI of 10. Flavopiridol (FVP) stocks were prepared in DMSO. At 1 hour post infection, DMSO alone or increasing amounts of FVP from 0 to 450 nM were added to cell monolayers. At 8 hours post infection, whole cell lysates were prepared and fractionated on 5-15% gradient SDS-polyacrylamide gels. Western blots were probed with N20, H5 and H14 as indicated. Lamin A/C served as the loading control. **B)** DMSO alone was added at 0 hour post infection or FVP (450 nM) was added at 1, 3 or 5 hours post infection as indicated. Whole cell lysates were prepared at 8 hours. Western blots were probed with anti-RNAP II antibody N20 or S2p CTD antibody H5 or S5p CTD antibody H14. HSV-1 protein ICP4 was detected using antibody P1101; ICP27 was detected with antibody P1119; gB was detected with antibody P1103 and gD was detected with antibody 1123. Lamin A/C served as a loading control.

DRB and FVP were added at earlier times after infection but later addition of FVP still decreased gB and gD levels.

In previous studies we showed that in HSV-1 KOS infected cells, when S2p RNAP II levels were reduced, immunofluorescent staining with antibody H5 was seen in speckled structures in the nucleus instead of diffuse staining throughout the nucleus as seen in mock infected cells (37,92). A similar result was also reported by Fraser and Rice (53). The reason for this change in the staining pattern is because it was reported that antibody H5 cross-reacts with a phospho-epitope in SR splicing proteins under conditions in which S2p RNAP II is less abundant compared to highly abundant SR proteins (40). This occurs during HSV-1 infection because of proteasomal degradation of elongating RNAP II complexes as described earlier (37) and because HSV-1 ICP22 can also cause a decrease in the phosphoserine-2 form (54). Therefore, H5 staining is a convenient method to detect loss of S2p RNAP II. When mock and KOS infected cells were stained with antibody ARNA3, which recognizes an epitope in the N-terminus, and thus all forms of RNAP II (Table 2-1), a diffuse nuclear staining was seen in mock and KOS infected cells (Figure 2-4A). When antibody H5 was used, this diffuse nuclear staining pattern was seen in mock infected cells that were not treated with inhibitors, whereas in KOS infected cells, a speckled staining pattern was seen, consistent with H5 recognizing SR proteins in splicing speckles as reported previously (37,53,92). Upon treatment with DRB or FVP, both mock and KOS infected cells showed the speckled staining pattern with antibody H5, consistent with a loss in the S2p RNAP II.

To assess the cytotoxicity of the inhibitors, percent cell death was estimated by trypan blue staining at 4 hour intervals in mock vs. KOS infected cells that were or were not treated with DRB or FVP (Figure 2-4B). Total cell counts were also estimated at 4 hour intervals (Figure 2-4C). A marked increase in cell death was not observed in the presence of the inhibitors.

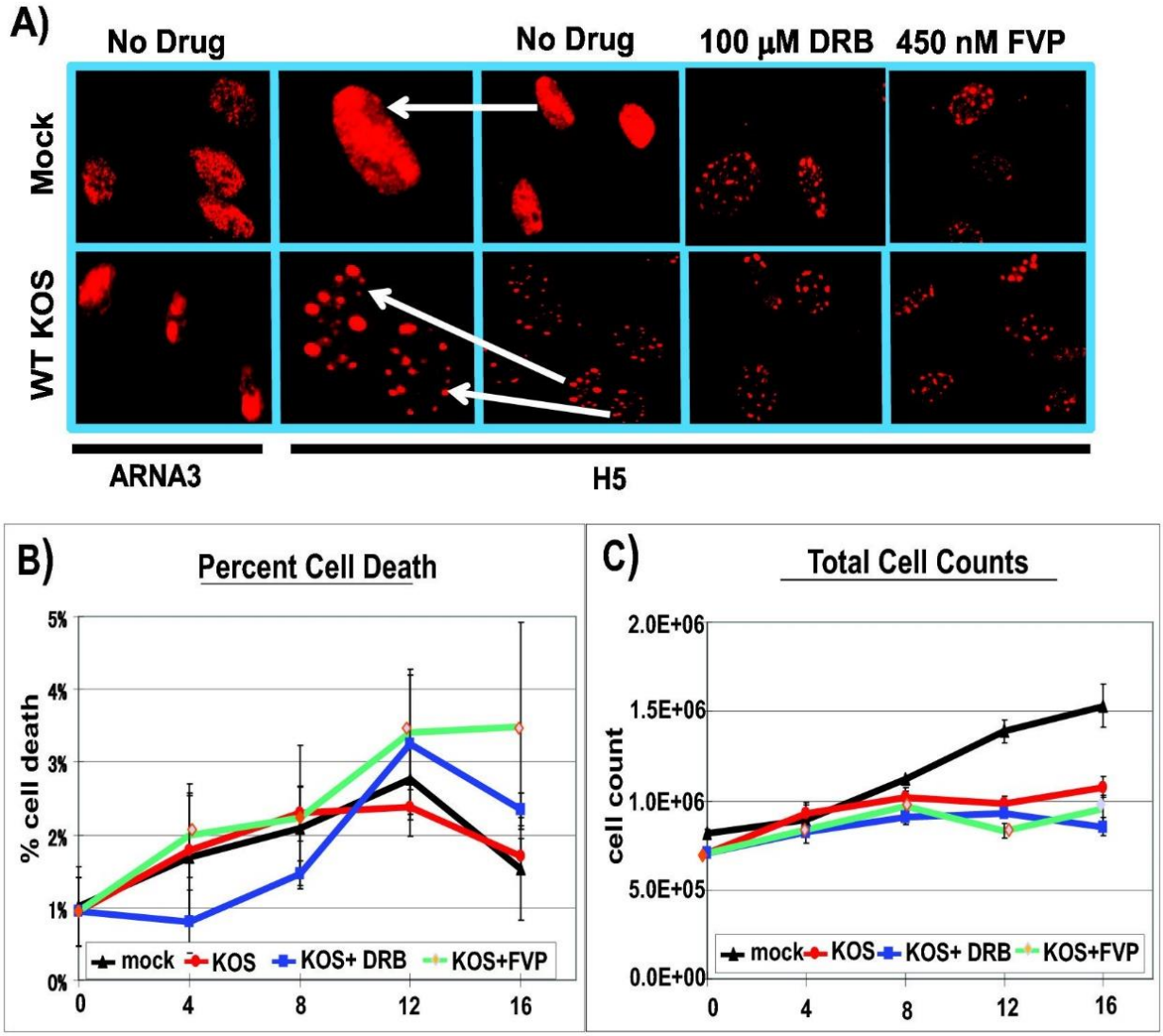

Figure 2-4: DRB and FVP altered the staining pattern of H5 antibody.
A) RSF cells were either mock infected or infected with WT HSV-1 KOS at an MOI of 10. Cells were either left untreated (no drug) or were treated with 100 µM DRB or 450 nM FVP as indicated. Cells were fixed at 8 hours post infection and stained with RNAP II antibody ARNA3, which recognizes all forms of RNAP II or S2p antibody H5. For the H5 no drug panels, cells from mock and KOS samples have been shown at higher magnification to show the nuclear staining patterns and are identified by white arrows. **B-C)** To account for cell toxicity, HeLa cells were either mock infected, or infected with HSV-1 KOS at an MOI of 1 for up to 16 hours as indicated. Infected cells were either untreated or treated with 100 µM DRB or 450 nM FVP. Cells were collected at 4 hour intervals, stained with Trypan Blue vital dye, and counted in triplicate using a hemocytometer to estimate **B)** percent cell death and **C)** total cell counts.

DRB and FVP reduced RNA synthesis in mock and HSV-1 infected cells

To determine the effect of adding CDK9 inhibitors on RNA synthesis and accumulation, mock and HSV-1 KOS infected cells were treated with DRB or FVP beginning 1 hour post infection (Figure 2-5). To monitor newly synthesized RNA, 5- bromouridine (BrU) was added for 30 min at 7.5 hours post infection to pulse label newly transcribed, nascent RNA. Cells were subsequently fixed and stained with anti-BrU antibody. In the absence of inhibitors, BrU incorporation was observed in mock and KOS infected cells (Figure 2-5A). However, BrU incorporation was not detected in mock or KOS infected cells treated with DRB or FVP (Figure 2-5A), suggesting that RNAP II transcription was curtailed by these CDK9 inhibitors. To assess the effect of these inhibitors on accumulation of poly(A)+ mRNA, *in situ* hybridization was performed with an oligo-dT probe (Figure 2-5B). In both mock and KOS infected cells (infected cells were marked by staining for ICP4), in the absence of inhibitors, poly(A)+ RNA was seen throughout the nucleus (marked by DAPI staining) and the cytoplasm (Figure 2-5B). However, after addition of DRB or FVP, poly(A)+ RNA was observed to be concentrated in large speckles in the nucleus and was barely detectable in the cytoplasm. These results indicate that inhibition of CDK9 by DRB and FVP negatively affected RNA synthesis and accumulation in both mock and HSV-1 infected cells, indicating that the S2p RNAP II is required for transcription during HSV-1 infection just as it is required in uninfected cells.

The effects of DRB and FVP on HSV-1 infection was reversible

To determine if the effects of these inhibitors could be reversed during HSV-1 infection, DRB or FVP were added for the first 4 hours of infection and then washed away and drug free medium was added for an additional 4 hours. These samples were compared to HSV-1 KOS infected cells that were left untreated and to KOS infected cells to which DRB or FVP were added at 3 hours post infection and remained in the medium until 8 hours when all cells were fixed and stained (Figure 2-6). In the absence of drugs, BrU incorporation was seen (Figure 2-6A) and poly(A)+ RNA was distributed throughout the nucleus and cytoplasm (Figure 2-6D). When DRB or FVP were added at 3 hours and remained in the medium until

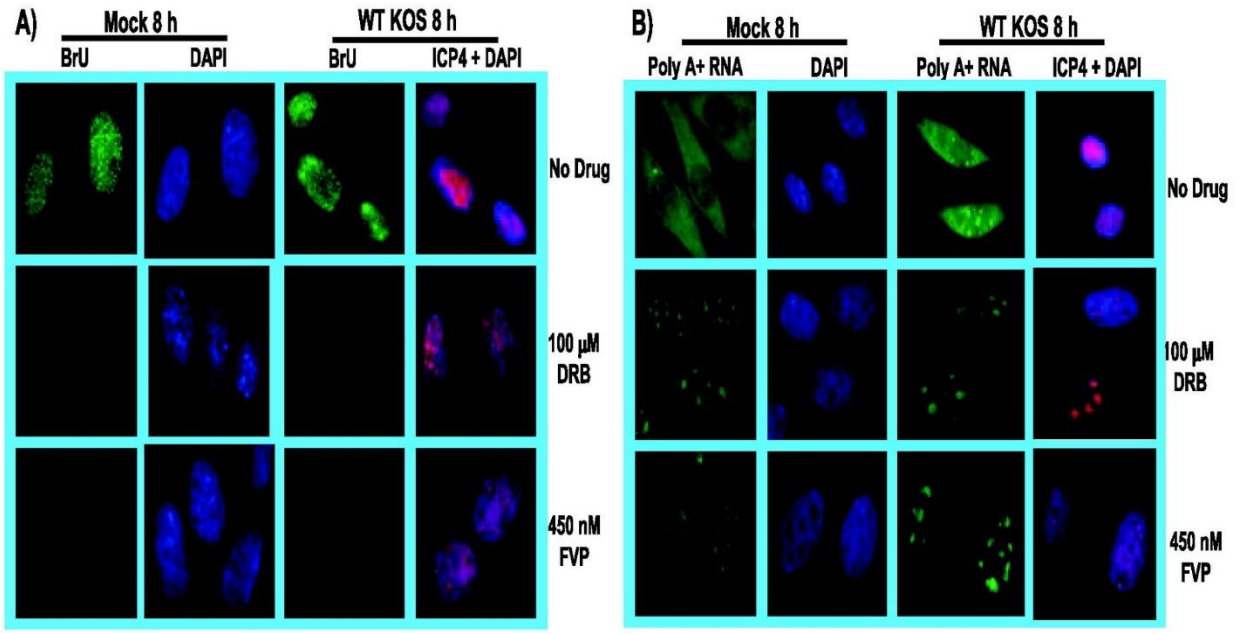

Figure 2-5: DRB and FVP reduced RNA synthesis in mock and HSV-1-infected cells.
RSF cells were mock infected or infected with WT HSV-1 KOS at MOI of 10. At 1 hour post infection, cells were treated with 100 µM DRB or 450 nM FVP. **A)** 4 mM Bromouridine (BrU) was added to the media at 7.5 hours to label nascent RNA. Cells were fixed at 8 hours post infection and stained with anti-BrU antibody (green). Mock infected cells were stained with DAPI to mark the nuclei. KOS-infected cells were stained with DAPI and with anti-ICP4 antibody as a marker of infection. **B)** Cells were fixed at 8 hours post infection and *in situ* hybridization with a biotinylated oligo-dT_{25} probe was performed to detect poly(A+) RNA. Mock infected cells were stained with DAPI and KOS infected cells were stained with DAPI and anti-ICP4 antibody as an infection marker. All images were captured on a Zeiss Axiovert 200M microscope at 100X magnification.

8 hours, there was no detectable incorporation of BrU during a 30 min pulse at 7.5 hours (Figure 2-6B) and poly(A)+ RNA was observed in large speckles in the nucleus and was barely detectable in the cytoplasm (Figure 2-6E). In the case of DRB or FVP addition from the start of infection until 4 hours, after which the drugs were washed away and drug free medium was added for an additional 4 hours, BrU incorporation was again observed during a 30 min pulse at 7.5 hours (Figure 2-6C). Poly(A)+ RNA was also observed in the nucleus and cytoplasm (Figure 2-6F), although for both BrU incorporation and poly(A)+ RNA hybridization, the fluorescence signals were less intense than those observed in the absence of drugs. Nevertheless, it appears that the effects of DRB and FVP on RNA synthesis and accumulation were reversible.

As a further test of whether the effects of these inhibitors on HSV-1 infection were reversible, we looked at the localization of viral IE proteins ICP4 and ICP27 in the presence of DRB or FVP and after the removal of the drugs. ICP4 is a transcriptional activator (61) that serves as a marker for viral transcription-replication compartments (85,163), which first form as pre-replicative sites at 4 hours post infection (Figure 2-7A) and which form full blown replication compartments by 8 hours post infection (Figure 2-7A). When DRB or FVP were present throughout infection, ICP4 was diffusely distributed in the nucleus (Figure 2-7B), however, when DRB and FVP were removed after 4 hours and infected cells were incubated an additional 4 hours, small replication compartments and pre- replicative sites were seen (Figure 2-7C) indicating that viral replication could resume. During HSV-1 infection, ICP27 is nuclear at early times but it begins shuttling between the nucleus and cytoplasm at later times in its role as a viral mRNA export factor (27,28,75,76,140) (Figure 2-7D). In the presence of DRB or FVP, ICP27 remained in the nucleus throughout infection (Figure 2-7E) but when the drugs were removed at 4 hours, ICP27 was detected in the cytoplasm 4 hours later (Figure 2-7F), again indicating that the inhibitory effects of DRB and FVP on viral infection were reversible when these inhibitors were removed.

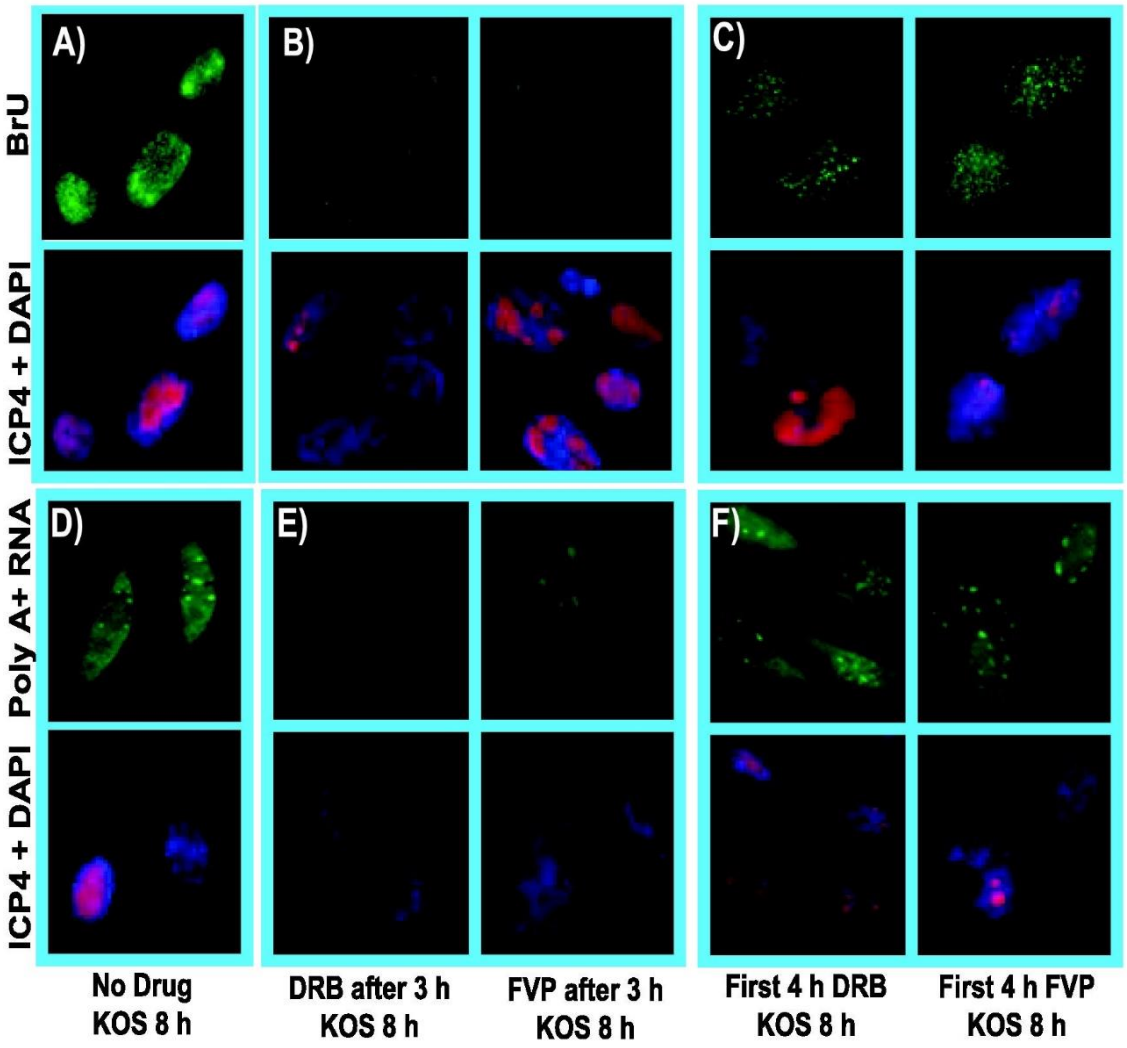

Figure 2-6: The inhibitory effects of CDK9 inhibiters DRB and FVP on RNA synthesis during HSV-1 infection could be reversed after removing the drugs.

RSF cells were infected with HSV-1 KOS at an MOI of 10. **A, D)** Infected cells were left untreated. **B, E)** Infected cells were treated with 100 µM DRB or 450 nM FVP at 3 hours post infection. **C,F)** Infected cells were treated with 100 µM DRB or 450 nM FVP as indicated for the first 4 hours of infection after which, cells were washed and drug-free medium was added. **A-C)** BrU was added to the media at 7.5 hours post infection to label nascent RNA. Cells were fixed at 8 hours and stained with anti- BrU and anti-ICP4 antibodies and with DAPI. **D-F)** Cells were fixed at 8 hours post infection and *in situ* hybridization was performed with a biotinylated oligo dT_{25}-probe, which was subsequently detected by FITC-conjugated streptavidin. ICP4 staining served as an infection marker and DAPI staining marked nuclei. All images were captured on a Zeiss Axiovert 200M microscope at 100X magnification.

A global reduction in HSV-1 mRNA expression in the presence of DRB and FVP

To determine the effect of CDK9 inhibitors DRB and FVP on individual HSV-1 transcript levels, total poly(A)+ RNA was isolated at 8 hours post infection from KOS infected cells to which no inhibitors were added and from KOS infected cells to which DRB or FVP were added at 3 hours post infection. Following reverse transcription of selected poly(A)+ RNA, cDNA from each fraction was hybridized to HSV-1 specific microarrays as described previously (76,92). A global reduction was seen in transcripts from all kinetic classes (IE, E, and L) when DRB or FVP were added at 3 hours post infection (Figure 2-8). We found strong statistical support that all transcripts analyzed were reduced (Table 2-2). We conclude that inhibition of CDK9 by DRB and FVP inhibited HSV-1 transcription.

To determine the effect of these inhibitors on viral replication, one-step growth curves were performed. In the presence of DRB or FVP added at the time of infection, viral replication was completely inhibited (Figure 2-9A). In contrast, when DRB or FVP were present for the first 4 hours post infection but were removed thereafter, viral replication resumed by 12 hours (Figure 2-9A). A single cycle growth curve was also performed in which DRB and FVP were added at the time of infection or at 3 hours post infection. Viral titers were similarly reduced in the presence of these inhibitors added either at the start of infection or 3 hours later (Figure 2-9B). These results indicate that inhibition of CDK9 prevented viral replication but removal of the inhibitors allowed viral replication to resume, which further supports the conclusion that S2p RNAP II is required for HSV-1 replication.

Effects of a dominant negative CDK9 mutant or overexpression of HEXIM1 on nascent RNA synthesis

As an alternative to chemical inhibitors, we also targeted CDK9 activity through expression of a dominant negative kinase-dead mutant and through over expression of hexamethylene bis-acetamide inducible protein 1 (HEXIM1). It has been shown that expression of mutant DN-CDK9, a kinase dead mutant (139), in HeLa cells results in the preferential inhibition of phosphorylation of RNAP II serine-2 without affecting phosphorylation of serine-5 (14,139). Here we transfected HeLa cells with empty vector

or a plasmid expressing DN-CDK9 tagged with an HA-epitope-tag. Western blot analysis was performed on cell lysates 24 hour after transfection to confirm DN-CDK9-HA expression (Figure 2-10A) and immunofluorescent staining with anti-HA antibody was also performed (Figure 2-10B). DN-CDK9-HA was found to be expressed at levels similar to endogenous CDK9 (Figure 2-10A). To determine the effect of DN-CDK9 expression on nascent RNA synthesis, HeLa cells transfected with DN-CDK-HA for 24 hours were either mock infected or were infected with HSV-1 KOS for 8 hours. At 7.5 hours post infection, BrU was added for 30 min and cells were fixed and stained. BrU incorporation was greatly reduced in the cell that expressed DN-CDK9-HA compared to the cell that did not in both mock and KOS infected samples (Figure 2-10E). About 50 fields of cells were assessed for BrU incorporation. Greater than 90% of the cells that were stained with HA antibody showed little to no incorporation of BrU, whereas cells that did not express DN-CDK9-HA did show staining with BrU antibody. This indicates that DN-CDK9 expression interfered with CDK9 activity and this impaired nascent RNA synthesis in both mock and KOS infected cells.

HEXIM1 is a negative regulator of P-TEFb, which consists of CDK9 and cyclin T1 (18,107,118,181). The PYNT motif of HEXIM1 is required to inhibit the kinase activity of CDK9, although the mechanism has not been elucidated. HEXIM1 binds 7SK non-coding RNA and P-TEFb associates with HEXIM1 forming an inactive P- TEFb complex (107,122). We transfected HeLa cells with FLAG- tagged HEXIM1 or empty vector and analyzed cell lysates 24 hours later by Western blot to monitor HEXIM1-FLAG expression (Figure 2-10C). HEXIM1-FLAG was expressed at levels similar to endogenous HEXIM1 levels. HEXIM1-FLAG expression was also confirmed by immunofluorescent staining (Figure 2-10D). To determine the effect of HEXIM1-FLAG expression on BrU incorporation, HeLa cells that were transfected with HEXIM1- FLAG for 24 hours were either mock infected or were infected with HSV-1 KOS and BrU was added for 30 min 7.5 hours post infection. Fixed cells were stained with anti-BrU and anti-FLAG antibodies. BrU incorporation

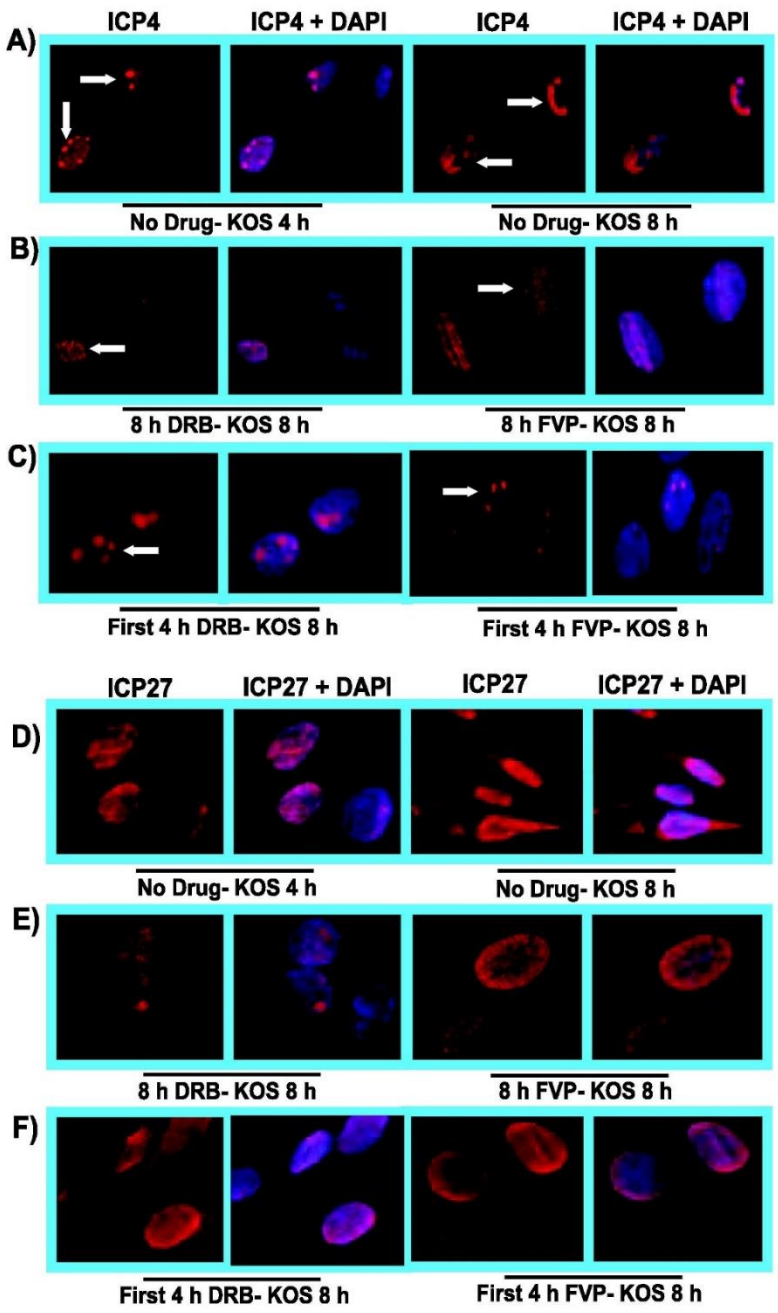

Figure 2-7: DRB and FVP hindered HSV-1 transcription-replication compartment formation but pre-replicative compartments were apparent after drug removal.

RSF cells were infected with WT KOS at an MOI of 10. **A,D)** Infected cells were untreated and were fixed at 4 hours and 8 hours as indicated. **B,E)** Cells were treated with 100 µM DRB or 450 nM FVP as indicated at the beginning of infection and were fixed at 8 hours. **C,F)** DRB or FVP were added at the start of infection and were removed at 4 hours and cells were incubated in drug-free medium for an additional 4 hours. Infected cells were fixed at 8 hours. **A,B,C)** Cells were stained with anti-ICP4 antibody to monitor viral transcription-replication compartment formation and DAPI to mark nuclei. **D,E,F)** Infected cells were stained with anti-ICP27 antibody to monitor ICP27 sub-cellular localization and DAPI to mark nuclei. Images were captured on a Zeiss Axiovert 200M microscope at 100X magnification.

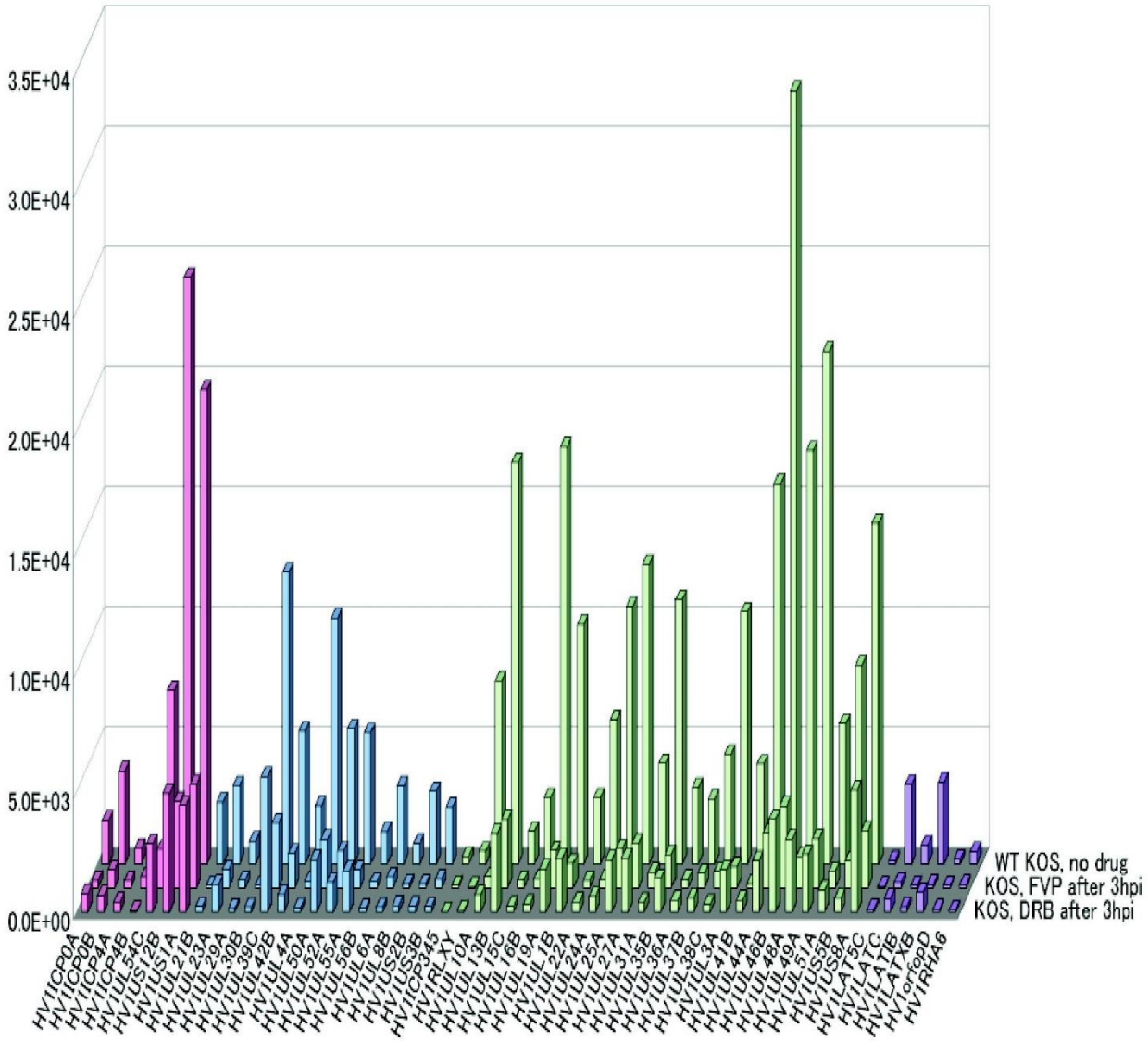

Figure 2-8: A global reduction in HSV-1 mRNA expression was seen in the presence of DRB and FVP.
HeLa cells were infected with HSV-1 KOS at an MOI of 10 and were either left untreated (no drug) or were treated with 100 µM DRB or 450 nM FVP starting at 3 hours post infection. Total RNA was isolated at 8 hours. Poly(A+) RNA was selected and reverse transcribed and the cDNA from each fraction was hybridized to HSV-1-specific microarray chips and quantified by using Array Vision software. The graph shown displays the averages of three independent experiments in which each transcript was represented three times on the array. The y-axis represents the intensity of the light scattering signal and the x-axis represents individual HSV-1 transcripts. Red bars represent immediate-early transcripts; early transcripts are in blue; late transcripts are in green, and LAT transcripts are in violet.

Table 2-2: Statistical analysis of HSV-1 microarray experiments

Feature Name	Class	P(T<=t critical)	
		DRB	FVP
ICP0 A	IE	3.34E-06	1.24E-05
ICP0 B	IE	8.61E-09	1.23E-08
ICP4 A	IE	1.52E-02	5.07E-03
ICP4 B	IE	2.20E-05	3.18E-05
ICP22 A	IE	6.52E-08	1.43E-08
ICP27 C	IE	4.52E-04	5.84E-08
ICP47 B	IE	9.00E-08	7.79E-09
U_L4 A	E	3.47E-08	2.10E-07
U_L6 A	E	9.21E-07	9.79E-07
U_L8 B	E	4.16E-03	1.39E-03
U_L21 B	E	4.02E-08	6.29E-08
U_L23 B	E	7.70E-04	2.09E-05
U_L29 A	E	8.00E-05	6.29E-03
U_L30 B	E	1.02E-04	6.65E-05
U_L39 C	E	4.89E-03	6.38E-09
U_L42 B	E	7.86E-09	3.06E-08
U_L50 A	E	8.49E-07	3.70E-07
U_L52 A	E	1.95E-04	7.67E-05
U_L55 A	E	2.12E-06	8.15E-09
U_L56 B	E	1.21E-05	1.87E-05
U_S2 B	E	4.57E-06	7.09E-06
U_S3 B	E	2.59E-07	3.62E-07

Feature Name	Class	P(T<=t critical)	
		DRB	FVP
U_L1 B	L	1.05E-05	1.48E-07
U_L3 A	L	5.78E-09	2.36E-08
U_L10 A	L	4.56E-05	5.22E-05
U_L13 B	L	6.65E-07	9.88E-07
U_L15 C	L	5.41E-05	5.83E-05
U_L16 B	L	8.07E-07	3.65E-06
U_L19 A	L	6.29E-07	2.73E-06
U_L22 A	L	1.37E-06	4.22E-06
U_L24 A	L	5.58E-05	5.71E-05
U_L25 A	L	6.86E-07	2.70E-06
U_L27 A	L	2.27E-07	3.35E-08
U_L31 A	L	3.52E-06	7.12E-06
U_L35 B	L	3.72E-07	3.87E-07
U_L36 A	L	6.79E-06	9.93E-06
U_L37 B	L	9.60E-05	3.15E-05
U_L38 C	L	3.57E-08	4.66E-08
U_L41 B	L	1.68E-06	3.12E-06
U_L44 A	L	9.89E-11	3.19E-09
U_L46 B	L	2.66E-08	4.64E-07
U_L48 A	L	5.66E-05	2.13E-05
U_L49 A	L	5.90E-12	7.12E-12
U_L51 A	L	2.67E-05	1.32E-05
U_S5 B	L	1.72E-08	3.42E-07
U_S8 A	L	1.03E-05	1.63E-07
ICP34.5	L	4.61E-04	4.60E-04
RLXY	L	1.14E-06	5.81E-06
LAT5 C	LAT	1.93E-01	3.01E-02
LATC	LAT	2.76E-06	5.21E-06
LATI B	LAT	4.62E-04	1.59E-04
LATX B	LAT	1.48E-04	1.13E-04
orfop D	LAT	8.43E-03	5.55E-04
RHA6	LAT	9.67E-04	2.19E-03

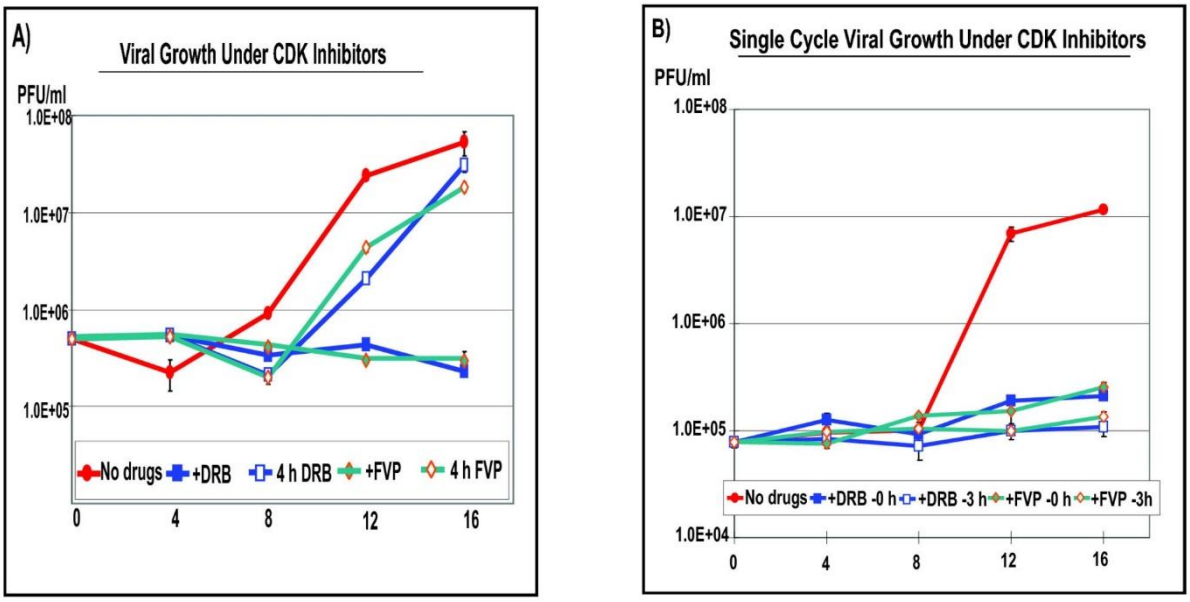

Figure 2-9: Viral replication was greatly reduced in the presence of DRB and FVP but viral replication resumed when the drugs were removed after 4 hours.

HeLa cells were infected with HSV-1 KOS at MOI of 1. **A)** Infected cells were either untreated (no drugs) or DRB (100 µM) or FVP (450 nM) were added at the time of infection for the duration of infection, or DRB and FVP were present for the first 4 hours and then were removed and cells were incubated in drug-free medium for the remainder of the time, as indicated. Samples were harvested at 0, 4, 8, 12 and 16 hours post infection and virus titers were determined by plaque assays. **B)** HeLa cells were infected with KOS at an MOI of 1 and were untreated (no drugs) or treated with DRB or FVP starting at 0 h or 3 h as indicated and the drugs were present for the duration of the experiment. Samples were harvested at 0, 4, 8, 12 and 16 hours as described in panel A. The experiments were performed in triplicate and error bars are shown.

was not detectable in the cells expressing HEXIM1-FLAG in both mock and KOS infected cells. Again, about 50 fields of cells were assessed and greater than 90% of the cells that were stained with anti-FLAG antibody displayed little to no BrU staining, whereas, cells that did not stain with anti-FLAG, indicating HEXIM1-FLAG was not being expressed, did stain with anti-BrU antibody. This indicates that over-expression of HEXIM1 inhibited the kinase activity of CDK9, which in turn resulted in an inhibition of nascent RNA synthesis in mock and KOS infected cells.

We conclude that inhibition of CDK9 by specific inhibitors DRB, FVP, DN-CDK9 or HEXIM1 results in decreased viral transcription, indicating that the S2p RNAP II is required during HSV-1 infection, just as it is required in uninfected cells.

Discussion

During HSV-1 infection there is a decrease in the S2p RNAP II at later times of infection when transcription of viral genes is very robust, and which results in part from proteasomal degradation of arrested elongating transcription complexes (37,92). It has also been reported that ICP22 contributes to the loss of the S2p RNAP II by an as yet undefined mechanism (54). Further, it has been shown that ICP22 and CDK9 are present in a complex with the CTD of RNAP II (41,42) and ICP22 and viral protein kinases U_L13 and US3 can cause a mobility shift change in the phosphorylation pattern of RNAP II resulting in an intermediately phosphorylated form detectable by CTD-specific antibody 8WG16 (41,94). This antibody does not recognize S2p because the serine at position 2 of the CTD is part of its epitope recognition, which appears to be altered or occluded upon phosphorylation (121). The actual CTD phosphorylated sites of the intermediately phosphorylated form have not been clarified. The sites of phosphorylation on the CTD by viral kinases U_L13 and U_S3 have also not been determined. It has also been proposed that the S2p RNAP II, which is required for transcription elongation, may not be required during HSV-1 infection. Here, we specifically targeted cellular kinase CDK9, which phosphorylates serine-2 and found that inhibition of

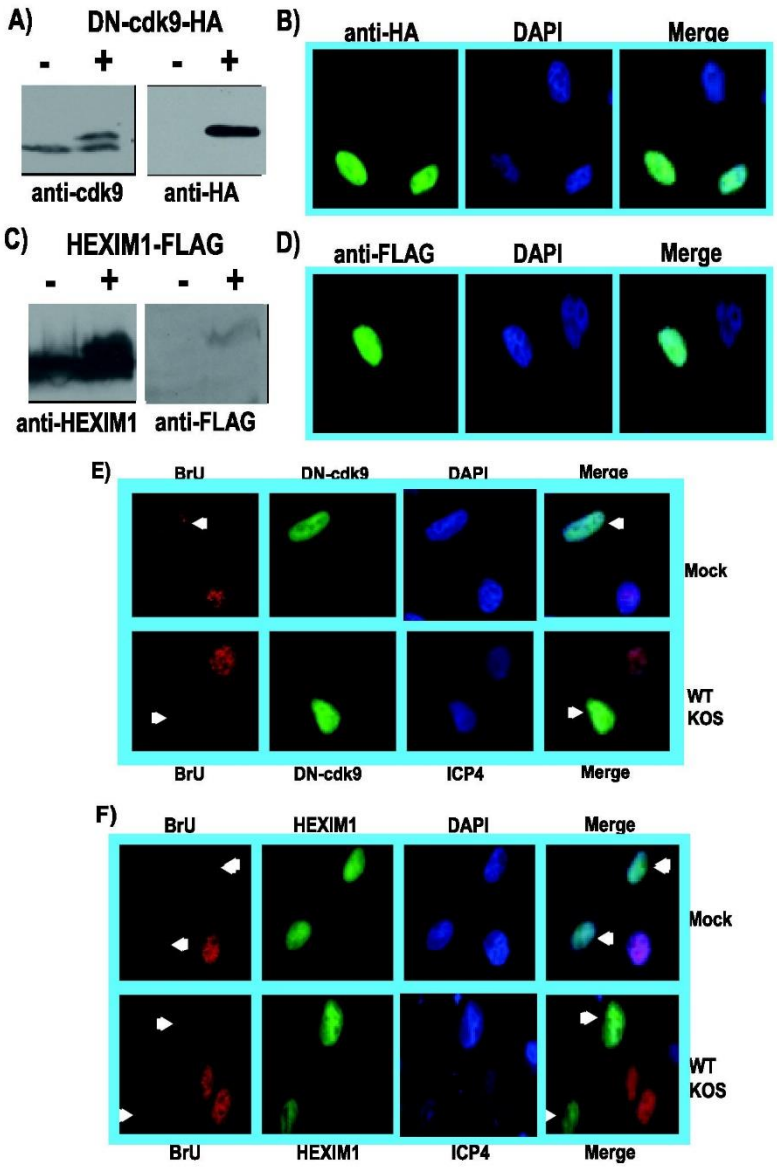

Figure 2-10: Expression of a dominant-negative kinase-dead CDK9 mutant or the CDK9 negative-regulator HEXIM1 inhibited nascent RNA synthesis.

A) HeLa cells were either transfected with empty vector or with 2 µg of DN-CDK9-HA plasmid DNA, which expresses an HA-tagged kinase-dead CDK9 dominant negative mutant. After 24 hours, whole cell lysates were prepared and fractionated by SDS-PAGE. Western blots were probed with anti-CDK9 antibody (left panel) or anti-HA antibody (right panel). **B)** HeLa cells transfected with DN-CDK9-HA were fixed 24 hours after transfection and stained with anti-HA antibody to visualize DN-CDK9-HA and DAPI to mark nuclei. **C)** HeLa cells were transfected with empty vector or with plasmid DNA expressing FLAG-tagged HEXIM1. Whole cell lysates were prepared as in panel A and Western blots were probed with anti-HEXIM1 antibody (left) and anti-FLAG (right). **D)** Indirect immunofluorescence was performed on HeLa cells transfected with HEXIM1-FLAG. Anti-FLAG antibody was used to visualize HEXIM1-FLAG and DAPI staining marked the nuclei. **E)** HeLa cells were transfected with DN-CDK9-HA for 24 hours and were subsequently mock infected or infected with HSV-1 KOS. Bromouridine (BrU) was added at 7.5 hours post infection for 30 min, at which time cells were fixed and stained with anti-BrU antibody to visualize newly transcribed RNA and

anti-HA antibody to visualize DN-CDK9-HA. DAPI staining in the upper mock panels marked nuclei and staining with anti-ICP4 antibody in the lower KOS panels was used as a marker for infection. White arrows point to cells expressing DN-CDK9-HA in the BrU and merged panels. **F)** HeLa cells transfected with HEXIM1-FLAG for 24 hours were mock infected or infected with HSV-1 KOS and BrU was added at 7.5 hours post infection for 30 min. Cells were fixed at 8 hours and stained with anti-BrU to detect newly transcribed RNA and anti-FLAG antibody to detect HEXIM1-FLAG. DAPI was used to mark nuclei in the upper mock panels and anti-ICP4 antibody was used in the lower KOS panels as a marker for infection. White arrows point to cells expressing HEXIM1-FLAG. All images were captured on a Zeiss Axiovert 200M microscope under 100X magnification.

CDK9 activity impaired HSV-1 transcription globally, indicating that S2p RNAP II is required for HSV-1 transcription as it is for cellular transcription.

The decrease in the S2p RNAP II during HSV-1 infection is unusual and is not seen with several other viruses, which have been shown to require CDK9 for their gene expression. Specifically, transcription elongation appears to be a critical regulator for viral latent infection. When the human immunodeficiency virus (HIV-1) genome is integrated, transcription through the long terminal repeat promoter is regulated at the level of transcription elongation (10,109,123). The HIV-1 transactivator Tat recruits P- TEFb to stalled RNAP II complexes that have initiated at the LTR, and phosphorylation by CDK9 results in processivity of HIV-1 transcription (109). The human T-lymphotropic virus (HTLV-1) protein Tax also complexes with P-TEFb through cyclin T1 to regulate the balance between active and inactive P-TEFb complexes (31). During Kaposi's sarcoma-associated herpesvirus (KSHV) latent infection, it has been shown that RNAP II transcription complexes are paused at the promoters of KSHV lytic genes OriLyt1, K5, K6 and K7 by the negative elongation factor NELF (164), which results in hyperphosphorylation of serine-5 and hypo-phosphorylation of serine-2. If these genes are induced to be expressed by the viral lytic activator Rta, the viral lytic phase ensues resulting in viral replication and cell death. Thus, negative regulation of transcription elongation of these lytic genes keeps KSHV in the latent state (164). Similarly, in another gamma herpesvirus, Epstein-Barr virus (EBV), the viral latent state is also maintained by NELF-DSIF (120). Specifically, the viral C promoter (Cp) that drives a viral pre-mRNA of about 120 kb, which is differentially spliced to produce several EBV products that are required for immortalization, displays high levels of promoter-proximal stalled RNAP II. P-TEFb is recruited to Cp by the cellular bromodomain protein Brd4 and inhibitor studies with DRB showed that P-TEFb is required for Cp transcription (120).

The beta herpesvirus, human cytomegalovirus (HCMV) recruits CDK9 to viral nuclear replication compartments during lytic infection and this recruitment results in hyperphosphorylation of RNAP II CTD

(48,79,80,162). HCMV proteins IE2 86 (79) and U_L69 (48) have been shown to be required for the recruitment of cyclin T1 and CDK9 to viral replication compartments. Thus, CDK9 appears to be important for HCMV lytic replication.

The studies that we have described here would also indicate that CDK9 is important for HSV-1 replication. One consequence of highly active HSV-1 transcription may be an increasing number of arrested transcription elongation complexes in crowded areas of the genome and clearing these by proteasomal degradation results in lower levels of S2p RNAP II from the arrested elongating complexes. How ICP22 causes a decrease in S2p RNAP II levels is still a bit of an enigma. Durand and Roizman (41,42) showed that CDK9 interacts with ICP22. They further showed that CDK9 and ICP22 colocalize with RNAP II. Inhibition of CDK9 with 50 μM DRB and with CDK9 siRNA resulted in decreased expression of several HSV-1 late genes that were previously shown to be regulated by ICP22 (64). In a recent study using an *in vivo* transient expression reporter system (64), ICP22 was coimmunoprecipitated with P-TEFb in accord with the results of Durand and Roizman. Further using ChIP assays, Guo *et al*. showed that ICP22 blocked the recruitment of P-TEFb to viral promoters, which inhibited transcription of these promoters. In this system, VP16 recruited P-TEFb to promoters and counteracted transcriptional repression by ICP22. Because this was a transient expression system, it is not clear if ICP22 would similarly repress viral promoters by preventing P-TEFb recruitment during viral infection. Another possibility might be that ICP22, like HIV Tat recruits inactive P-TEFb in complex with 7SK snRNA and HEXIM1 to viral promoters and another factor, perhaps VP16, can cause its disassociation into active P-TEFb. Thus, HSV-1 might have a complex regulatory mechanism to insure that transcription of early and late viral genes can occur during very active times after infection when both DNA replication and transcription are proceeding robustly. It will be necessary to parse and define many details of this regulation during HSV-1 infection and to determine how ICP22 affects CDK9 activity, all of which are beyond the scope of this study. In conclusion, we showed here that CDK9 activity is required for HSV-1 transcription and replication.

Materials and Methods

Cells, viral strains and plasmids

HeLa cells were grown on minimal essential medium (MEM) containing 10% newborn calf serum. Rabbit skin fibroblasts (RSF) and Vero cells were grown on minimal essential medium supplemented with 8% fetal calf serum and 4% donor calf serum. HSV-1 wild-type (WT) strain KOS was described previously (151). ICP27 null mutant 27-GFP encodes green fluorescent protein (GFP) in place of ICP27 coding sequences and has been described previously (153,157). Mammalian expression vector pRc/CMV-dnCDK9-HA encoding a kinase- dead CDK9 was generously provided by Dr. Xavier Graña (139). Plasmid pCMV2-FLAG-HEXIM1 was a generous gift from Dr. Qiang Zhou and it has been described previously (118).

Virus infection and transfection

HeLa cells were infected with WT HSV-1 KOS or 27-GFP as indicated at a multiplicity of infection (MOI) of 10 and were incubated at 37°C for the times indicated in the figure legends. For transfection/ infection experiments, plasmid DNA was transfected into cells using Lipofectamine 2000 reagent (Invitrogen) according to the manufacturer's protocol. Cells were infected 24 h after transfection.

Cell viability assay and single cycle viral growth curve analysis

HeLa cells seeded on 6-well tissue culture dishes were either mock infected or infected with HSV-1 KOS at an MOI of 1.0 for up to 16 hours as indicated in the figure legends. Cells were either incubated in MEM or MEM containing 100 µM 5.6- dichloro-1-β-D-ribofuranosyle-1H-benzimidazole (DRB) or 450 nM flavopiridol (FVP). For cell viability assays, cells were harvested at 4 h intervals and stained with the vital dye trypan blue solution (Sigma), followed by cell counting using a hemocytometer. For single-cycle viral growth assays, cells were infected with HSV-1 KOS at an MOI of 1.0 in the presence or absence of DRB or FVP as indicated and were harvested at 4, 8, 12, and 16 hours post infection. Virus titers were measured by plaque assays on Vero cells. The experiments were performed in triplicate.

Western blot analysis

HeLa cells were infected or transfected and then infected as indicated in the figure legends. At the times indicated, cells were washed with cold phosphate-buffered saline (PBS) and harvested in 2X ESS loading buffer (20 mM Tris, 5 mM EDTA, 4% SDS, 10% 2-mercaptoethanol, 20% glycerol), as described previously. Cell lysates were fractionated on 5-15% gradient sodium dodecyl sulfate polyacrylamide gels (SDS-PAGE) and transferred to nitrocellulose membranes. Membranes were probed as described previously (153,154). Primary antibodies used for immuno-blotting were as follows: rabbit polyclonal anti-RPB1 N20 (Santa Cruz Biotechnology, Inc.) at 1:1,000; mouse monoclonal anti-RNAP II CTD phosphoserine-2 H5 (Abcam) at 1:2,500; mouse monoclonal anti-RNAP II CTD phosphoserine-5 H14 (Abcam) at 1:2,500; rabbit monoclonal anti-CDK9 C12F7 (Cell Signaling Technology) at 1:2,000; rabbit polyclonal anti-HEXIM1 ChIP grade (Abcam) at 1:1,000; mouse monoclonal anti-HA epitope HA-7 (Sigma-Aldrich) at 1:250; mouse monoclonal anti-FLAG epitope M2 (Sigma- Aldrich) at 1:1,000; rabbit polyclonal anti-Lamin A/C (Cell Signaling Technology) at 1:2,000; rabbit monoclonal anti-YY1 (Abcam) at 1:500; mouse monoclonal anti-ICP27 (P1119; Virusys) at 1:5,000, mouse monoclonal anti-ICP4 (P1101; Virusys) at 1:5,000, mouse monoclonal anti-glycoprotein D (gD) (P1103;Virusys) at 1:5,000 and mouse monoclonal anti-glycoprotein B (gB) (P1123; Virusys) at 1:5,000.

Immunofluorescence microscopy

RSF cells grown on glass cover slips were infected or transfected as described in the figure legends. Cells were either untreated or were incubated with MEM supplemented with DRB or FVP as indicated in the figure legends. Cells were fixed with 3.7% formaldehyde at the times indicated and immunofluorescent staining was performed as described previously (27,37,92). Cells were stained with anti-ICP4 (P1101) at 1:500; anti-ICP27 (P1119) at 1:500; anti-RNAP II antibody ARNA3 (Research Diagnostics) at 1:50; anti-bromodeoxyuridine Ab-3 (Calbiochem) at 1:100; anti-HA (Sigma) at 1:500 and anti-FLAG (Sigma) at 1:500.

Bromouridine labeling and in situ hybridization

To label nascent, newly synthesized RNA, 4 mM 5- Bromouridine (BrU-Sigma-Aldrich) was added to the culture medium for 30 min at 37°C before fixation of the cells, which were subsequently stained with anti-BrU antibody (Ab3; Calbiochem). For poly(A)+ RNA hybridization, cells grown on coverslips in 24 well dishes were infected as described in the figure legends and were fixed with 3.7% formaldehyde and then overlaid with 70% ethanol at 4°C. Cells were rehydrated for 5 min at room temperature in 15% dimethylformamide in 2X SSC (1X SSC is 0.15 M NaCl plus 0.015 M sodium citrate) and then overlaid with 40 µl hybridization solution (15% formamide, 10% dextran sulfate, 40 µg yeast tRNA, 0.02% bovine serum albumin, 40 ng biotinylated oligo[dT_{25}] (Promega), RNAsin, 0.5 M dithiothreitol, 2X SSC) for 2 h at 37°C. Cells were washed twice with wash solution (15% formamide, 2X SSC and 0.1% NP-40) for 30 min at 37°C. Images were captured using a Zeiss Axiovert 200M microscope at a magnification of 100X.

Microarray analysis

HeLa cell monolayers were infected with WT HSV-1 KOS at an MOI of 10 for 8 hours. At 3 hour post infection, cell culture medium was replaced with medium without inhibitors or medium containing 100 µM DRB or 450 nM FVP and incubation was continued for an additional 5 hours. Total RNA was isolated from whole cell lysates with TrIzol reagent (Invitrogen). Poly(A)+ RNA was selected using an Oligotex mRNA mini kit (QIAGEN) according to the manufacturer's protocol. Synthesis of cDNA and subsequent hybridization to custom arrays of HSV-1 transcript-specific probes was performed as previously described (76,156). Statistical analysis was performed using a one-tailed t-test assuming unequal variance, comparing drug treated samples to corresponding control samples, with a 97.5% confidence limit.

Chapter 3
Assessing RNAP II Occupancy on the HSV-1 Genome by Chromatin Immunoprecipitation (ChIP)

Summary

Herpes simplex virus type 1 (HSV-1) genome is compact and harbors multiple nested open reading frames (ORFs) that are expressed in a well-defined temporal cascade. The DNA virus hijacks cellular RNA polymerase II (RNAP II) early in infection for viral transcription, but as we have previously shown, at late time in infection, elongating RNAP II was found to be degraded by the proteasome pathway. We proposed that the compact viral genome might be over burdened by transcribing RNAP II at late times in infection and leading to colliding RNAP II complexes that might eventually become arrested. Here we attempted to substantiate this collision model by examining the RNAP II occupancy on the viral genome during lytic HSV-1 infection. Anti-RNAP II chromatin immunoprecipitation quantitative PCR (ChIP-qPCR) analysis was performed on two HSV-1 gene clusters that were predicted to differ in their frequency of potentially colliding RNAP II complexes. Moderate IP efficiencies were demonstrated for the anti-RNAP II antibodies used but three of the four antibodies used did not yield reliable above-background ChIP signals . The Early gene cluster containing the ORFs for U_L39 and U_L40 produced a ChIP profile that matched well with their know expression patterns, but the Late gene cluster containing the ORFs for U_L44 and U_L45 did not yield comparable results. At this time, we are unable to demonstrate trends in RNAP II occupancy on the HVS-1 genome and expansion of coverage is required.

Introduction

Herpes simplex virus type 1 (HSV-1) is an enveloped DNA virus that replicates inside the nucleus of an infected host cell. Its double-stranded DNA genome is approximately 152 kilo base-pairs in length and encodes 94 open reading frames (ORFs), of which 84 are unique (136). During lytic infection of host cells, viral gene expression is divided into three distinct temporarily regulated phases: immediate-early (IE), early (E), and late (L). With the help of viral tegument proteins such as VP 16 that are packaged with the virion, IE gene expression is activated soon after viral genome entry into the nucleus of the infected cell. The IE gene products are responsible for regulating viral gene expression, and sufficient build-up of IE gene products, usually at about 3 hours post infection, stimulates E gene expression. E gene products are involved in viral DNA replication and viral DNA replication promotes L gene expression of viral structural and tegument proteins, starting at about 5 hours post infection. Once activated, each gene class continues to be expressed until packaging and egress are complete, at approximately 16 hours post infection (reviewed in (170)).

Within the HSV-1 genome, many of ORFs are nested within one another and often share either transcriptional start sites but different polyadenylation sites or vice versa. Transcription occurs on both strands of the viral genome. With the exception of U_L10, U_L22, and U_L23, nested ORFs tend to be transcribed in the same direction. Adjacent ORF clusters often are transcribed from the anti-sense strand (127). In the case of U_L10, U_L22, and U_L23 ORFs, their anti-sense nature with adjacent ORFs interferes with the production of transcripts to which they can hybridize. These anti-sense ORFs are transcribed with different kinetics compared to neighboring ORFs and the anti-sense hybridization mechanism appears to delay L gene expression until E gene expression tapers off. The U_L1, U_L23 U_L24 ORFs contain a weak and a strong polyadenylation signal, and two transcripts variants are made from the same coding sequence (34,35,150). The shorter variants are more abundant early in infection while the longer variants dominate at late time in infection. This compact genome arrangement potentially could result in collisions of

transcribing RNAP II, either within the nested ORFs, or near the polyadenylation sites of opposing ORFs. At late times in infection, nearly all of the viral ORFs are being transcribed at high levels, crowding the genome with RNAP II complexes. In addition, viral DNA synthesis on viral genomes ensues about 4-5 hours after infection, further increasing the number of complexes that are potentially on the viral genome. The high occupancy of transcription/replication complexes could result in these complexes becoming arrested and unable to complete their tasks. Indeed, it has been demonstrated that at late times in HSV-1 infection, elongating RNAP II complexes were ubiquitinated and degraded by the proteasome (37,54). Inhibition of transcription by actinomycin D prevented degradation of transcribing RNAP II, adding support to the collision model. Lastly, though inhibition of proteasome degradation did keep levels of elongating RNAP II in HSV-1 infected cells similar to uninfected counterparts, it appeared to negatively impact viral yield (37). These findings suggested that on congested regions of the HSV-1 genome RNAP II might become stalled or arrested and as a response, stalled RNAP II complexes could be degraded by the proteasome.

Currently there is no direct evidence supporting the collision model in which transcribing RNAP II becomes arrested on the HSV-1 genome. We investigated RNAP II occupancy during HSV-1 lytic infection of two separate regions of the viral genome with overlapping transcripts of different kinetic classes using chromatin immunoprecipitation (ChIP) quantitative polymerase chain reaction (qPCR) analysis. While there was an average 11-fold increase of viral DNA in 10 hours, poor signal-to-noise ratios in the ChIP analysis as well as insufficient genome coverage did not allow accurate estimates of RNAP II occupancy in these experiments.

Results

Chromatin Immunoprecipitation (ChIP) optimization

One of the critical factors for successful ChIP analysis is uniform DNA fragmentation. We tested a Bioruptor, a water bath type sonicator, and a Misonix Microson XL sonicator, a traditional probe type sonicator for their ability to achieve consistent 200-500 nucleotide DNA fragmentation. Initial success with

the Bioruptor was achieved yielding uniform fragmentation in the desired size range with twenty 30-second pulses on the highest output setting. Subsequent tests failed to produce DNA fragment sizes in this range despite no change in protocol (Figure 3-1A, B). The Misonix Microson XL was initially less efficient and there was a persistent presence of high molecular weight DNA in the preparations (Figure 3-1C, D). We were able to achieve uniform DNA fragmentation when there was a switch from wet ice to wet ice augmented with 20% volume ethanol during sonication using the Misonix Microson.

It has been shown that RNAP II levels decreases at late time in HSV-1 infection due to proteasome degradation of S2p RNAP II (37,54). To ensure that we were able to immunoprecipitate (IP) RNAP II efficiently in our experiment, several RNAP II antibodies were tested that recognize either all forms or specific phospho-forms of RNAP II (Table 3-1). Initially, N20x and 4H8, two pan-RNAP II antibodies were tested and we were able to detect both phosphorylated and unphosphorylated RNAP II in the input fractions when the cells were crosslinked prior to IP, however, we were unable to detect RNAP II in the eluted fraction, in uninfected and infected cells. Figure 3-2 shows representative Western blots of ChIP experiments using N20x and 4H8 antibodies. Thus, the ChIP protocol was too inefficient.

To enhance the efficiency of the ChIP experiment, a two-step crosslinking ChIP protocol that was developed to detect NF-κB inducible genes by Nowak *et. al* (117) was used. In addition to the traditional formaldehyde crosslinking step, the authors introduced a disuccinididyl glutarate (DSG) crosslinking step to improve protein-protein crosslinking. This enhanced protein-protein crosslinking should allow the use of antibodies that recognize other subunits of the RNAP II holoenzyme and not be restricted to antibodies specific to RPB1, the largest subunit that physically makes contact with the DNA template. To this end, we selected the 1Y27 antibody, a mouse monoclonal antibody that recognizes RPB3, the third largest subunit of RNAP II. In the test ChIP experiments, we found that among the pan-RNAP II antibodies, only 4H8 and 1Y27 showed enrichment

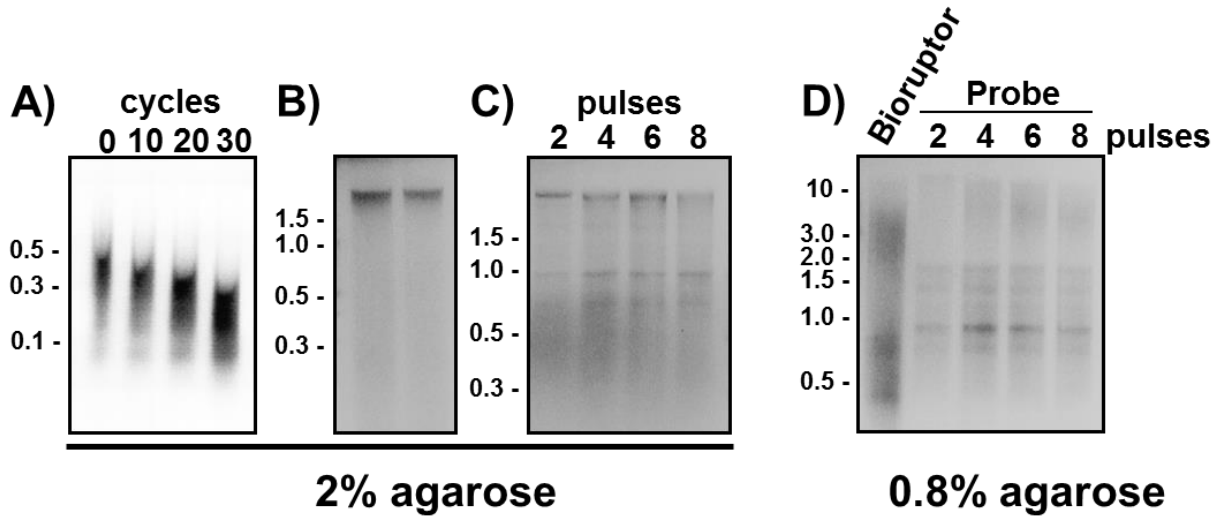

Figure 3-1: Optimizing sonication homogenization for ChIP.
HeLa cells were crosslinked in 10% formaldehyde and harvested in PBS. Cells were then pelleted and re-suspended in ChIP sonication buffer and sonicated using **A**, **B)** a Bioruptor set to 30-second cycles on/off cycle on its high setting, or **C**, **D)** a conventional probe sonicator set to pulse 15 seconds at 10 watt output over ice. Samples were uncrosslinked and Proteinase-K digested prior to DNA extraction by phenol-chloroform. Samples were fractionated on either **A-C)** 2% agarose or **D)** 0.8% agarose gels and visualized with ethidium bromide.

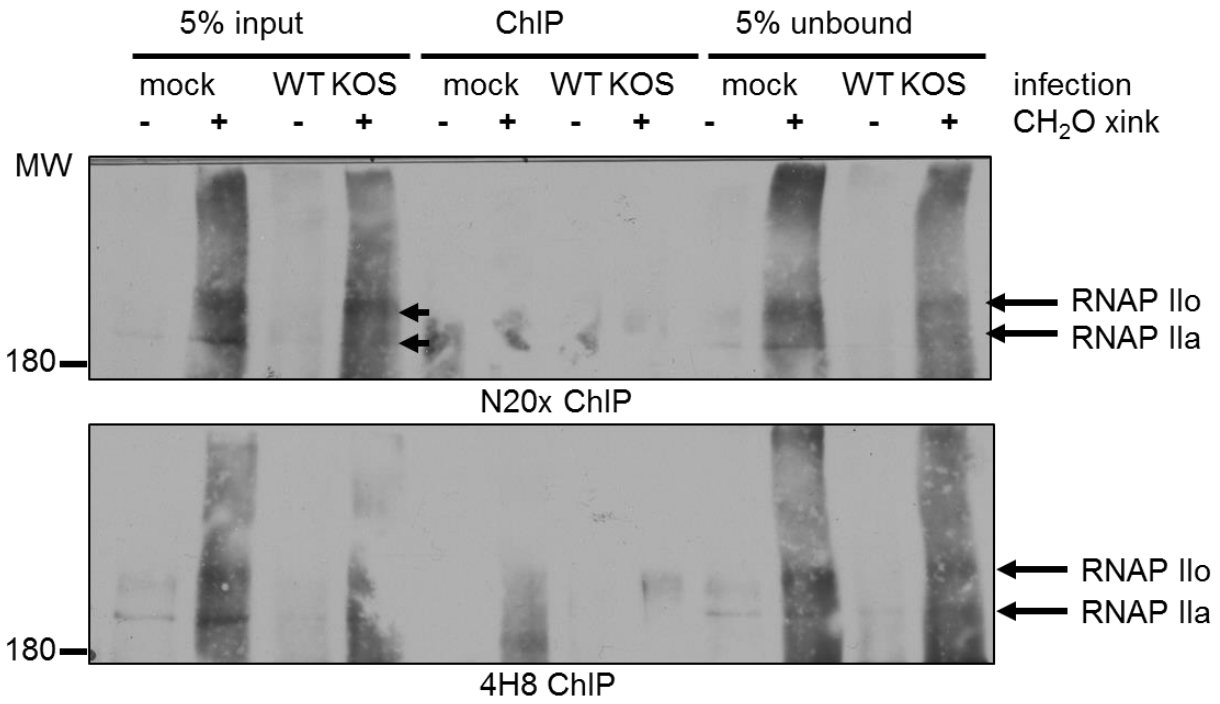

Figure 3-2: Formaldehyde crosslinking was not sufficient for chromatin immunoprecipitation (ChIP). HeLa cells were mock infected or infected with WT KOS HSV-1 at MOI of 10. At 8 hours post infection, cells were crosslinked in 10% formaldehyde (CH2O) and homogenized by sonication. 5% of each sample was collected as the input fraction. Approximately 80% of each cell lysate sample was incubated with Dynabeads conjugated with either N20x or 4H8 antibodies overnight at 4°C to immunoprecipitate RNAP II. 5% volume of each immunoprecipitated lysate sample was collected prior to washes and elution. The input, unbound and elution samples were fractionated on 5-15% gradient SDS-polyacrylamide gels and probed with the cognate antibody in Western blot analysis.

over isotype controls (Figure 3-2A – C). The positive enrichment in 1Y27 testing suggested that the two-step crosslinking protocol was working and we were able to immunoprecipitate the RNAP II holoenzyme with this antibody. The 4H8 ChIP Western blot showed a strong band above the 250 kDa marker, suggesting that it was actively transcribing RNAP that it was captured, and not the unphosphorylated free RNAP II species. Among the phospho-form-specific antibodies that were tested, H5 and H14 both showed enrichment over the isotypic mouse IgM controls, albeit not as clean as the pan-RNAP II antibodies (Figure 3-2D – E). These antibodies are mouse IgM and require the use of rabbit anti-mouse IgM linker antibodies for efficient binding to the Protein G moiety on the Dynabeads used in the ChIP reactions. A higher background was observed in the mouse IgM controls than in the mouse or rabbit IgG controls, suggesting that perhaps the linker antibody contributed to more non-specific binding. To test the efficiency of the ChIP protocol, we also performed Western blot analysis on three independent samples of WT HSV-1 infected cells and assessed the percentage of the RNAP II that was pulled down (Figure 3-3). The densitometry analysis showed an average of 15.3% and 21.6% pull-down efficiency for the 4H8 and H14 antibody respectively. As these samples were generated from cells that were infected with WT HSV-1 for 8 hours, a time when RNAP II levels are decreasing, we were encouraged to able to achieve over 15% pull-down efficiency. Based on these test results, the ChIP experiments were continued with 4H8, 1Y27, H5, and H14 antibodies.

ChIP analysis of two gene clusters that are predicted to be high traffic regions at different times in HSV-1 infection

The HSV-1 genome encodes approximately 80 open reading frames (ORFs) in 152 kb. Several parts of the viral genome contain nested ORFs and/or opposing ORFs and many of these ORFs are expressed at the same time during lytic infection. The collision model proposed by Dai-Ju *et al*. suggests that when viral transcription is high, the regions of the HSV-1 genome with several actively transcribing RNAP II complexes

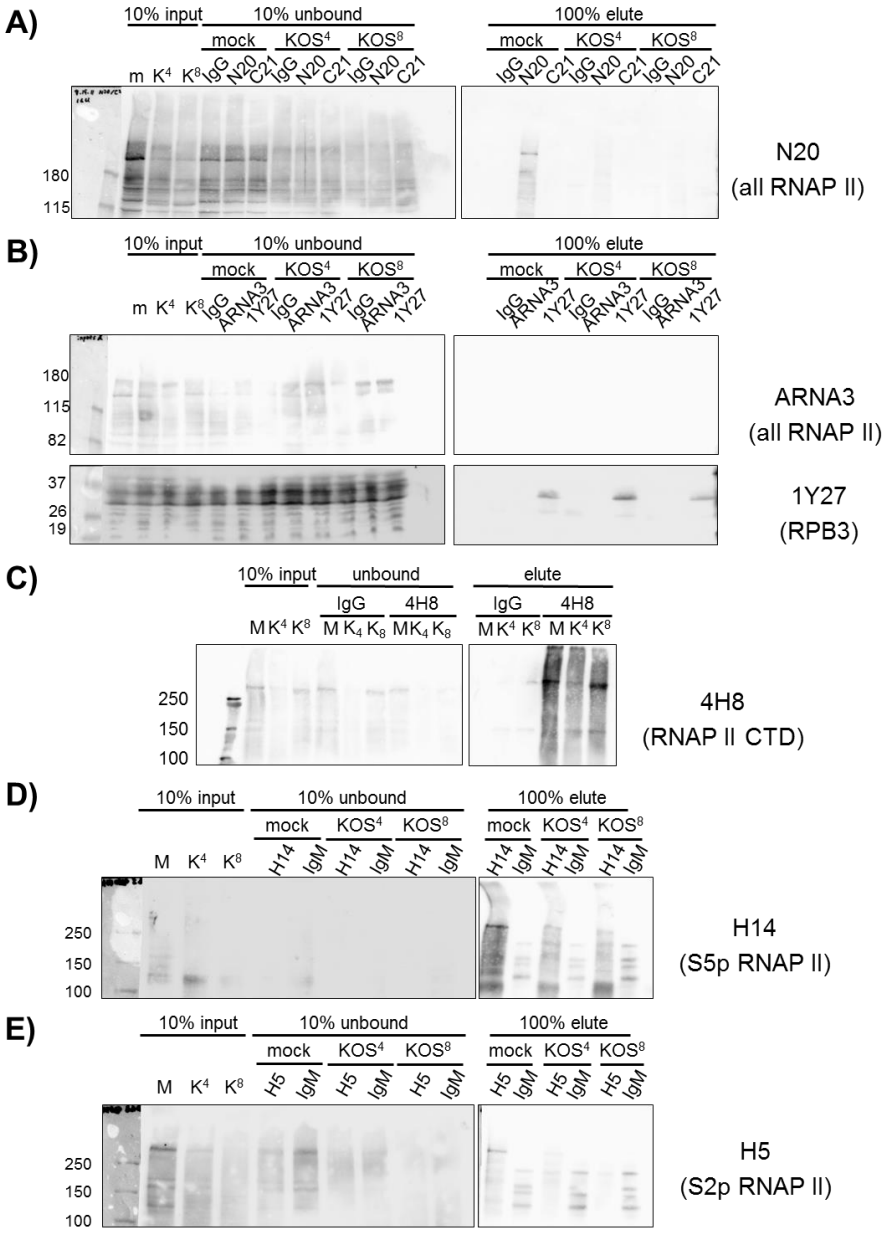

Figure 3-3: ChIP antibody testing.

HeLa cells were mock infected or infected with WT KOS HSV-1 at MOI of 10. Cells were crosslinked first in 2 mM disuccinimidyl glutarate (DSG), then in 1% (v/v) formaldehyde at 4 or 8 hours post infection. Cells were homogenized by sonication and 10% of each cell lysate sample was collected as the input fraction. Approximatedly 25% of each cell lysate sample was incubated overnight at 4°C with Dnyabeads conjugated with anti-RNAP II antibodies as indicated in the figure to immunoprecipitate RNAP II. 10% volume of each immunoprecipitated sample was collected as the unbound fraction prior to washes and elution. The input, unbound, and elution samples were fractionated on 5-15% gradient SDS-polyacrylamide gels and probed with N20, ARNA3, 1Y27, H14, H5, and 4H8 in Western blot analysis as indicated. Normal rabbit IgG instead of N20 and C21 antibodies, normal mouse IgG instead of ARNA3, 1Y27, and 4H8 antibodies, and normal mouse IgM instead of H14 and H5 antibodies conjugated to Dyanbead served as isotype controls.

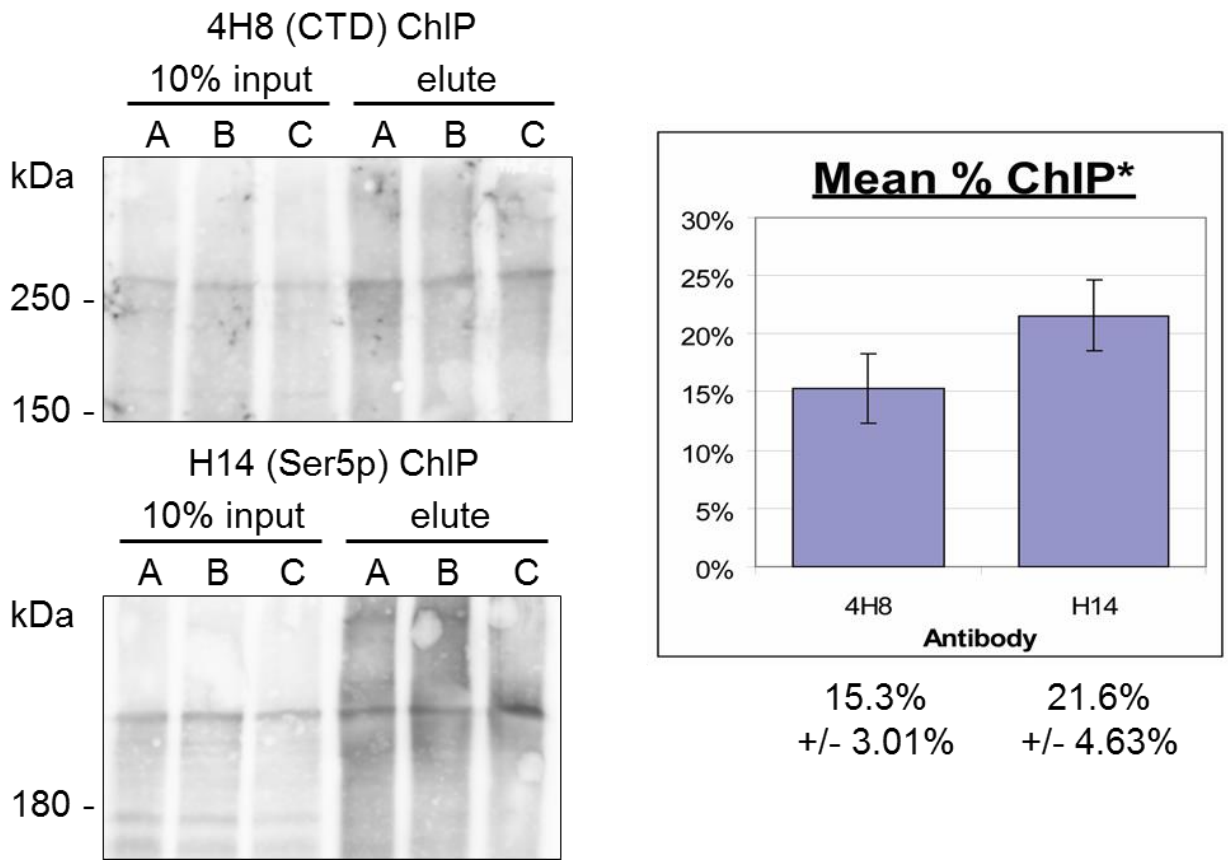

Figure 3-4: Quantification of ChIP efficiency.

HeLa cells were infected with WT KOS HSV-1 at MOI of 10 for 8 hours and processed for ChIP independently to quantify IP reaction efficiencies of the 4H8 and H14 antibodies. The graph shows mean % ChIP efficiency based on the mean intensity of the respective input sample; error bars represent standard deviations.

may have collisions or piling up of complexes and could lead to arrested RNAP II in infected cells (37). Arrested RNAP II is in turn recognized by the host cell machinery, perhaps the transcription-coupled nucleotide excision repair (TC-NER) pathway, and targeted for proteasome degradation (52,66,88). The model predicts that regions of the genome that harbor more nested ORFs would be occupied with more transcriptional complexes and therefore be more prone to collisions than regions of the genome that do not harbor nested ORFs that are expressed at the same time. To test the collision model, we selected an Early gene (U_L39/40) that is predicted to be a low traffic region and a Late gene (U_L44) that is predicted to be a high traffic region at the peak of expression and examined RNAP II occupancy in these regions by ChIP analysis.

U_L39/40 encodes the viral ribonucleotide reductase subunits 1 and 2. As Early proteins involved in viral DNA replication, their expression begins at approximately 3 hours post-infection and peaks at about 5 or 6 hours post-infection. While U_L39/40 are nested ORFs, the flanking U_L38 and U_L41 are both Late genes and are not expected to be highly transcribed at the peak of UL39/40 expression. The collision model predicts this region to have relatively low traffic. We designed quantitative polymerase chain reaction (qPCR) primer pairs to detect the promoter, proximal coding sequence (CDS), distal CDS, and poly-A signal segments of U_L39/40 ORFs (Figure 3-4A) and performed ChIP analysis. To normalize ChIP signals across the time points, we measured viral genome copy number using the same primer pairs and found that the viral genome copy number increased on average 11 fold over the course of a 10-hour infection (Figure 3-4B). All four primer pairs showed similar progression over the course of the infection and significantly higher than the background amplification levels detected in mock infected cell samples, therefore validating one another in their efficacy.

To examine total RNAP II occupancy in the U_L39/40 ORFs, we used the 4H8 and 1Y27 antibodies that recognize all forms of RNAP II. Mouse IgG served as isotypic control in these experiments. Strong ChIP

A)

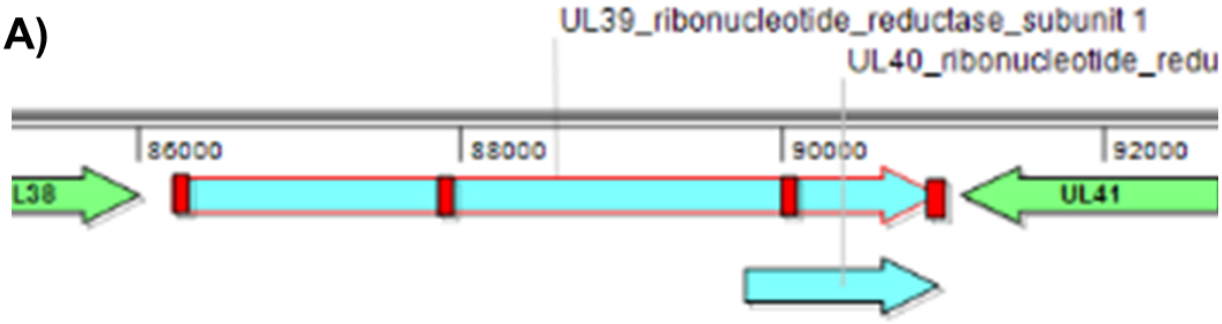
UL39_ribonucleotide_reductase_subunit 1
UL40_ribonucleotide_redu
86000
88000
90000
92000
L38
UL41

B)

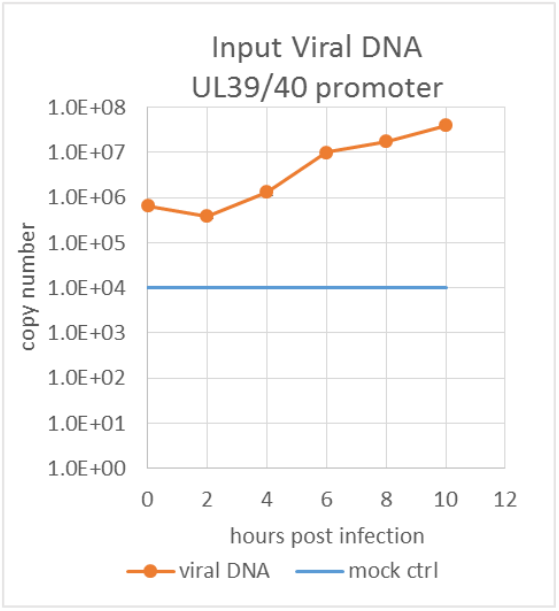
Input Viral DNA
UL39/40 promoter
copy number
1.0E+08
1.0E+07
1.0E+06
1.0E+05
1.0E+04
1.0E+03
1.0E+02
1.0E+01
1.0E+00
0 2 4 6 8 10 12
hours post infection
viral DNA
mock ctrl

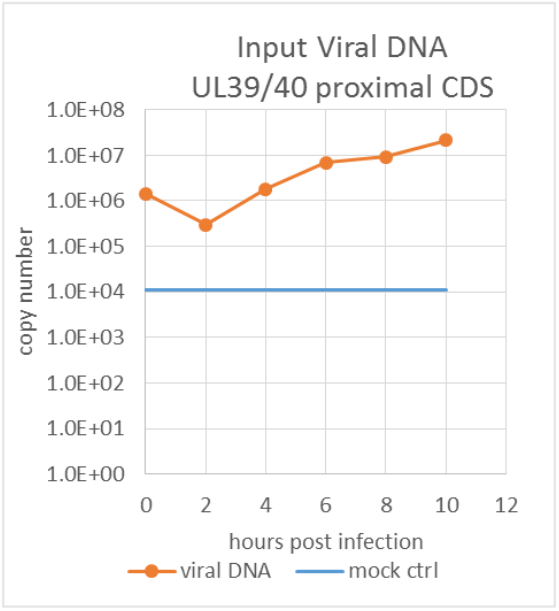
Input Viral DNA
UL39/40 proximal CDS
copy number
1.0E+08
1.0E+07
1.0E+06
1.0E+05
1.0E+04
1.0E+03
1.0E+02
1.0E+01
1.0E+00
0 2 4 6 8 10 12
hours post infection
viral DNA
mock ctrl

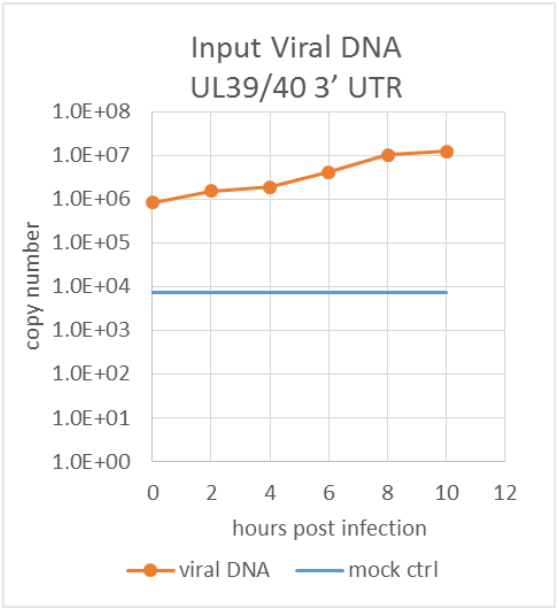
Input Viral DNA
UL39/40 3' UTR
copy number
1.0E+08
1.0E+07
1.0E+06
1.0E+05
1.0E+04
1.0E+03
1.0E+02
1.0E+01
1.0E+00
0 2 4 6 8 10 12
hours post infection
viral DNA
mock ctrl

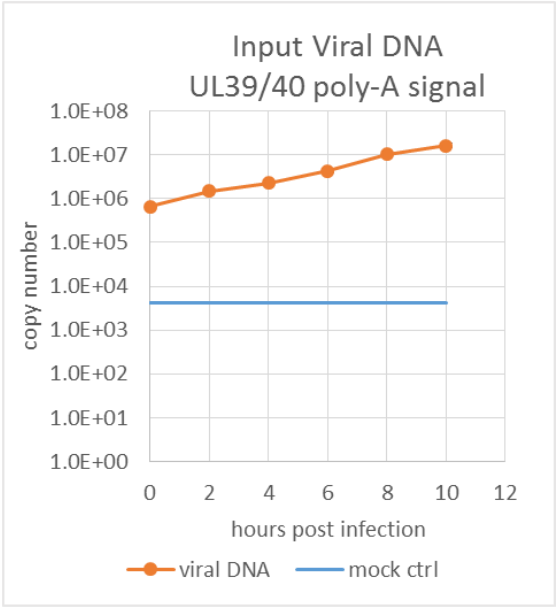
Input Viral DNA
UL39/40 poly-A signal
copy number
1.0E+08
1.0E+07
1.0E+06
1.0E+05
1.0E+04
1.0E+03
1.0E+02
1.0E+01
1.0E+00
0 2 4 6 8 10 12
hours post infection
viral DNA
mock ctrl

C)

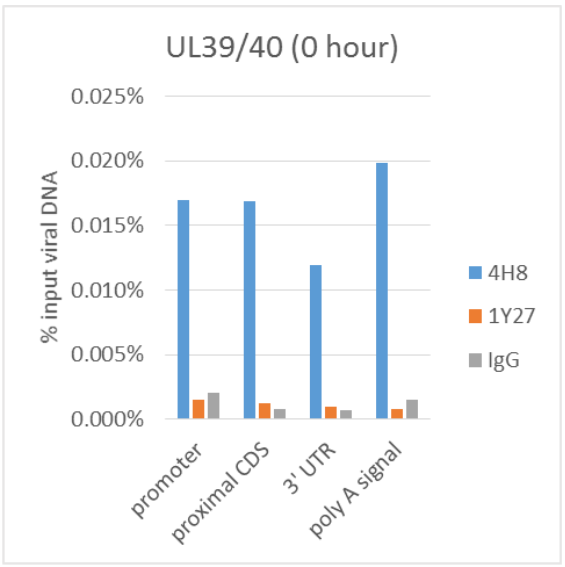
UL39/40 (0 hour)
% input viral DNA
0.025%
0.020%
0.015%
0.010%
0.005%
0.000%
promoter
proximal CDS
3' UTR
poly A signal
4H8
1Y27
IgG

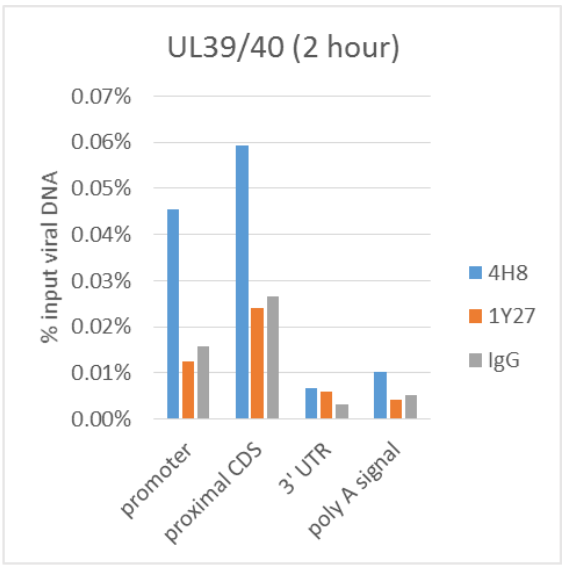
UL39/40 (2 hour)
% input viral DNA
0.07%
0.06%
0.05%
0.04%
0.03%
0.02%
0.01%
0.00%
promoter
proximal CDS
3' UTR
poly A signal
4H8
1Y27
IgG

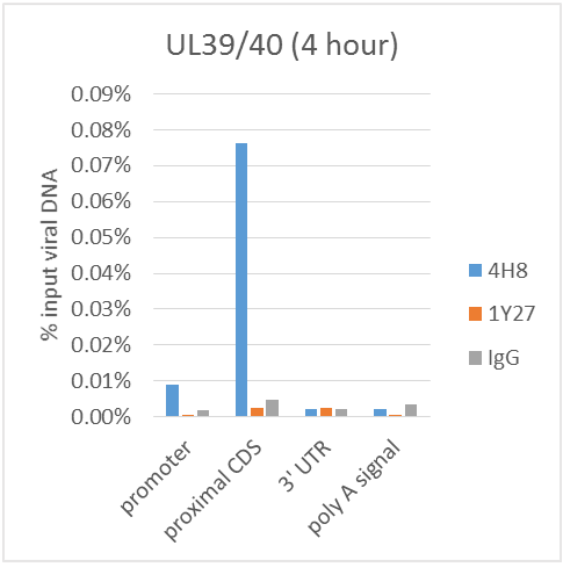
UL39/40 (4 hour)
% input viral DNA
0.09%
0.08%
0.07%
0.06%
0.05%
0.04%
0.03%
0.02%
0.01%
0.00%
promoter
proximal CDS
3' UTR
poly A signal
4H8
1Y27
IgG

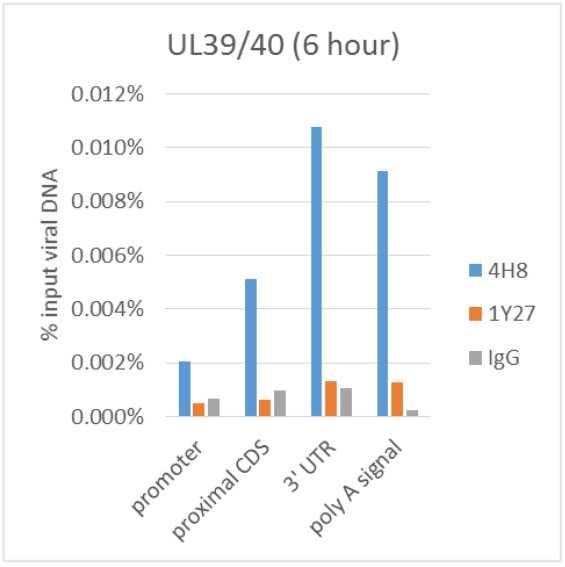
UL39/40 (6 hour)
% input viral DNA
0.012%
0.010%
0.008%
0.006%
0.004%
0.002%
0.000%
promoter
proximal CDS
3' UTR
poly A signal
4H8
1Y27
IgG

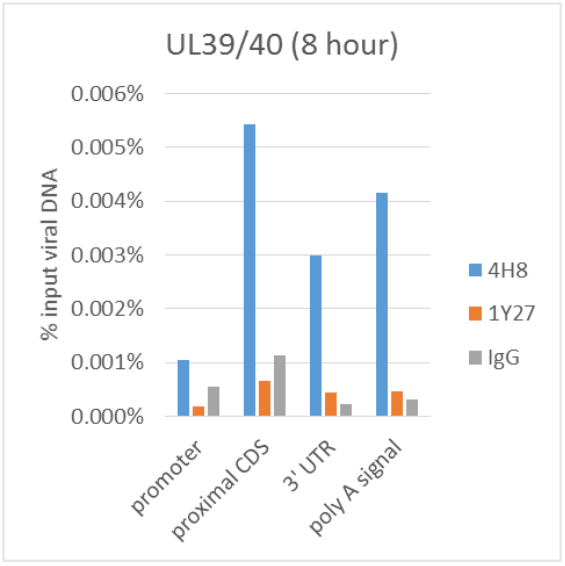
UL39/40 (8 hour)
% input viral DNA
0.006%
0.005%
0.004%
0.003%
0.002%
0.001%
0.000%
promoter
proximal CDS
3' UTR
poly A signal
4H8
1Y27
IgG

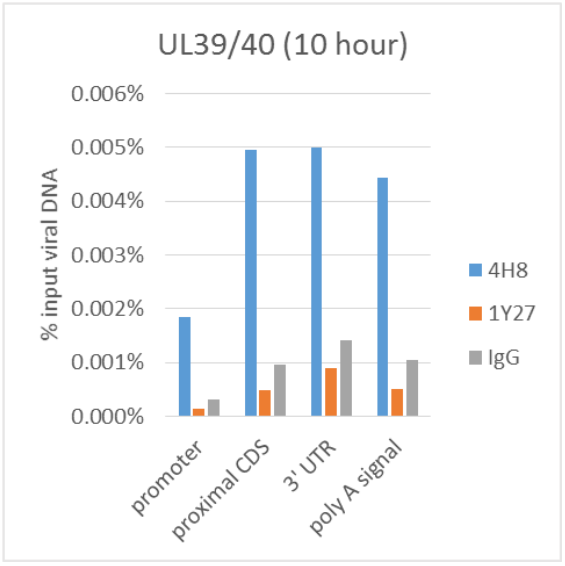
UL39/40 (10 hour)
% input viral DNA
0.006%
0.005%
0.004%
0.003%
0.002%
0.001%
0.000%
promoter
proximal CDS
3' UTR
poly A signal
4H8
1Y27
IgG

D)

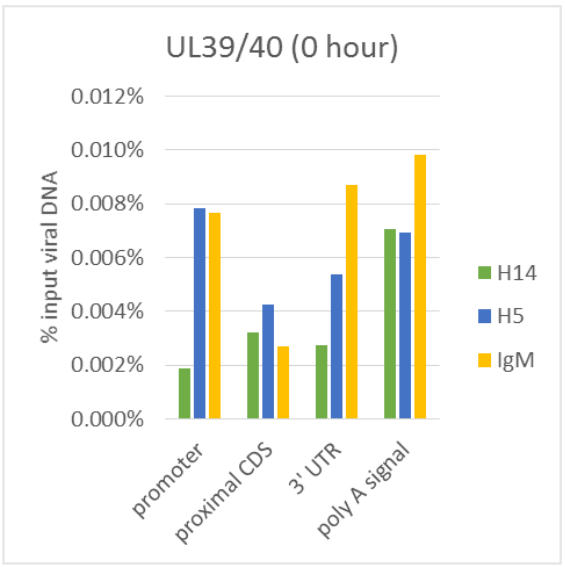
UL39/40 (0 hour)
% input viral DNA
0.012%
0.010%
0.008%
0.006%
0.004%
0.002%
0.000%
promoter
proximal CDS
3' UTR
poly A signal
H14
H5
IgM

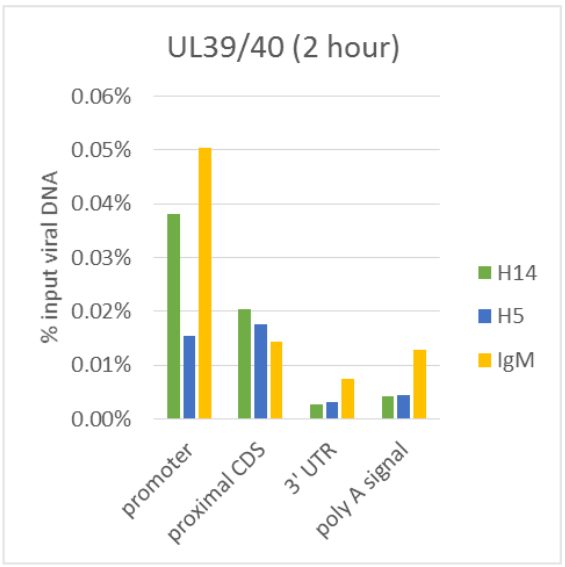
UL39/40 (2 hour)
% input viral DNA
0.06%
0.05%
0.04%
0.03%
0.02%
0.01%
0.00%
promoter
proximal CDS
3' UTR
poly A signal
H14
H5
IgM

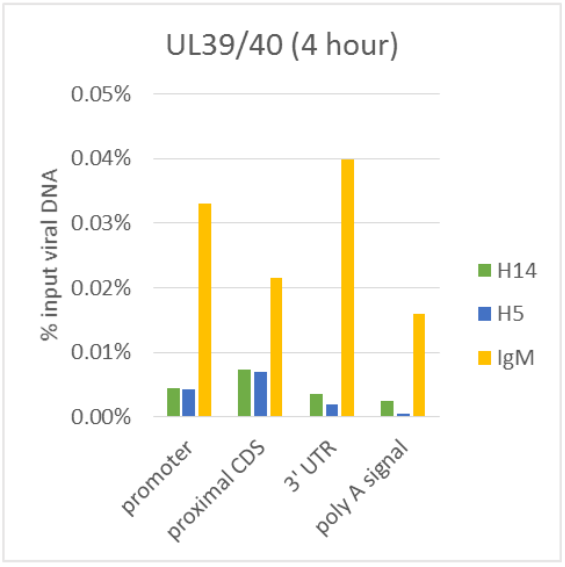
UL39/40 (4 hour)
% input viral DNA
0.05%
0.04%
0.03%
0.02%
0.01%
0.00%
promoter
proximal CDS
3' UTR
poly A signal
H14
H5
IgM

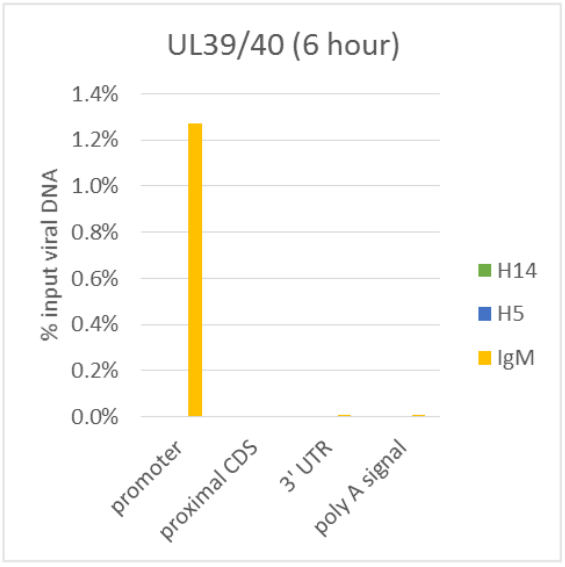
UL39/40 (6 hour)
% input viral DNA
1.4%
1.2%
1.0%
0.8%
0.6%
0.4%
0.2%
0.0%
promoter
proximal CDS
3' UTR
poly A signal
H14
H5
IgM

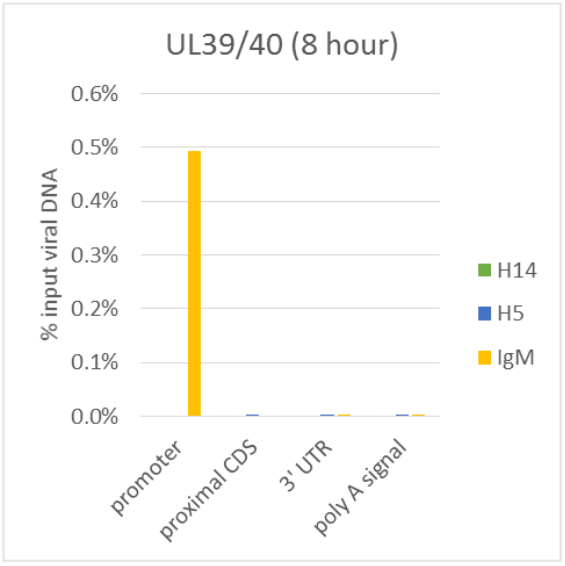
UL39/40 (8 hour)
% input viral DNA
0.6%
0.5%
0.4%
0.3%
0.2%
0.1%
0.0%
promoter
proximal CDS
3' UTR
poly A signal
H14
H5
IgM

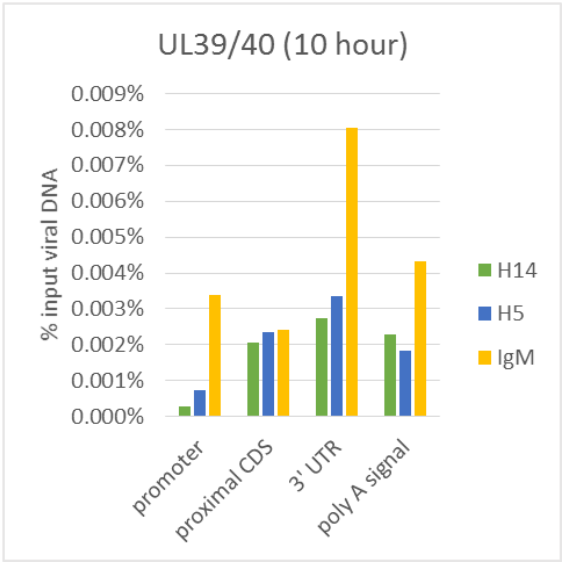
UL39/40 (10 hour)
% input viral DNA
0.009%
0.008%
0.007%
0.006%
0.005%
0.004%
0.003%
0.002%
0.001%
0.000%
promoter
proximal CDS
3' UTR
poly A signal
H14
H5
IgM

Figure 3-5: ChIP analysis of a HSV-1 Early gene.
HeLa cells were infected with WT HSV-1 at MOI of 10 and crosslinked with DSG and formaldehyde at two hour intervals. Cell lysates were homogenized by sonication and immunoprecipitated with antibodies against RNAP II as indicated in figure. Immunoprecipitated complexes were treated to reverse the crosslinks and digested with proteinase K to release DNA fragments, which were extracted with phenol/chloroform. Ten percent of each purified DNA sample was used as input template to amplify signal by quantitative PCR targeting the HSV-1 $U_L39/40$ gene region. **A)** Schematic of the UL39/40 gene region and positions of amplicons. **B)** Assessing viral DNA content of the $U_L39/40$ gene region through qPCR of input viral DNA samples. ChIP qPCR analysis of the HSV-1 $U_L39/40$ gene region using **C)** pan-RNAP II antibodies and **D)** phospho-form-specific RNAP II antibodies. Graphs present median copy numbers of each amplicon form three independent infections, normalized to input viral DNA of the same amplicon.

signals were observed from the 4H8 samples with an increase in ChIP signal starting at 2 hours post infection and peaking at 4 hours post infection. ChIP signals began to decrease at 6 hours post infection and were stable by 8 hours post infection (Figure 3-4C). 4H8 ChIP signals were highest in the promoter and proximal CDS segments in the first 4 hours of infection, with much lower signals from the distal CDS and poly-A signal segments. This suggests that perhaps the genes were being transcribed but only a few RNAP II complexes were able to finish transcribing at those time points. Starting at 6 hours post infection, 4H8 ChIP signals were lower than those observed at earlier time points, but now signals from the distal CDS and poly-A signal segments were on par with the promoter and proximal CDS segments. These data suggest that although fewer RNAP II complexes were transcribing the U_L39/40 genes, many appeared to reach the end of the genes and therefore produce full-length transcripts. The overall 4H8 ChIP signal profile matched with the expected expression profile of Early genes.

Despite having demonstrated enrichment over mouse IgG control ChIP reactions by Western blot analysis, 1Y27 ChIP signals showed no clear pattern in these experiments. In many cases, the 1Y27 ChIP signals were in fact lower than those of mouse IgG controls. The H5 and H14 ChIP signals were consistently lower than the mouse IgM controls as well. Thus, no conclusions could be drawn from the ChIP analysis using these three antibodies in this experiment regarding initiating or elongating RNAP II occupancy on the U_L39/40 genes.

The HSV-1 U_L44 ORF encodes the viral glycoprotein C, an envelope protein that in conjunction with glycoprotein B, binds to heparin sulfate on host cells to mediate viral adsorption (71,89,146). As a Late gene, U_L44 expression begins at approximately 6 hours post infection and remains high for the rest of the infection. The short UL45 ORF is nested in the last 520 nucleotides of the U_L44 ORF and the two ORFs share a common poly-A signal. The U_L44 ORF is flanked by two other Late genes, U_L43 and U_L46/47 ORFs. All five ORFs in this region have similar expression profiles and the collision model predicts that this would be a high traffic region at late time in infection. We designed qPCR primer pairs to detect the

promoter, proximal CDS, and distal CDS of the U_L44 ORF (Figure 3-5A) and performed ChIP analysis. Similar to the results analyzing the U_L39/40 ORFs, there was an average 10.5 fold increase in viral genomes measured by the same qPCR primer pairs as used in the U_L44 ChIP analysis (Figure 3-5B). All three primer pairs showed similar progression over the course of the 10 hour infection and significantly higher than the mock infected cell samples.

Both of the pan-RNAP II ChIP antibodies 4H8 and 1Y27 were able to achieve strong signals above mouse IgG isotype controls at all time points. The overall ChIP signal levels were quite low however, with 4H8 maxing out at 0.031% and 1Y27 no higher than 0.016% of input viral DNA at 2 hours and 6 hours post infection respectively (Figure 3-5C). Neither 4H8 nor 1Y27 ChIP revealed a clear pattern of RNAP II occupancy at the U_L44 ORF region and this did not match the expression profile of a Late gene. The H14 and H5 ChIP experiments only achieved above background signals at the earliest time points, possibly reflecting the fact that the overall RNAP II level was higher at the start of the infection. At 4 hours post infection and beyond, the mouse IgM controls were always much higher than either H14 or H5 ChIP signals, much like the UL39/40 ORFs. We are unable to draw any conclusions from the ChIP data set on the U_L44 ORF.

Discussion

The genome of HSV-1 is highly compact, encoding a total of 94 ORFs and multiple repeated regions within 152 kbp (127,136). Many of the viral ORFs share initiation sites but differ in termination, while other ORFs may begin at different loci but terminate at the same locus (127). Furthermore, studies have shown that a few of the viral ORFs such as U_L1 and U_L24, harbor two polyadenylation signals and are expressed in two distinct variants at different times in infection (34,35,150). Three of the ORFs (U_L10, U_L22, and U_L23) are transcribed in an anti-sense manner relative to ORFs residing in the same gene cluster. In addition to coding functional polypeptides of their own, these anti-sense transcripts appear to exhibit a regulatory

A)

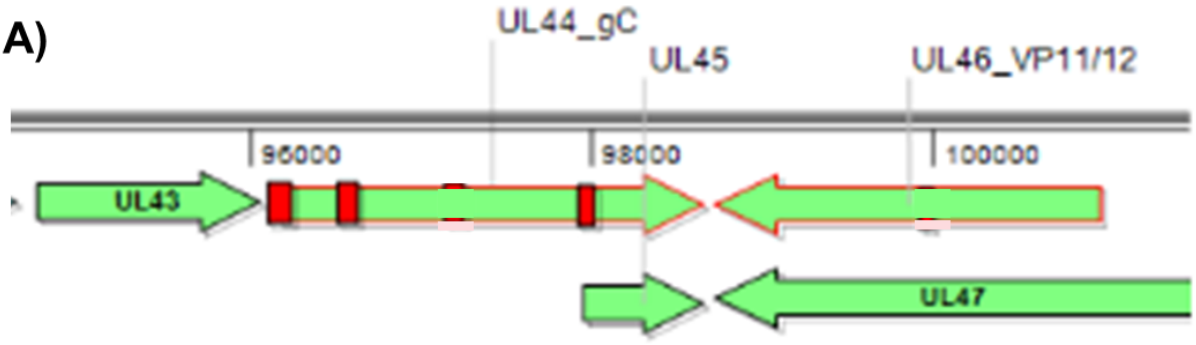
UL44_gC
UL45
UL46_VP11/12
96000
98000
100000
UL43
UL47

B)

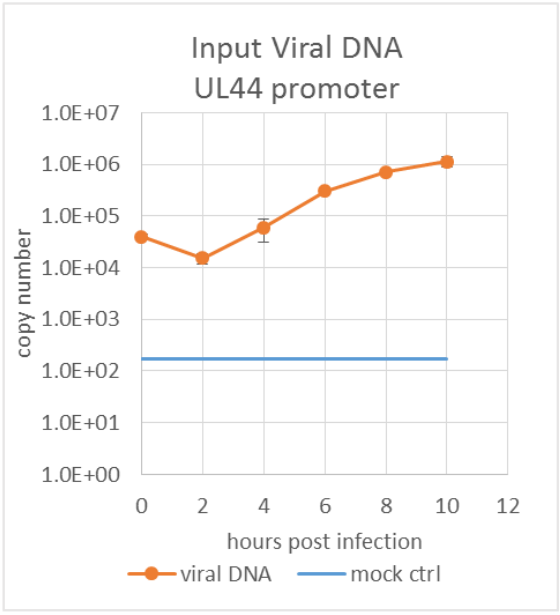
Input Viral DNA
UL44 promoter
copy number
1.0E+07
1.0E+06
1.0E+05
1.0E+04
1.0E+03
1.0E+02
1.0E+01
1.0E+00
0
2
4
6
8
10
12
hours post infection
viral DNA
mock ctrl

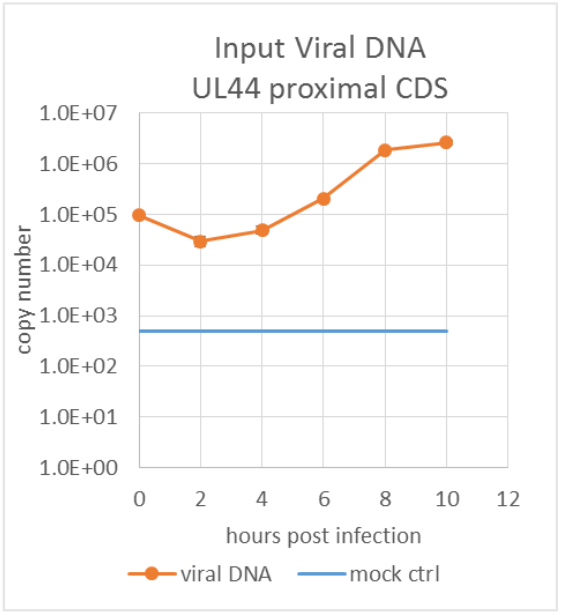
Input Viral DNA
UL44 proximal CDS
copy number
1.0E+07
1.0E+06
1.0E+05
1.0E+04
1.0E+03
1.0E+02
1.0E+01
1.0E+00
0
2
4
6
8
10
12
hours post infection
viral DNA
mock ctrl

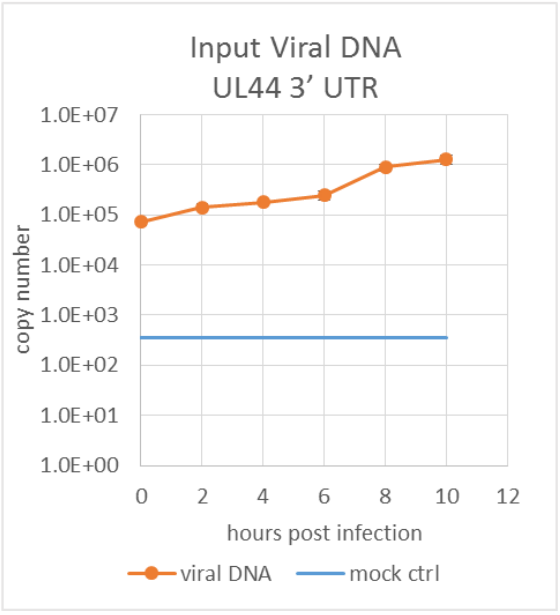
Input Viral DNA
UL44 3' UTR
copy number
1.0E+07
1.0E+06
1.0E+05
1.0E+04
1.0E+03
1.0E+02
1.0E+01
1.0E+00
0
2
4
6
8
10
12
hours post infection
viral DNA
mock ctrl

C)

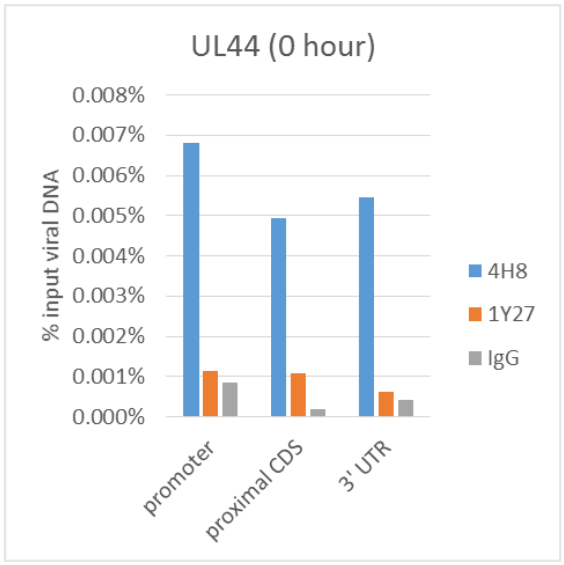
UL44 (0 hour)
0.008%
0.007%
0.006%
0.005%
0.004%
0.003%
0.002%
0.001%
0.000%
% input viral DNA
promoter
proximal CDS
3' UTR
4H8
1Y27
IgG

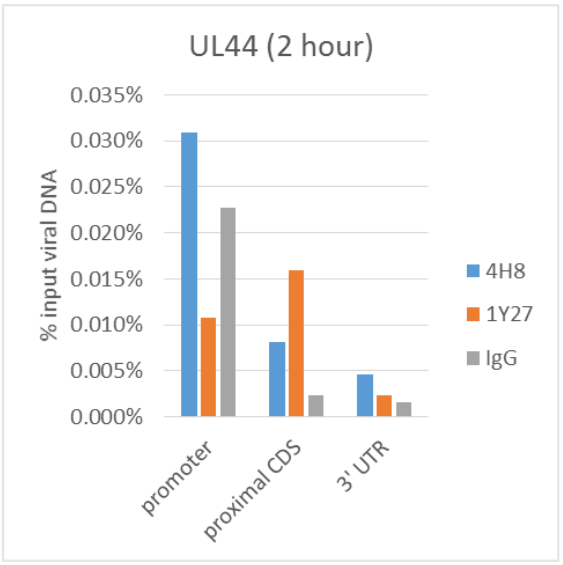
UL44 (2 hour)
0.035%
0.030%
0.025%
0.020%
0.015%
0.010%
0.005%
0.000%
% input viral DNA
promoter
proximal CDS
3' UTR
4H8
1Y27
IgG

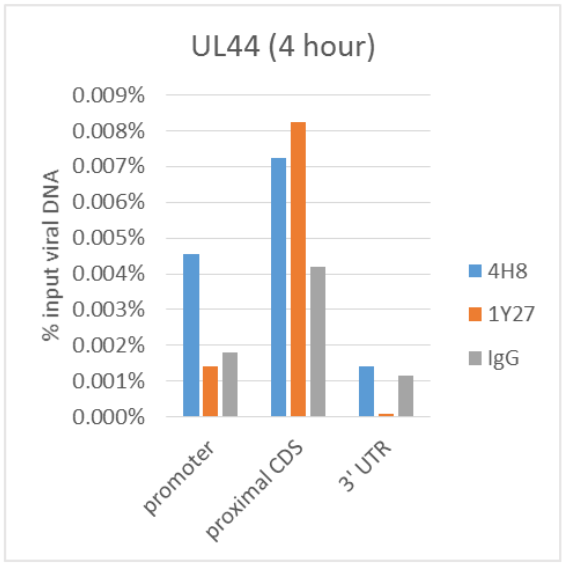
UL44 (4 hour)
0.009%
0.008%
0.007%
0.006%
0.005%
0.004%
0.003%
0.002%
0.001%
0.000%
% input viral DNA
promoter
proximal CDS
3' UTR
4H8
1Y27
IgG

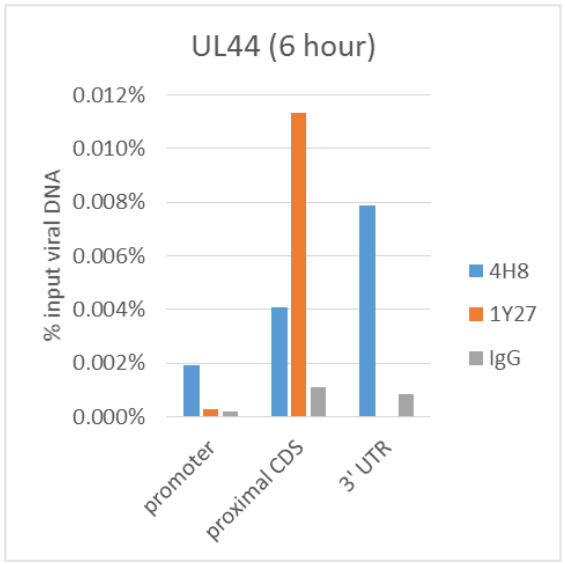
UL44 (6 hour)
0.012%
0.010%
0.008%
0.006%
0.004%
0.002%
0.000%
% input viral DNA
promoter
proximal CDS
3' UTR
4H8
1Y27
IgG

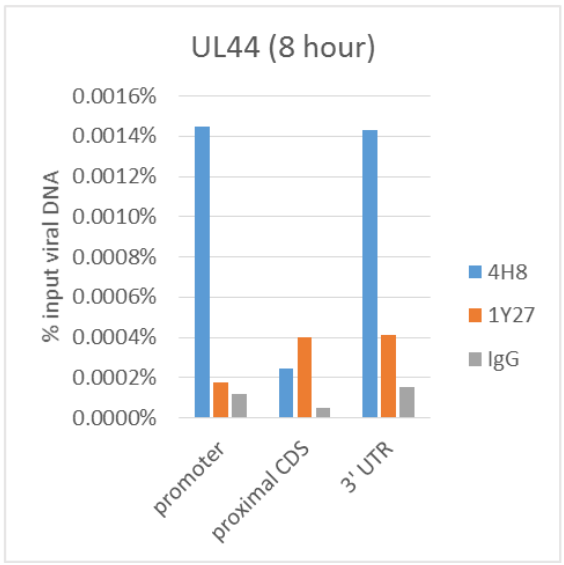
UL44 (8 hour)
0.0016%
0.0014%
0.0012%
0.0010%
0.0008%
0.0006%
0.0004%
0.0002%
0.0000%
% input viral DNA
promoter
proximal CDS
3' UTR
4H8
1Y27
IgG

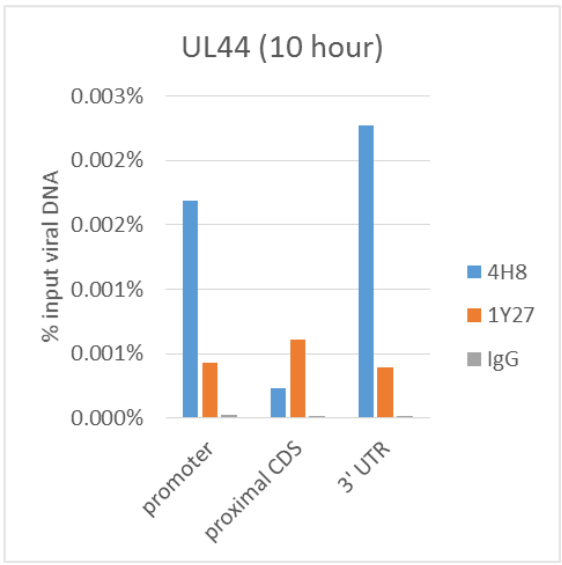
UL44 (10 hour)
0.003%
0.002%
0.002%
0.001%
0.001%
0.000%
% input viral DNA
promoter
proximal CDS
3' UTR
4H8
1Y27
IgG

D)

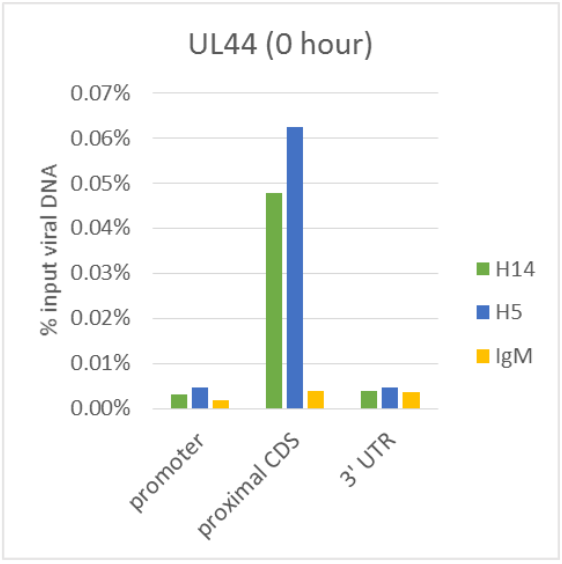
UL44 (0 hour)
% input viral DNA
0.07%
0.06%
0.05%
0.04%
0.03%
0.02%
0.01%
0.00%
promoter
proximal CDS
3' UTR
H14
H5
IgM

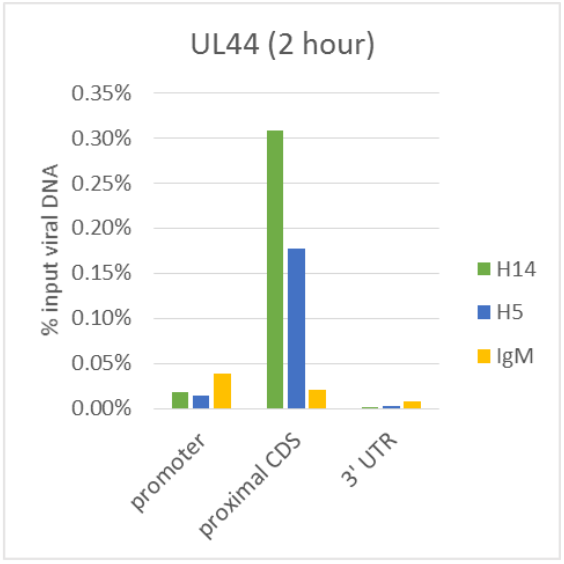
UL44 (2 hour)
% input viral DNA
0.35%
0.30%
0.25%
0.20%
0.15%
0.10%
0.05%
0.00%
promoter
proximal CDS
3' UTR
H14
H5
IgM

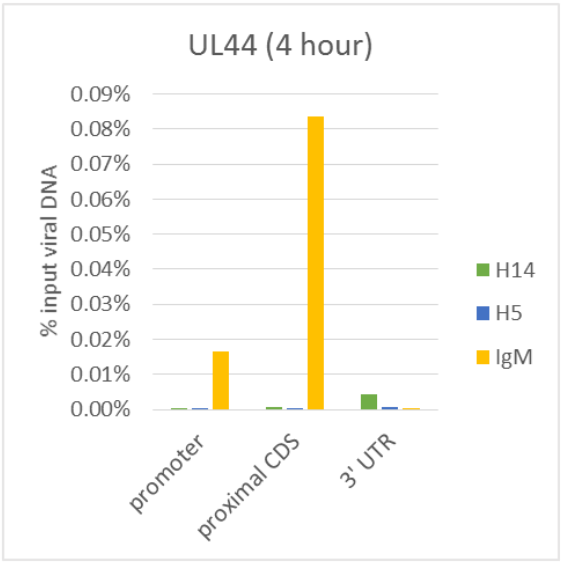
UL44 (4 hour)
% input viral DNA
0.09%
0.08%
0.07%
0.06%
0.05%
0.04%
0.03%
0.02%
0.01%
0.00%
promoter
proximal CDS
3' UTR
H14
H5
IgM

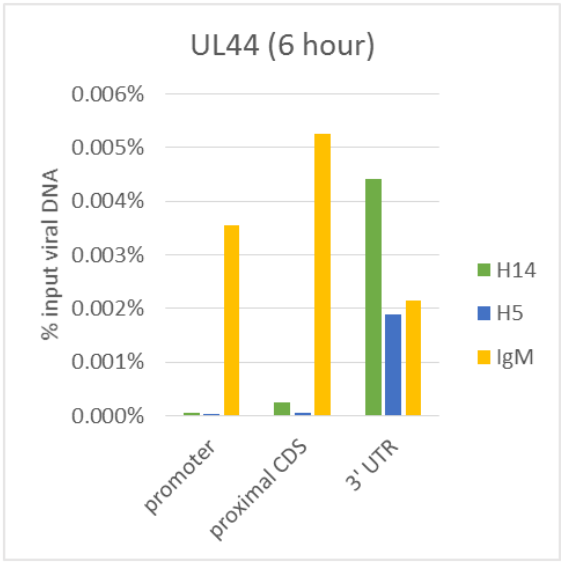
UL44 (6 hour)
% input viral DNA
0.006%
0.005%
0.004%
0.003%
0.002%
0.001%
0.000%
promoter
proximal CDS
3' UTR
H14
H5
IgM

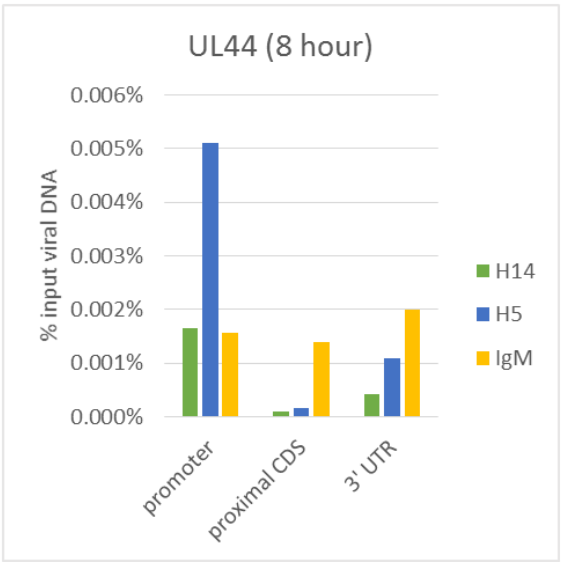
UL44 (8 hour)
% input viral DNA
0.006%
0.005%
0.004%
0.003%
0.002%
0.001%
0.000%
promoter
proximal CDS
3' UTR
H14
H5
IgM

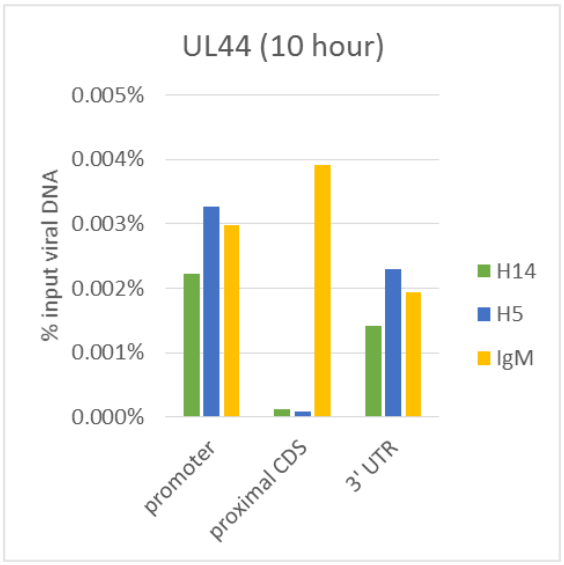
UL44 (10 hour)
% input viral DNA
0.005%
0.004%
0.003%
0.002%
0.001%
0.000%
promoter
proximal CDS
3' UTR
H14
H5
IgM

Figure 3-6: ChIP analysis of a HSV-1 Late gene.
HeLa cells were infected with WT HSV-1 at MOI of 10 and cross-linked with DSG and formaldehyde at two hour intervals. Cell lysates were homogenized by sonication and immunoprecipitated with antibodies against RNAP II as indicated in figure. Immunoprecipitated complexes were treated to reverse cross-linking and digested with proteinase K to release DNA fragments, which were extracted with phenol/chloroform. Ten percent of each purified DNA sample was used as input template to amplify signal by quantitative PCR targeting the HSV-1 U_L44 gene region. **A)** Schematic of the U_L44 gene region and positions of amplicons. **B)** Assessing viral DNA content of the UL44 gene region through qPCR of input viral DNA samples. ChIP qPCR analysis of the HSV-1 U_L44 gene region using **C)** pan-RNAP II antibodies and **D)** phospho-form-specific RNAP II antibodies. Graphs present median copy numbers of each amplicon form three independent infections, normalized to input viral DNA of the same amplicon.

Table 3-1: ChIP antibodies against RNA polymerase II.

Antibody	RNAP II form	Epitope
ARNA3 (mouse monoclonal IgG)	All forms; unphosphorylated, Initiating, and elongating	N-terminal epitope in largest subunit of RNAP II holoenzyme
4H8 (mouse monoclonal IgG)	All forms; unphosphorylated and phosphorylated	CTD repeats of $YSPTS_pPS$ in the largest subunit of RNAP II
N20x (rabbit polyclonal)	All forms; unphosphorylated, Initiating, and elongating	N-terminal epitope in largest subunit of RNAP II holoenzyme
C21 (rabbit polyclonal)	All forms; unphosphorylated and phosphorylated	CTD repeats of the largest subunit of RNAP II holoenzyme
H14 (mouse monoclonal IgM)	RNAP II initiating complex	Ser-5-phosphorylated (S5p) CTD
ab5131 (rabbit polyclonal IgG)	RNAP II initiating complex	Ser-5-phosphorylated (S5p) CTD
H5 (mouse monoclonal IgM)	RNAP II elongating complex	Ser-2-phosphorylated (S2p) CTD
ab5095 (rabbit polyclonal IgG)	RNAP II elongating complex	Ser-2-phosphorylated (S2p) CTD
1Y27 (mouse monoclonal IgG)	All forms; unphosphorylated, Initiating, and elongating	RPB3, the third largest subunit of RNAP II holoenzyme

function in the expression of the sense transcripts (9,34,35). Even with a complex genomic structure, HSV-1 gene expression follows a well-defined cascade of IE, E, and L phases. Structuraldifferences in promoter sequences appear to play a role in orchestrating the timing of viral gene expression. Expression of the IE genes is enhanced by the potent transcription transactivator VP16 (13,59,69), which is packaged inside the virion, and which recognizes a cis element within the IE gene promoters. ICP4, an IE protein acts as the major transactivator of early genes (47,128,137). Forty-four out of fifty-five L gene promoters lack upstream regulatory elements but harbor a downstream activation signal (DAS) located at +20 to +33 nt instead. The absence of upstream regulatory elements may explain in part why L gene expression is dependent on viral DNA replication (127).

Once activated, HSV-1 genes maintain active expression throughout the course of the infection. Until the onset of robust viral DNA replication, most of the genome is not being actively transcribed. However, when the Late genes becomes activated, the viral genome also becomes enriched with actively transcribing RNAP II. Because of the complex structure of the HSV-1 genome, multiple RNAP II complexes might compete for the same transcription start site, or conversely, transcription may start in the middle of what would be the coding sequence of an upstream ORF. Gene clusters adjacent to each other might also terminate very close in proximity. The combination of a high level of transcription and complex genome structure lends itself to possible collisions among transcribing RNAP II complexes. If left unresolved, the colliding RNAP II complexes could eventually become arrested and viral transcription would stall. Mammalian cells degrade elongating RNAP II that has become arrested due to DNA lesions through the transcription-coupled nucleotide excision repair (TC-NER) pathway (52,66,88,104). As Dai-Ju *et al*. have demonstrated, at late times in HSV-1 infection, RNAP II was ubiquitinated and subsequently degraded by the proteasome (37), similar to TC-NER. Proteasome inhibition in infected cells lead to a significant reduction in viral yield, supporting the idea that degradation of stalled elongating RNAP II complexes is necessary for productive HSV-1 infection.

In the current study, we attempted to establish direct evidence that transcription elongation complexes were becoming arrested on the HSV-1 genome by assessing RNAP II occupancy with ChIP-qPCR analysis. We tested U_L39/40, an E gene cluster that is simpler in genomic structure and thus predicted to be less prone to experience arrested RNAP II. Though we found RNAP II occupancy that corroborated with the known expression patterns of U_L39 and U_L40 when using a pan-RNAP II antibody, we were unable to draw any conclusions about specific phosphoforms of RNAP II due to exceedingly high background levels. We also tested U_L44, a L gene cluster that contains nested ORFs converging on termination sites in very close proximity, thus is predicted to be more prone to arrested RNAP II complexes at the peak of expression. We found the ChIP signals were too low to draw conclusions in the U_L44 data sets, with pan-RNAP II and with phospho-form-specific RNAP II antibodies. We were unable to decipher a trend in RNAP II occupancy on the HSV-1 genome from these data.

We measured viral genomic DNA at all times tested in the experiment as a way to normalize ChIP signals over the course of the infections and found that on average, viral DNA increased 11 to 17 fold in an 10-hour period. Over the same time period, mean transcript copy numbers increased 4.85 and 5.62 fold after subtracting mouse IgG or IgM isotype controls for U_L39/40 and U_L44 respectively. Because ChIP signals were normalized to viral input DNA, the increase in transcript copy numbers was masked by the more rapid increase in viral genomic DNA, especially at late times in infection. ChIP signals could have been normalized to a cellular housekeeping gene such GAPDH or 18s rRNA, but cellular transcripts levels are not as stable in HSV-1 infected cells due to the de-stabilizing effect of the ICP0 protein (20,65) as well as inhibition of pre-mRNA splicing (141) and the degradation of cellular mRNA by the virion host shutoff ribonuclease vhs. Indeed, Watson *et al*. demonstrated that qPCR-based measurements of GAPDH and 18s rRNA showed large variability in HSV-1 infected cells (169). In a recent study, Eisenberg and Levanon examined the stability of human housekeeping genes by next generation RNA-seq analysis and found that expression of many traditional housekeeping genes was not as uniform as once thought (45). Given the

study was done in uninfected cells, it is currently unknown if the RNA-seq results will show similar results in HSV-1 infected cells.

With the advances in massive parallel sequencing techniques, it is conceivable to perform our study using an RNA-seq approach. By analyzing the RNA species present in infected cells, one can infer the locations of pause/arrested RNAP II in the viral genome. RNA-seq should in theory, allow less dependence on the low efficiency of immunoprecipitation, which was exacerbated by a dwindling RNAP II population during HSV-1 lytic infection. This approach however, would not yield information regarding the phospho-state of RNAP II nor does it truly provide direct evidence of colliding RNAP II complexes on the viral genome.

This current study was unable to achieve its goal due to low immunoprecipitation efficiencies and lack of sufficient coverage of the vial genome. We could potentially address the low IP efficiency with a larger cell population and thereby increase the abundance of RNAP II in input material. Just as before, it remains critical to accurately quantify the amount of input chromatin prior to the IP reactions. The lack of coverage was due to the long preparative time required to generate the materials needed in the experiment, and could be addressed given more time. The only conclusion that can be drawn from these data is that HSV-1 DNA replication appeared to outpace viral transcription. This suggests that perhaps not all viral genomes participate in transcription, but given that we were only able to cover two gene clusters in this study, it will require more supporting data to substantiate.

Materials and Methods

Cells, viral strains and virus infections

HeLa cells were grown on minimal essential medium (MEM) containing 10% newborn calf serum. Rabbit skin fibroblasts (RSF) were grown on minimal essential medium supplemented with 8% fetal calf serum and 4% donor calf serum. HSV-1 wild-type (WT) strain KOS was described previously. HeLa cells

were infected with WT HSV-1 KOS as indicated at a multiplicity of infection (MOI) of 10 and were incubated at 37°C for the times indicated in the figure legends.

Western blot analysis

HeLa cells were infected as indicated in the figure legends. At the times indicated, cells were washed with cold phosphate-buffered saline (PBS) and harvested in 2X ESS loading buffer (20 mM Tris, 5 mM EDTA, 4% SDS, 10% 2-mercaptoethanol, 20% glycerol), as described previously (153,154). Cell lysates were fractionated on 5-15% gradient sodium dodecyl sulfate polyacrylamide gels (SDS-PAGE) and transferred to nitrocellulose membranes. Membranes were probed as described previously. Primary antibodies used for immuno-blotting were as follows: rabbit polyclonal anti-RPB1 N20 (Santa Cruz Biotechnology, Inc.) at 1:500; mouse monoclonal anti-RPB1 ARNA3 (EMD Millipore) at 1:500; mouse monoclonal anti-RPB3 1Y27 ChIP grade (Abcam) at 1: 1,000; mouse monoclonal anti-RNAP II CTD 4H8 ChIP grade (Abcam) at 1:1,000; mouse monoclonal anti-RNAP II CTD phosphoserine-2 H5 ChIP grade (Abcam) at 1:2,500; mouse monoclonal anti-RNAP II CTD phosphoserine-5 H14 ChIP grade (Abcam) at 1:2,500.

Two-step chromatin immunoprecipitation (ChIP)

ChIP protocol was modified from Nowak *et al* (117). 4 X 10^7 HeLa cells were infected as indicated in the figure legends. At the times indicated, cells were washed with room temperature phosphate-buffered saline (PBS) augmented with 1 mM $MgCl_2$ (PBS/Mg) three times. Cells were crosslinked at room temperature with 2 mM discuccinimidyl glutarate (DSG) in PBS/Mg on a platform rotator set to 80 rpm for 45 minutes, then washed with room temperature PBS three times. Cells were then crosslinked again at room temperature with 1% (v/v) formaldehyde in PBS/Mg rotating at 80 rpm for 15 minutes, then washed with room temperature PBS three times. Cells were scraped and transferred to 14 ml conical tubes; pelleted by centrifuging at 5,000 RPM (4°C) in a SS-34 fixed angle rotor for 3 minutes. The supernatant was aspirated and the cell pellet was flash frozen in liquid nitrogen and stored at -80°C until samples were ready for lysis and homogenization by sonication. Cell were lysed by gently re-suspending

the cell pellet in 900 µl L1 buffer (50 mM Tris-HCl, pH 8.0, 2 mM EDTA, 0.1% IGEPAL® 630 (Sigma-Aldrich), 10% glycerol, 1 mM dithiothreitol (DTT)) supplemented with protease inhibitors (4 mM Pefabloc® and 0.1 mg/ml leupectin) on ice for 15 minutes. Cytoplasmic content was separated by centrifuging at 1,200 x g in a refrigerated microfuge for 5 minutes and aspirated with the supernatant. The nuclear pellet was re-suspended in 500 µl sodium docecyl sulfate (SDS) lysis buffer (50 mM Tris-HCl, pH 8.0, 10 mM EDTA, 1% SDS) at room temperature. Chromatin was sonicated ten times at 10 watt in 15-second pulses with a minimum of a 1-minute break on ethanol-ice bath in between pulses to prevent overheating, using a Misonix Microson XL sonicator (Misonix, Inc.).

Average DNA fragment size was analyzed using a 20 µl aliquot of the sonicated chromatin taken from each sample. Samples were un-crosslinked at 65°C for 1 hour in 200 mM NaCl, 0.5% SDS, 200 µg/ml proteinase K (Life Technologies), and DNA was extracted with the phenol/chloroform, followed by ethanol precipitation overnight. DNA fragment sizes were visualized on 2% Tris-borate-EDTA (TBE) agarose gels, while DNA quantification was measured through absorbance at 260 nm using a NanoDrop® ND-1000 spectrophotometer (Thermo Scientific). Approximately 2.75 µg (55 OD_{260} units) of soluble chromatin per sample in no more than 100 µl volume was diluted with low ionic strength ChIP dilution buffer (50 mM NACl, 10 mM HEPES, pH 7.4, 1% IGEPAL® 630, 10% glycerol, 1 mM DTT) supplemented with proteinase inhibitors (4 mM Pefabloc® and 0.1 mg/ml leupectin) to a total volume of 900 µl. Five such dilutions were made for each sample prepared from 4 X 10^7 cells.

50 µl of Dynabead® Protein G were rinsed with 200 µl low ionic strength ChIP dilution buffer three times and blocked with 100 µg/ml sheared salmon sperm DNA (Life Technologies) in 200 µl low ionic strength ChIP dilution buffer on an end-over-end rotator at 4°C for 10 minutes. Four µg of anti-RNAP II antibodies, with the exceptions of H14 and H5, were added to the beads to bind at room temperature on an end-over-end rotator for 30 minutes. For the H14 and H5 antibodies, beads were first bound to 10 µg

rabbit anti-mouse IgM (Thermo Scientific) linker antibody, then 4 µg H14 or H5 antibody in the same manner as the other antibodies. Beads were then rinsed with 200 µl low ionic strength ChIP dilution buffer three times and gently re-suspended in 50 µl low ionic strength ChIP dilution buffer supplemented with protease inhibitors. Antibody-bound beads were added to diluted soluble chromatin samples to immunoprecipitate on a rotator at 4°C overnight.

Dynabeads, along with immunoprecipitated complexes were captured with a magnet and the supernatant was aspirated. Beads were washed twice with 500 µl low ionic strength ChIP dilution buffer, once with high-salt ChIP wash buffer (500 mM NaCl, 0.1% SDS, 1% IGEPAL® 630, 2 mM EDTA, 20 mM Tris-HCl, pH 8.0), once with LiCl ChIP wash buffer (0.25 M LiCl, 1% IGEPAL® 630, 1% deoxycholate, 1 mM EDTA, 10 mM Tris-HCl, pH 8.0), and twice with TE (10 mM Tris-HCl, pH 8.0, 1 mM EDTA). Immunoprecipitated complexes were eluted off the beads in 250 µl freshly prepared elution buffer (1% SDS, 0.1 M $NaHCO_3$) at 50°C for 15 minutes once, then again in 50 µl elution buffer at 50°C for 15 minutes. Both elution were combined and adjusted to 200 mM NaCl, 50 mM Tris-HCl, pH 6.8, 10 mM EDTA, 200 µg/ml proteinase K to un-crosslink at 65°C for 2 hours. DNA was extracted with the phenol/chloroform, followed by ethanol precipitation overnight. The resulting DNA pellet was re-suspended in 30 µl TE and the five identical ChIP reactions were pooled back as a single sample.

Quantitative polymerase chain reaction (qPCR) was performed using 3 µl of the ChIP DNA as the template, 2 pmole each of the forward and reverse primer, and 10 µl of the 2X iQ™ SYBR® Green Supermix (Bio-Rad Laboratories) on a Bio-Rad MyiQ real-time PCR detection system. PCR reactions with serially diluted known quantities of either pUC18-U_L39/40 or pUC18-U_L44 plasmid as templates were setup as standard curves, and known quantities of pUC18-h18srRNA with primer pair specific for the human 18s rRNA were setup as interplate calibrators in each run. PCR primer sequences can be found in Table 3-2.

Table 3-2: Genes and primers used in this study

Gene	Segment	Primers	
		Forward	Reverse
HSV-1 U_L39/40	Promoter	5’ CACAGGTGGGTGCTTTGGAAAC 3’	5’ GAAGAGTAGGCGAGAGCAGGTC 3’
	Proximal CDS	5’ TCTGGACCATTACGACTGTCTGATC 3’	5’ GCCCGCCAAAACGCTTTAGG 3’
	3’ UTR	5’ GGCGATCCAGATTCCAAAGTGC 3’	5’ GTTTCCAGCCAGCGGTTAAGG 3’
	Poly-A signal	5’ GTGTCGCAGCACCTCCTACG 3’	5’ CCCTGACAAGAATCACAATGAGACC 3’
HSV-1 U_L44	Promoter	5’ TGATTTCGCCATAACACCCAAACC 3’	5’ GCATGAAAACGACCTCCACACG 3’
	Proximal CDS	5’ CACCCGCATGGAGTTCCG 3’	5’ GCTGTCGACACCAGGAGTC 3’
	3’ UTR	5’ ATAAAGCCGCCACCCTCTCTTC 3’	5’ GCCGTTGTGTTGGTAGGAAAGC 3’
Human 18s rRNA	CDS	5’ CGGACAGGATTGACAGATTGATAGC 3’	5’ GAGTCTCGTTCGTTATCGGAATTAACC 3’

Chapter 4
Investigation of Possible Involvement of Cellular General Transcription Factor TFIIS during HSV-1 Transcription

Summary

Transcription by RNAP II is intrinsically prone to pause and require the activities of general transcription factors (GTFs) to stimulate elongation. The GTF TFIIS has been shown to cleave the extendable 3' end of the nascent transcript to promote proper alignment between DNA-RNAP II-RNA when the polymerase becomes blocked and therefore arrested on the template. Prolonged association of TFIIS with the polymerase might act as a trigger for the transcription-coupled nucleotide excision repair (TC-NER) pathway and could lead to proteasomal degradation of the elongating RNAP II. This may be similar to degradation of stalled elongating RNAP II by the proteasome at late times during herpes simplex virus type 1 infection, in a transcription dependent manner. We attempted to investigate possible involvement of TFIIS in HSV-1 transcription by examining its co-localization with RNAP II but inconsistent patterns were found among the three isoforms. Functional analysis by protein knock down experiments were not successful. Western blot analysis revealed that the antibodies used in the immunofluorescence experiments lacked specificity for their cognate target proteins. Thus, we do not have data supporting a role for TFIIS in HSV-1 transcription.

Introduction

Eukaryotic mRNA transcription by RNA polymerase II (RNAP II) is critical to the cell and thus is regulated at several points during the process. Beyond the basic regulation conferred by the promoters and sequence-specific transcription factors, transcription elongation can be influenced by chromatin modification, splicing, and termination (7,17,23,39,49,87). Even in the absence of nucleosomes, transcription elongation by RNAP II on a naked DNA template is non-continuous and pauses, backtracks and becomes arrested along the length of the template. Addition of general transcription factors (GTFs) such as TFIIS and TFIIF to highly purified *in vitro* systems have been found to increase the rate of transcription elongation (reviewed in (159)). While both TFIIS (6,81) and TFIIF (179,182) have been shown independently to stimulate resumption of RNAP II transcription after pausing, recent data demonstrated that the two GTFs might work synergistically (74,143).

The original TFIIS protein was first identified by Natori *et. al.* in 1973 as a protein with ribonuclease H (RNase H) activity that stimulated RNAP II transcription (112,113). Subsequent studies found two related proteins with similar activities that were expressed in a tissue-specific manner (78,111). All three TFIIS proteins consist of three domains (I-III), with domain II being an alpha helical region that makes direct contact with RNAP II (8,81,172). When RNAP II becomes arrested on the DNA template while elongating, the polymerase loses physical contact with the 3' end of the nascent transcript and backtracks 7-9 nucleotides (49,63). The RNase H activity of TFIIS cleaves the now extended 3' end of the RNA and thereby re-establishes contact between the polymerase and the transcript to ensure proper alignment upon resumption of transcription. When RNAP II is physically blocked from elongation however, TFIIS activity is insufficient to help the polymerase bypass the obstacle, and the cell senses this as a potential site for DNA damage. Components of the transcription coupled nucleotide excision repair (TC-NER) pathway are then recruited to the site of the blockage and RNAP II becomes ubiquitinated to mark it for degradation by the proteasome, prior to DNA repair (reviewed in (158,174). It is thought that TFIIS might act as a sensor for

the TC-NER pathway in identifying DNA damage in the genome, and data showing TFIIS dynamically associating with elongating RNAP II lends support that perhaps prolonged association with the polymerase by TFIIS acts as a signal for TC-NER (33,83,125).

Dai-Ju *et al*. showed previously that elongating RNAP II was ubiquitinated and then degraded by the proteasome in HSV-1 infected cells at late times in infection (37). This degradation of elongating RNAP II was negated under transcription inhibition by actinomycin D. Dai-Ju *et al*. postulated that late in infection, the HSV-1 genome, which contains many nested open reading frames (ORFs), becomes crowded with actively transcribing RNAP II complexes and the complexes may collide or pile up. This would lead to arrest of the elongating RNAP II complexes and this could triggers degradation by the proteasome, similar to the TC-NER response. We set out to investigate if TFIIS is involved in HSV-1 transcription by immunofluorescence (IF) co-localization studies in HSV-1 infected cells and found that although some co-localization between TFIIS and RNAP II was observed, the patterns differed from those seen between TFIIS and viral transcription compartments. To examine if TFIIS plays a functional role in viral transcription transient knock down experiments were attempted but detection of the target proteins by Western blot analysis was obscured because the antibodies used were relatively non-specific. In light of the Western blot analysis, the validity of the IF co-localization results as well is also questionable.

Results

TCEA2, a TFIIS isoform appeared to be relocalized in HSV-1 infected cells

Transcription of mRNA by RNAP II is not continuous and there are many loci in the genome where the polymerase pauses before resuming transcription. These pause sites influence the *in vivo* kinetics of RNAP II transcription and there is evidence these pauses affect processing events such as splice site or poly-A signal choices (21,38,115). The GTF TFIIS was first identified as a positive transcription factor that stimulates RNAP II elongation (113). Subsequent experiments found that TFIIS stimulates RNPA II elongation by cleavage of the 3’ end of the paused transcript thereby promoting the proofreading activity

of the polymerase to maintain the proper alignment between the DNA-RNA-RNAP II complex when transcription resumes (81). Although a monomeric protein, TFIIS is encoded by three separate genes in humans (TCEA1-3) and appears to be expressed in a tissue-specific manner. The redundancy of protein function suggests that TFIIS activity is important for the cell.

Because TFIIS is involved in reinitiating transcription after RNAP II has encountered a pause site, we postulated that if robust HSV-1 transcription at late times in infection might lead to colliding RNAP II elongation complexes on the viral genome, perhaps TFIIS would be triggered to attempt to rescue viral transcription. To explore this possibility, immunofluorescence (IF) staining of all three isoforms of TFIIS was performed in RSF cells that were either mock infected or infected with WT HSV-1 for 8 hours (Figure 4-1). Both TCEA1 and TCEA3 were nuclear as expected and they remained nuclear in HSV-1 infected cells at 8 hours post infection. Unexpectedly, TCEA2 staining was much weaker and appeared to be diffusely localized in the cytoplasm in mock infected cell controls. At 8 hours post infection, approximately 25% of the HSV-1 infected cells showed TCEA2 staining that appeared globular within the nuclei (Figure 4-1, middle panel). These data suggested that although all three isoforms of TFIIS were expressed in the cultured RSF cells, only TCEA2 showed a change in its localization pattern in HSV-1 infected cells, which hinted at its possible involvement in HSV-1 transcription.

The initial TCEA2 IF staining was weak in mock infected cell controls and the increased intensity of the globular staining pattern observed in HSV-1 infected cells could have been due to upregulation of the TCEA2 gene. To examine this possibility, the transcript levels of both TCEA1 and TCEA2 was measured in HeLa cells infected with WT HSV-1 by reverse transcription quantitative polymerase chain reaction (RT-qPCR) at 0, 2, 4, and 8 hours post infection (Figure 4-2). qPCR primer pairs were designed to cover both proximal and distal coding sequences (CDS) of each transcript to ensure accurate quantification. Mock infected cells served as a baseline control for this experiment and the transcript levels for both TCEA1 and TCEA2 remain steady during the 8 hour timed course. In WT HSV-1 infected cells,

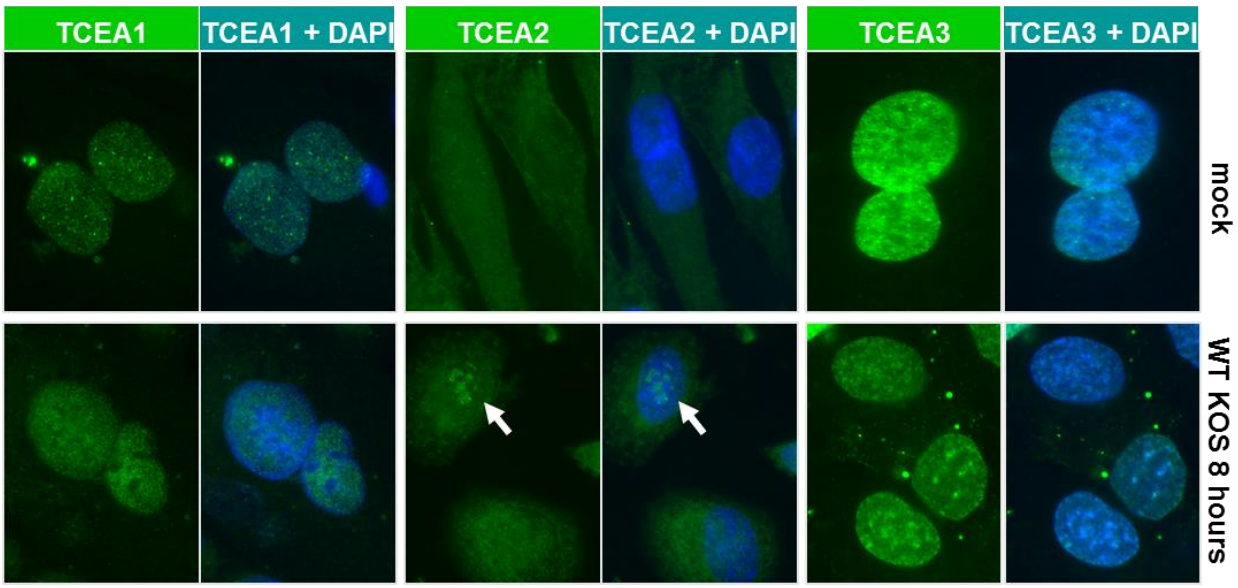

Figure 4-1: HSV-1 infected cells exhibited altered localization patterns in one of the TFIIS isoforms. RSF cells were mock infected or infected with WT KOS HSV-1 at MOI of 10. At 8 hours post infection, cells were fixed in 3.7% formaldehyde and stained with primary antibodies against different isoforms of TFIIS (TCEA1-3). Detection of the primary antibodies was done with FITC conjugated anti-mouse IgG secondary and DAPI marked the nuclei. All images were captured on a Zeiss Axiovert 200M microscope at 100X magnification.

TCEA1 and TCEA2 transcript levels decreased steadily and by the end of the 8 hour time course, levels fell an average of 23.8 and 52.3 fold respectively. Given that both TECA1 and TCEA2 transcript levels were decreased in HSV-1 infected cells, but only TCEA2 appeared to exhibit differential localization compared to mock infected cells, it appeared that the difference in TCEA2 staining patterns was not due to upregulation of the gene in HSV-1 infected cells.

To further examine the altered localization of TCEA2 in cells infected with WT HSV-1, we performed confocal IF microscopy to examine if TCEA2 co-localized with RNAP II in HSV-1 infected cells (Figure 4-3A). In mock-infected cells, the diffused cytoplasmic distribution of TCEA2 was still observed, but now TECA2 also appeared in small nuclear puncta owing to better optical resolution of the confocal microscope. RNAP II was also seen in small nuclear puncta but there did not appear to be significant co-localization ofTCEA2 and RNAP II. At an early time in infection (4 hours), little or no cytoplasmic TCEA2 staining was observed while nuclear TCEA2 staining appeared to be in larger puncta compared to those seen in mock infected cells. RNAP II was observed either in small puncta that resembled splicing speckles, or in globular structures, which resembled HSV-1 transcription-replication compartments. Co-localization between TCEA2 and RNAP II was not observed. At a late time in infection (8 hours), TCEA2 was seen in large globular structures that resembled full-blown HSV-1 transcription-replication compartments and RNAP II appeared to be co-localized with TCEA2. These observations could suggest that RNAP II was paused on viral templates at a late time in infection and TFIIS might be associated with RNAP II to overcome the pause.

Because TCEA2 staining patterns resembled HSV-1 viral transcription compartments, the co-localization experiments were repeated to examine possible co-localization of TCEA2 and ICP4, the major transcription transactivator of HSV-1, and which serves as a marker for viral transcription-replication compartments. TCEA2 was co-localized with ICP4 at both 4 and 8 hours post infection (Figure 4-3B). These results suggested that TCEA2, one of the TFIIS isoforms might be involved in HSV-1 transcription.

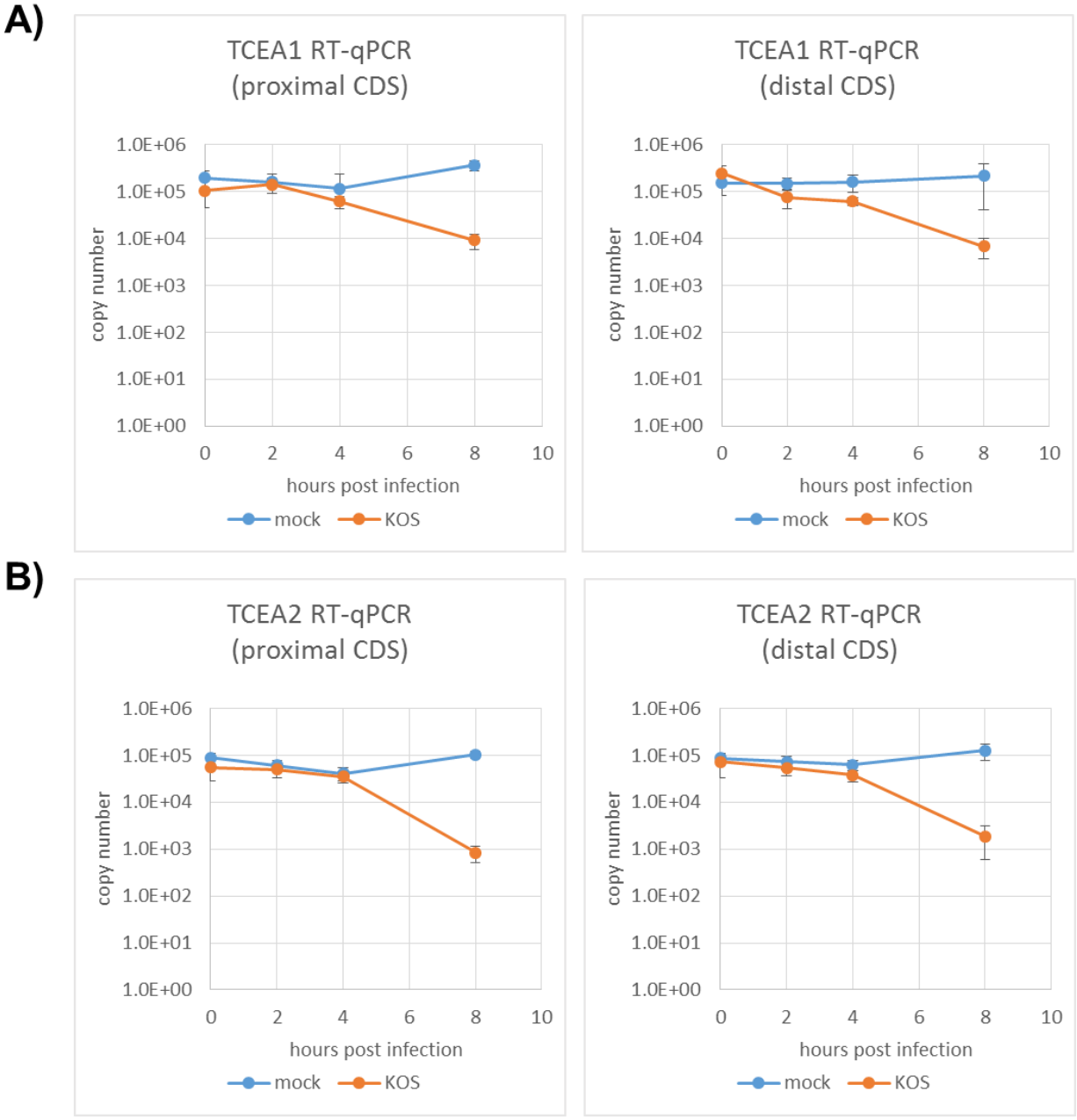

Figure 4-2: TFIIS transcript levels were lower in HSV-1 infected cells.
HeLa cells were infected with WT HSV-1 at MOI of 10 and total RNA was extracted at times indicated. Total RNA was reverse-transcribed into cDNA and 1% of the cDNA was used as input template DNA in quantitative PCR analysis using primers targeting the A) TCEA1 transcripts and B) TCEA2 transcript. Data points represent the median copy number from three independent experiments and error bars represent the SEM.

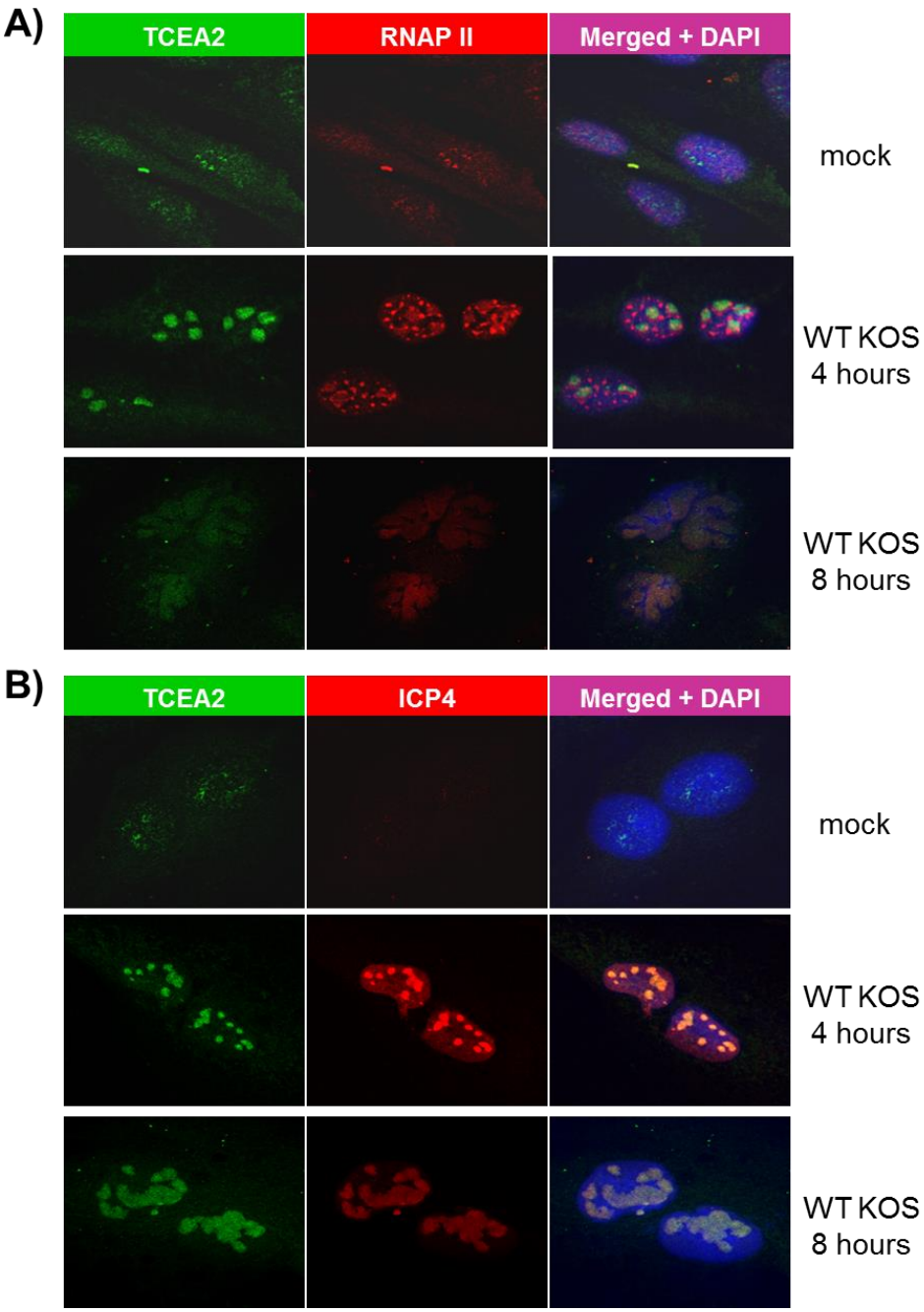

Figure 4-3: TCEA2 was associated with RNAP II in both mock infected and HSV-1 infected cells, and appeared to be in HSV-1 transcription compartments.

RSF cells were mock infected or infected with WT KOS HSV-1 at MOI of 10 at 37°C. Cells were fixed in 3.7% formaldehyde at 4 or 8 hours post infection and stained with B01, a mouse polyclonal anti-TCEA2 antibody and **A)** ARNA3, a mouse monoclonal antibody recognizing all forms of RNAP II or **B)** P1101, a mouse monoclonal antibody recognizing HSV-1 ICP4 to mark viral transcription compartments. Anti-TCEA2 primary antibodies were detected using FITC conjugated anti-mouse IgG2a secondary antibodies, and anti-RNAP II/anti-ICP4 primary antibodies were detected with Texas Red conjugated anti-mouse IgG1 secondary antibodies. Cells were counterstained with DAPI to mark nuclei. All images were captured on a Zeiss LSM510 confocal microscope at 63X magnification.

Transcription inhibition by α-amanitin had different effects on TFIIS isoforms in HSV-1 infected cells

Previous studies by Dai-Ju *et al*. found that inhibition of RNAP II transcription by actinomycin D treatment in HSV-1 infected cells prevented degradation of RNAP II, compared to untreated controls (37). The collision model predicts many arrested RNAP II complexes on the viral genome and if true, one might expect a higher degree of co-localization between RNAP II and TFIIS, a protein that functions in re-initiation of paused polymerases. To test if TFIIS plays a functional role in HSV-1 transcription, we examined the co-localization patterns of TFIIS isoforms and RNAP II in the absence or presence of the potent RNAP II transcription inhibitor α-amanitin.

In mock infected cells treated with α-amanitin, RNAP II became highly associated with either TCEA1 or TCEA3 (Figures 4-4 and Figure 4-6, panels A and B). We did not observe any change in TCEA2 association with RNAP II in mock infected cells treated with α-amanitin however (Figure 4-5A-B). In WT HSV-1 infected cells, α-amanitin appeared to affect each of the TFIIS isoforms differently. For TCEA1, transcription inhibition by α-amanitin unexpectedly eliminated much of its association with RNAP II (Figure 4-4C-F). Localization of RNAP II and TCEA2 following α-amanitin treatment showed slightly more RNAP II associated with TCEA2 in HSV-1 infected cells at an early time in infection and but treated cells were indistinguishable from untreated controls at a later time in infection (Figure 4-5C-F). TCEA3 appeared to be highly associated with RNAP II in HSV-1 infected cells throughout the course of the infection and treatment of α-amanitin did little to alter that pattern (Figure 4-6C-F).

In a parallel experiment, ICP4 was co-stained to mark viral transcription compartments, with each of the TFIIS isoforms to determine if α-amanitin treatment affected TFIIS localization to viral replication compartments. The patterns observed between RNAP II and each of the TFIIS isoforms did not coincide with those seen between ICP4 and the same TFIIS isoforms. TCEA1 co-localized with ICP4 at both early and late times in infection, regardless of α-amanitin treatment status (Figure 4-4I-L). Contrary to previous results, TCEA2 co-localized with ICP4 early in infection but not at late times (Figure 4-5I, K).

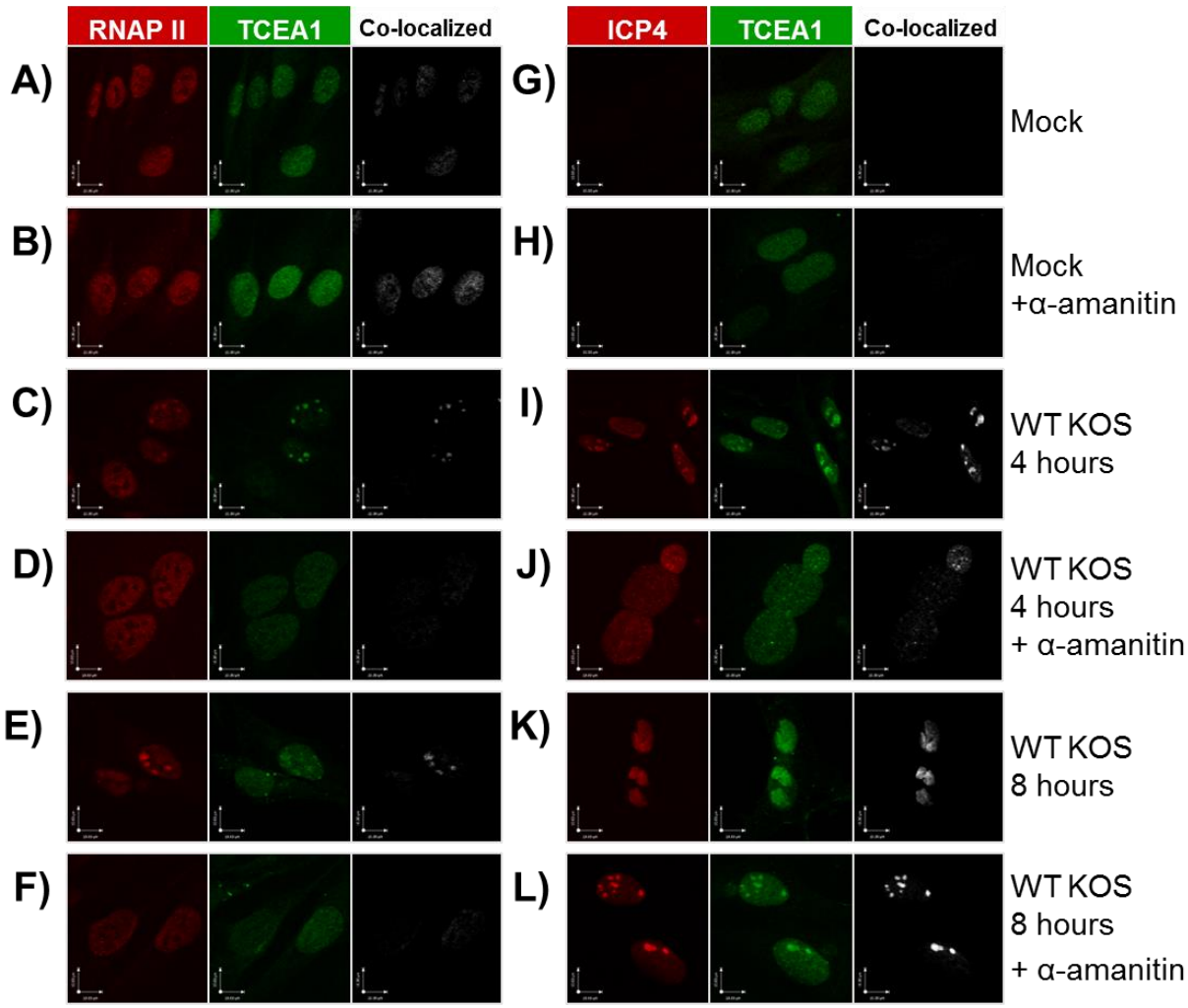

Figure 4-4: TCEA1 and RNAP II co-localized in HSV-1 infected cells when treated with α-amanitin.
HeLa cells were mock infected or infected with WT HSV-1 at MOI of 10. Cells were either left untreated or treated with 20 µg/ml α-amanitin for the duration of the infection. Cells were fixed in 3.7% formaldehyde and stained with primary antibodies against TCEA1 and **A-F)** RNAP II or **G-L)** HSV-1 ICP4 to mark viral transcription compartments at times indicated in figure. Mouse anti-TCEA1 monoclonal antibody was detected using the Alexa Fluor 488 conjugated anti-mouse IgG2a secondary antibody and anti-RNAP II and anti-ICP4 monoclonal antibodies were detected using the Alexa Fluor 595 conjugated anti-mouse IgG1 secondary antibody. All images were captured on a Zeiss LSM510 confocal microscope using a 63X oil immersion objective with Z-stacks. Each Z-stack was represented as max projections and analyzed at the pixel level to generate the co-localized panels using the Volocity software.

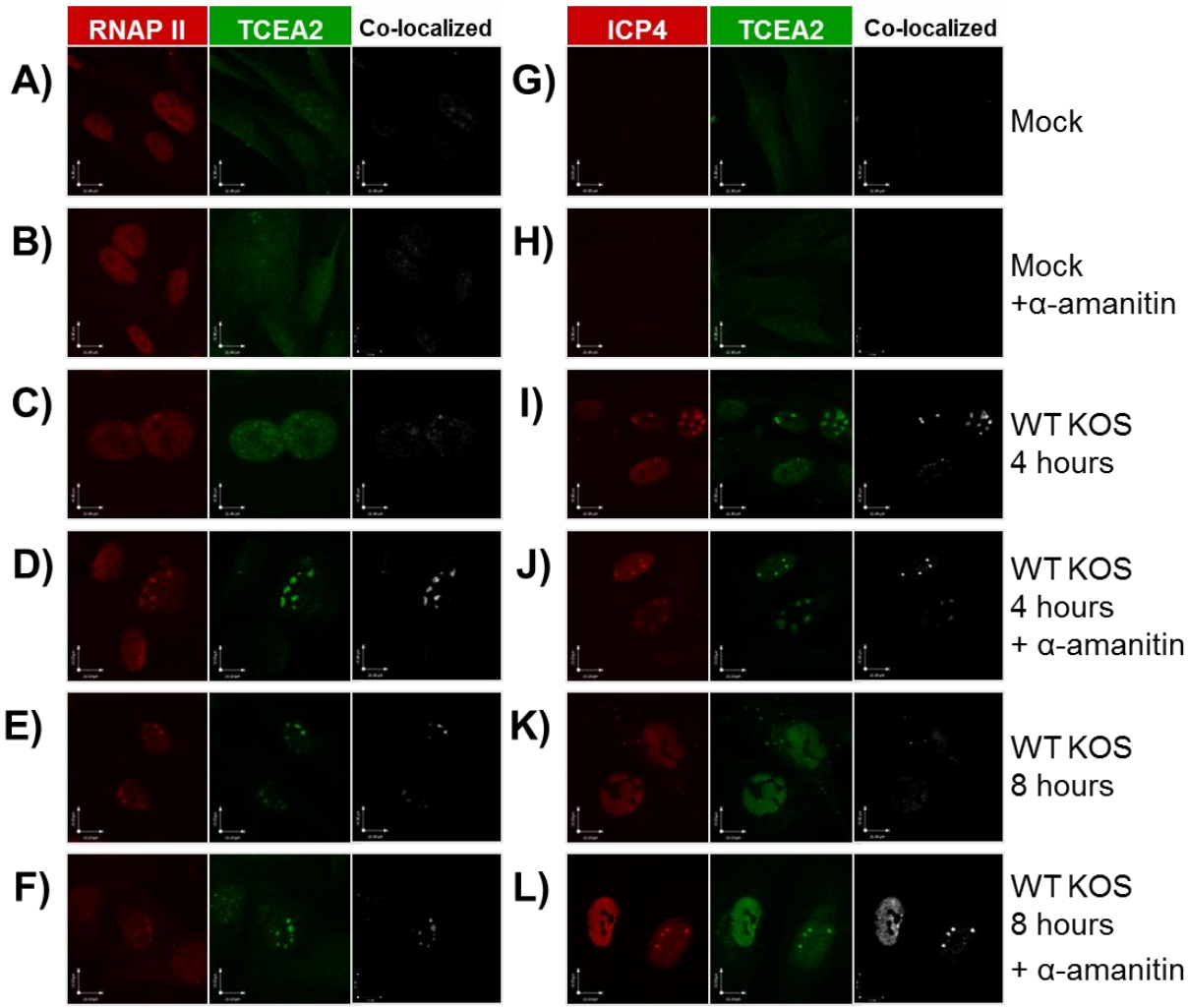

Figure 4-5: TCEA2 and RNAP II co-localized in HSV-1 infected cells when treated with α-amanitin.
HeLa cells were mock infected or infected with WT HSV-1 at MOI of 10. Cells were either left untreated or treated with 20 µg/ml α-amanitin for the duration of the infection. Cells were fixed in 3.7% formaldehyde and stained with primary antibodies against TCEA2 and **A-F)** RNAP II or **G-L)** HSV-1 ICP4 to mark viral transcription compartments at times indicated in figure. Mouse anti-TCEA2 polyclonal antibody was detected using the Alexa Fluor 488 conjugated anti-mouse IgG2a secondary antibody and anti-RNAP II and anti-ICP4 monoclonal antibodies were detected using the Alexa Fluor 595 conjugated anti-mouse IgG1 secondary antibody. All images were captured on a Zeiss LSM510 confocal microscope using a 63X oil immersion objective with Z-stacks. Each Z-stack was represented as max projections and analyzed at the pixel level to generate the co-localized panels using the Volocity software.

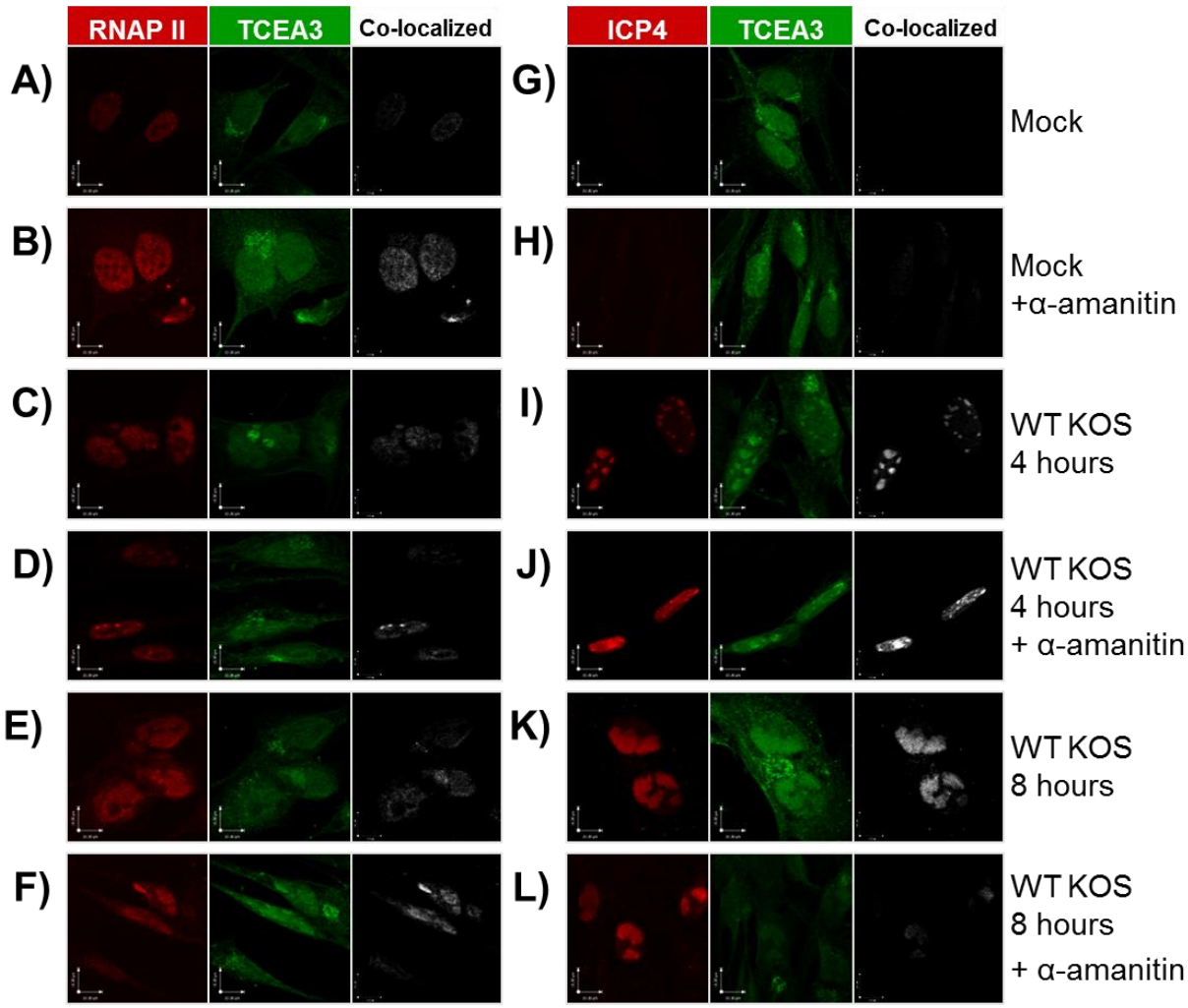

Figure 4-6: TCEA3 and RNAP II co-localized in HSV-1 infected cells.
HeLa cells were mock infected or infected with WT HSV-1 at MOI of 10. Cells were either left untreated or treated with 20 µg/ml α-amanitin for the duration of the infection. Cells were fixed in 3.7% formaldehyde and stained with primary antibodies against TCEA3 and **A-F)** RNAP II or **G-L)** HSV-1 ICP4 to mark viral transcription compartments at times indicated in figure. Mouse anti-TCEA3 monoclonal antibody was detected using the Alexa Fluor 488 conjugated anti-mouse IgG2a secondary antibody and anti-RNAP II and anti-ICP4 monoclonal antibodies were detected using the Alexa Fluor 595 conjugated anti-mouse IgG1 secondary antibody. All images were captured on a Zeiss LSM510 confocal microscope using a 63X oil immersion objective with Z-stacks. Each Z-stack was represented as max projections and analyzed at the pixel level to generate the co-localized panels using the Volocity software.

Transcription inhibition by α-amanitin did not appear to affect this localization pattern at 4 hours post infection, but at 8 hours post infection, there was an increase in co-localization between TCEA2 and ICP4 when the cells were treated with α-amanitin. HSV-1 infected cells treated with α-amanitin exhibited a much lower level of co-localization of TCEA-3 with ICP4 late in infection (Figure 4-6I-L). There was no consensus from these results across the three isoforms of TFIIS and even within each isoform. No correlation was observed between changes in TFIIS-RNAP II co-localization and those in TFIIS-ICP4 co-localization with or without transcription inhibition using α-amanitin.

Assessing TFIIS involvement in HSV-1 transcription by functional knockdown assays

With no consistent results from the IF co-localization experiments, we attempted to assess the possible role of TFIIS in HSV-1 lytic infection by individual knockdown of the isoforms. The pSuperior plasmid based shRNA expression system was used with its additional selective puromycin marker to ensure that nearly all of the infected cells would also express anti-TFIIS shRNA. To establish the level of puromycin selection in HeLa cells, we mock transfected or transfected cells with 2 μg of pSuperior vector plasmid for 24 hours and then incubated the cells either in the absence or presence of 1 μg/ml puromycin for up to 36 additional hours. Cell survival was estimated by counting crystal violet stained cells that remained on the culturing vessels at 12, 24, and 36 hours post selection (Figure 4-7A). In the pSuperior-transfected but not puromycin-selected controls, an overall lower rate of survival was observed compared to mock transfected counterparts, indicating that transfection of the pSuperior plasmid itself carried a survival cost to the cells. When cells under puromycin selection were compared to non-selected controls, it was found that at 36 hours post selection, the pSuperior vector did not confer protection compared to mock transfection. Approximately 49% of the mock transfected cells survived under puromycin selection, while 59% of the pSuperior transfected cells survived under the same conditions by the end of the experiment. The difference in survival was statistically insignificant.

To account for the possibility that pSuperior transfection did not confer protection from puromycin selection, we repeated the experiment with the addition of pGFP controls. Cells were mock transfected or transfected with 2 μg of either pGFP or pSuperior vector plasmid for 24 hours and then incubated in the absence or presence of 1 μg/ml puromycin for additional 24 or 48 hours (Figure 4-7B-C). Without puromycin selection, mock transfected controls remained constant in estimated cell counts, while pGFP transfected cells although fewer in estimated number, also remained relatively constant. pSuperior transfected cells again showed a decrease of 39% and 70% at 24 and 48 hours respectively compared to the initial estimate at the start of the experiment. At 24 hours post selection, mock transfected cells had a relative 77% survival compared to the same cells without puromycin selection, comparable to the 76% relative survival for cells that were transfected with pSuperior vector. At 48 hours post selection, mock transfected cells had a relative survival rate of 17% compared to 44% relative survival rate among pSuperior transfected cells. While pSuperior transfection appeared to confer protection from puromycin, the loss in cell counts from transfection alone was too high and there were too few cells to work with.

In an attempt to reduce toxicity from transfection, a puromycin kill curve analysis was performed comparing a reduced amount of plasmid DNA at 0.5 μg per 10^5 cells to the standard 2 μg per 10^5 cells Figure 4-8). pGFP once again served as our transfection efficiency control in the experiment, and we did not observe more GFP positive cells when transfection was done with 2 μg of DNA compared to 0.5 μg of DNA. However, we observed similar levels of protection from puromycin whether the cells were transfected with 0.5 μg or 2 μg of the pSuperior vector, at both 24 and 48 hours post selection. The mock transfection controls continued to exhibit resistance to puromycin selection, with relative survival rates at 78% and 51% at 24 and 48 hours post selection respectively. These results suggested that 1 μg/ml puromycin selection was insufficient.

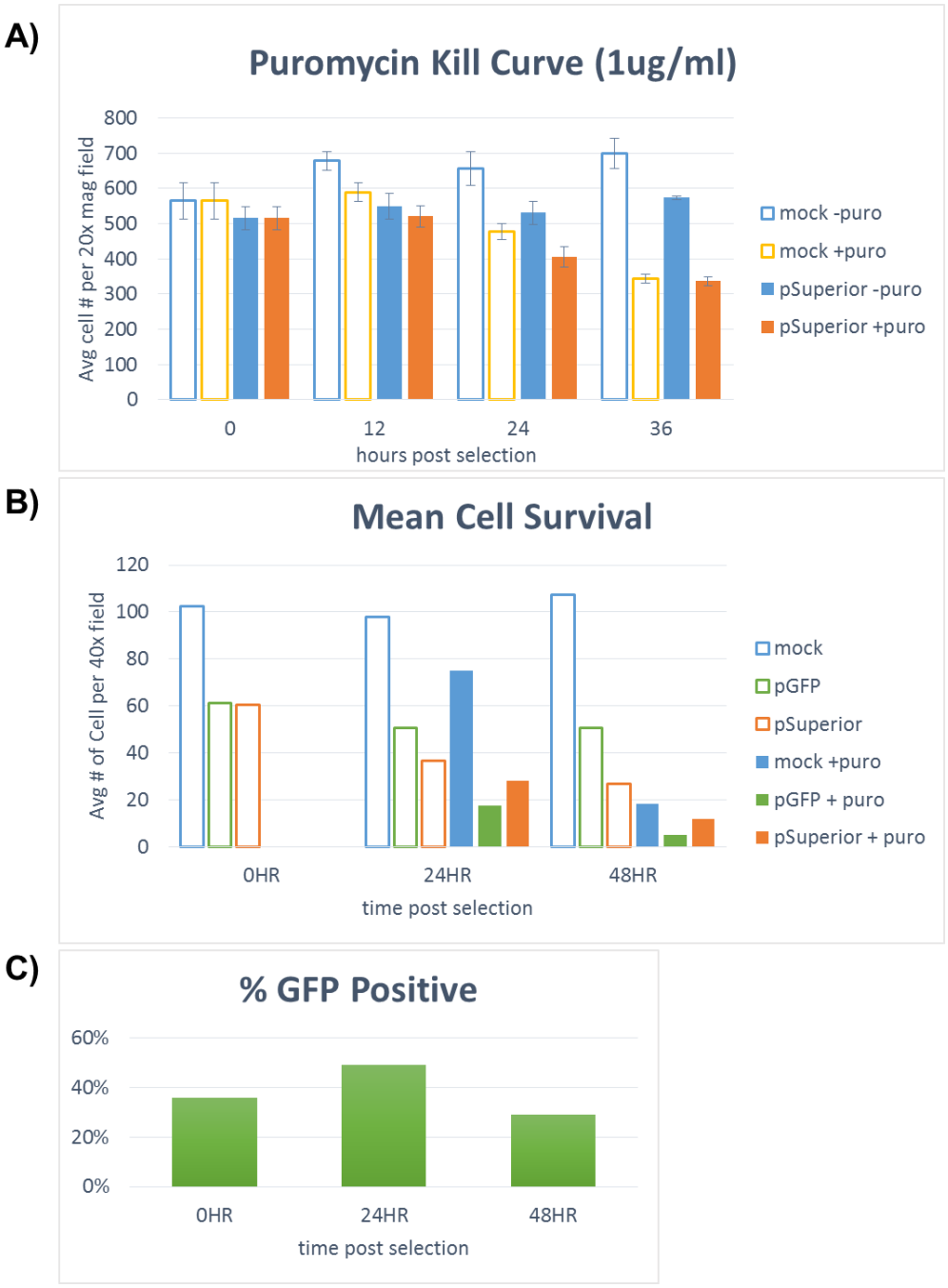

Figure 4-7: pSuperior vector did not protect HeLa cells from puromycin selection.
HeLa cells were mock transfected or transfected with 2 µg pSuperior vector plasmid DNA for 24 hours. Cells were then incubated in the absence or presence of 1 µg/ml puromycin for up to 36 hours after transfection. Cells were stained with crystal violet and ten fields at 20X magnification were counted to estimate the average number of cells remaining in each field at times indicated. Error bars represent standard deviations. All images were captured on a Zeiss Axiovert 200M microscope at 20X magnification, and analyzed using the Volocity software. (

To establish a more efficient puromycin selection scheme, a protocol was tested in which cells were placed under higher puromycin selection at 5 μg/ml for 24 hours after the initial 24-hour transfection period, followed by puromycin maintenance at either 1 or 2 μg/ml for up to additional 72 hours. Cell were stained with DAPI and counted using the Volocity software. We found pSuperior transfected cells were able to maintain a steady cell count when the initial selection phase was skipped and cells were maintained under 1 or 2 μg/ml of puromycin. This was in contrast to mock transfected controls where both 1 and 2 μg/ml of puromycin in the maintenance phase resulted in total cell death, despite no initial selection phase (Figure 4-9A). When the 5 μg/ml puromycin selection was applied prior to the maintenance phase, higher numbers of cells were lost as expected, but some pSuperior transfected cells were able to persist in contrast to significant decreases in mock transfected controls after 24 hour of maintenance (Figure 4-9B). Thus, HeLa cells required a more stringent puromycin selection scheme and the greater loss in cell counts post selection can be countered by increasing the initial population.

Prior to testing TFIIS knockdown by short hairpin RNA (shRNA) expression, we tested the antibodies that were used in the IF experiments for specificity on Western blots (Figure 4-10A-C, left panels). The 35kDa (TCEA1/2) and 38kDa (TCEA3) bands from fractionating HeLa whole cell lysates were visible but faint. In additional to the bands at the expected molecular weight, several strong bands of higher molecular weight were also observed. Because TFIIS proteins are not known to be post-translationally modified, these other protein species may be due to non-specific cross-reactivity. However because a faint band of the correct size could be detected in each case, protein levels in the knockdown experiments relative to vector controls were compared using these antibodies.

Short hairpin RNA (shRNA) inserts were cloned into the pSuperior vector to be expressed under a RNAP III promoter and the reduction in TFIIS protein levels in transfected cells was monitored. Four shRNA expression constructs were made for each of the three TFIIS isoforms and one WWP2-specific shRNA construct was made to account for possible off-target effects. HeLa cells were transfected for 24 hours,

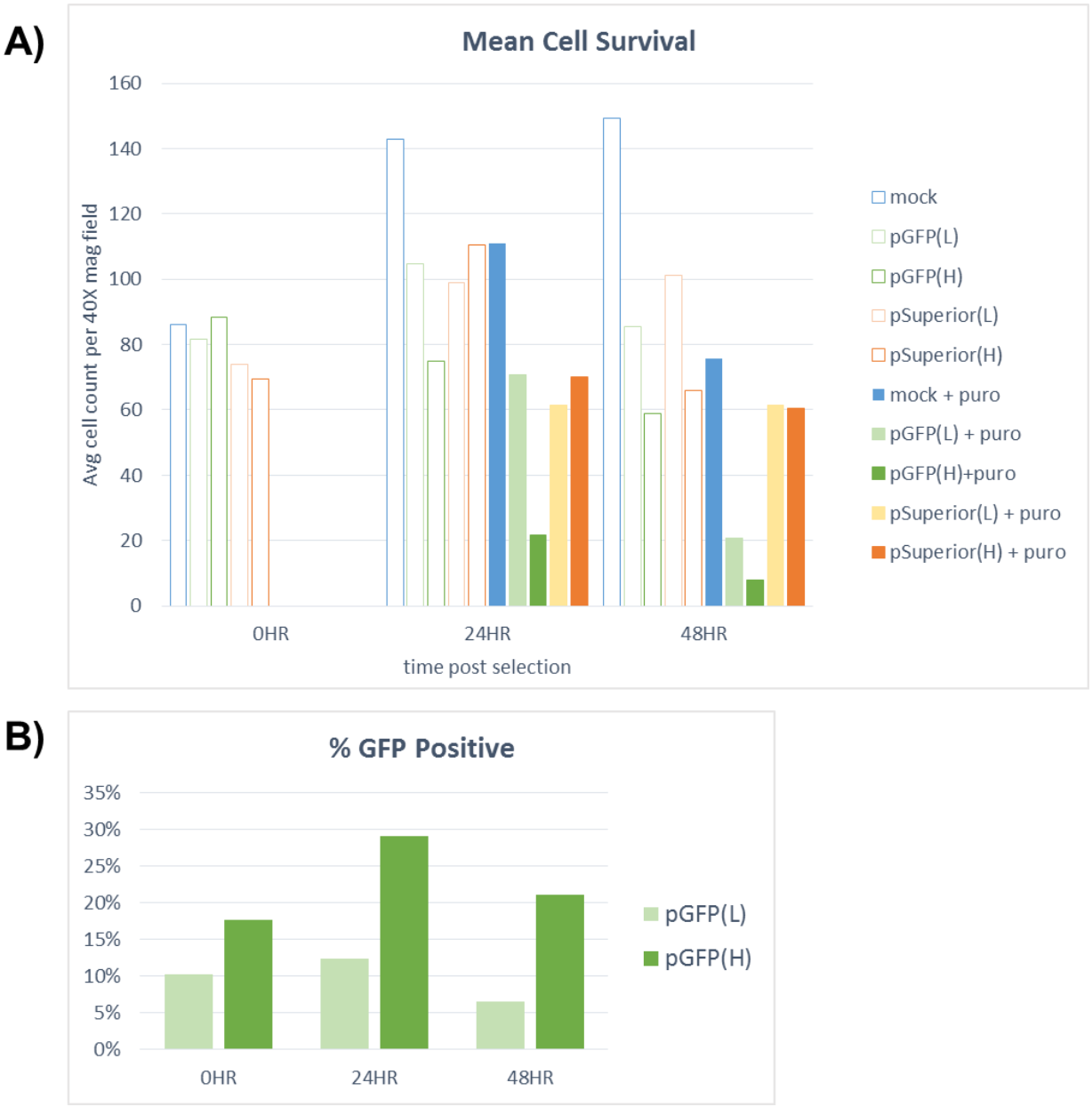

Figure 4-8: HeLa cells exhibited resistance to puromycin selection.
HeLa cells were mock transfected or transfected with either 0.5 µg (L) or 2 µg (H) pGFP or pSuperior vector plasmid DNA for 24 hours. Cells were incubated in the absence or presence or 1 µg/ml puromycin selection agent for up to 48 hours after transfection. **A)** Cells were stained with DAPI and ten fields at 40X magnification were counted to estimate the average number of cells remaining in each field at times indicated. **B)** GFP-positive cells were counted to estimate transfection efficiency in the experiment. Error bars represent standard error of means. All images were captured on a Zeiss Axiovert 200M microscope at 20X magnification, and analyzed using the Volocity software.

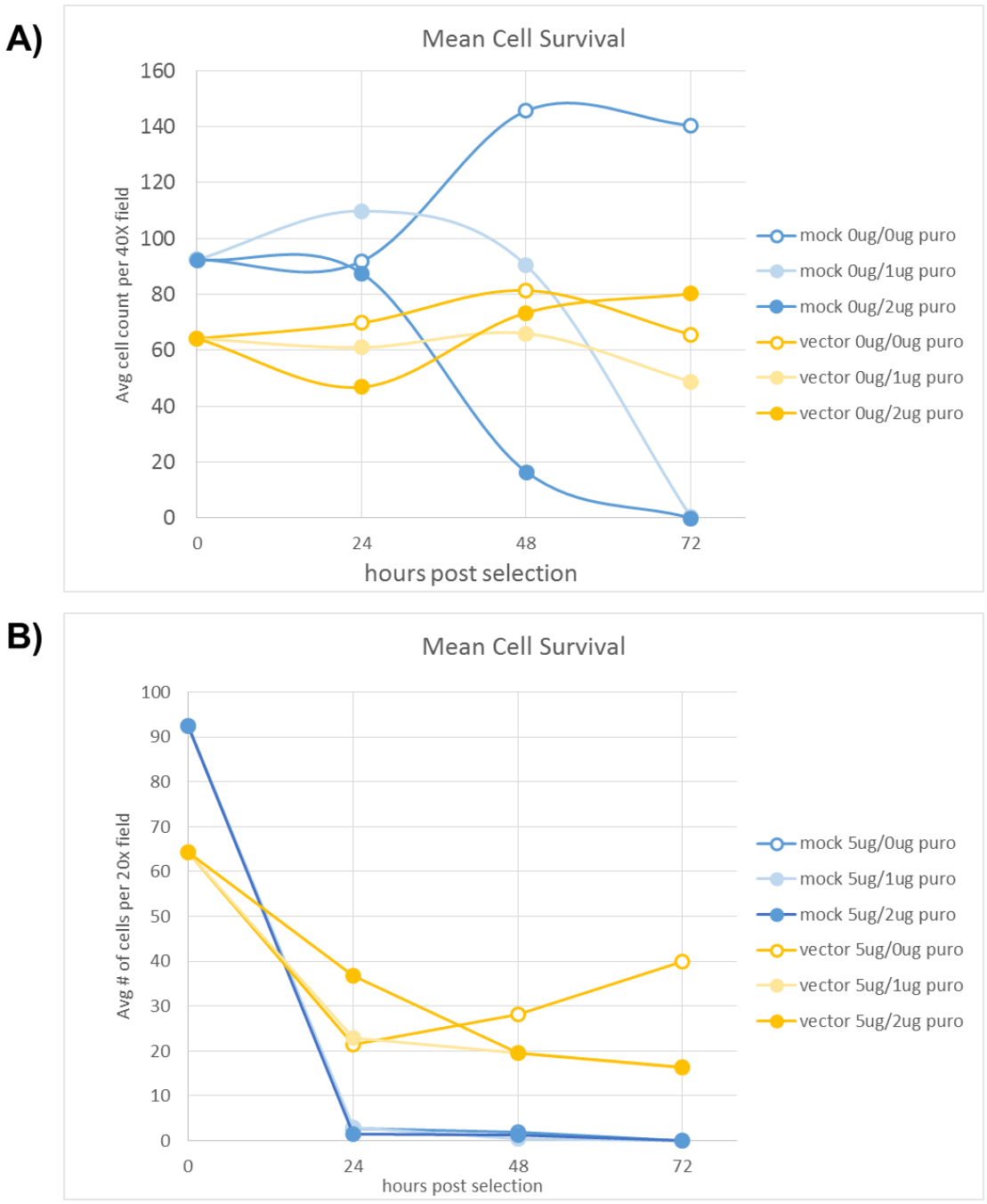

Figure 4-9: HeLa cells were unable to recover from strong puromycin selection.
HeLa cells were mock transfected or transfected with 2 µg pGFP or pSuperior vector plasmid DNA for 24 hours. Cells were then incubated in the **A)** absence or **B)** presence of 5 µg/ml puromycin selection agent for 24 hours after transfection. Cells were rinsed with PBS and then incubated in the absence or presence of 1 µg/ml or 2 µg/ml puromycin to maintain selection for additional 72 hours. Cells were stained with DAPI and ten fields at 40X magnification were counted to estimate the average number of cells remaining in each field at times indicated. All images were captured on a Zeiss Axiovert 200M microscope at 20X magnification, and analyzed using the Volocity software.

followed by a 24-hour 5 μg/ml puromycin selection period and cells were maintained on 1 μg/ml puromycin for an additional 48 hours after selection to ensure that only transfected cells survived. We found that none of the shRNA expression constructs was able to reduce its putative target protein level (Figure 4-10A-C, right panels) in these experiments based upon the Western blot analysis. In some cases, the Western blots showed that expression of some of the shRNA constructs actually resulted in higher putative target protein levels. These results again raised serious concerns as to the specificity of the antibodies used in these experiments.

To test the specificity of the antibodies, HeLa cells were transfected with FLAG-tagged TCEA constructs FLAG-TCEA1 or FLAG-TCEA2 for 48 hours and then mock infected or infected with WT HSV-1 for 8 hours. Cell lysates were analyze by Western blots. Cells transiently expressing FLAG-tag alone or FLAG-tagged cap-binding protein 80 (FLAG-CBP80) or hexamethylene bis-acetamide inducible protein 1 (FLAG-HEXIM1) served as controls (Figure 4-11). When the blot was probed with anti-FLAG antibody, strong signals were observed from HSV-1 infected cells expressing FLAG-CBP80, as well as cells expressing FLAG-TCEA1 and FLAG-TCEA2 at the expected molecular weight. FLAG-HEXIM1 appeared to be under-expressed in this experiment for reasons unknown. Probing the same blot with anti-TCEA1 antibody yielded similar banding patterns as before, with a double band at approximately 35 kDa. Not only was this was a mismatch to the 40 kDa band of FLAG-TCEA1 when probed with anti-FLAG antibody, the anti-TCEA1 antibody failed to pick up elevated TCEA1 protein levels in cells that were over expressing FLAG-TCEA1 (compare Figure 4-11A and B). These results provide strong evidence that the anti-TCEA1 antibody did not in fact recognize TCEA1 as its cognate target. A satisfactory signal from anti-TCEA2 Western blots could not be observed at the time of writing of this dissertation, but because a 37 kDa band was not observed in previous anti-TCEA2 blots, it is likely that this antibody also lacked specificity for its intended target protein.

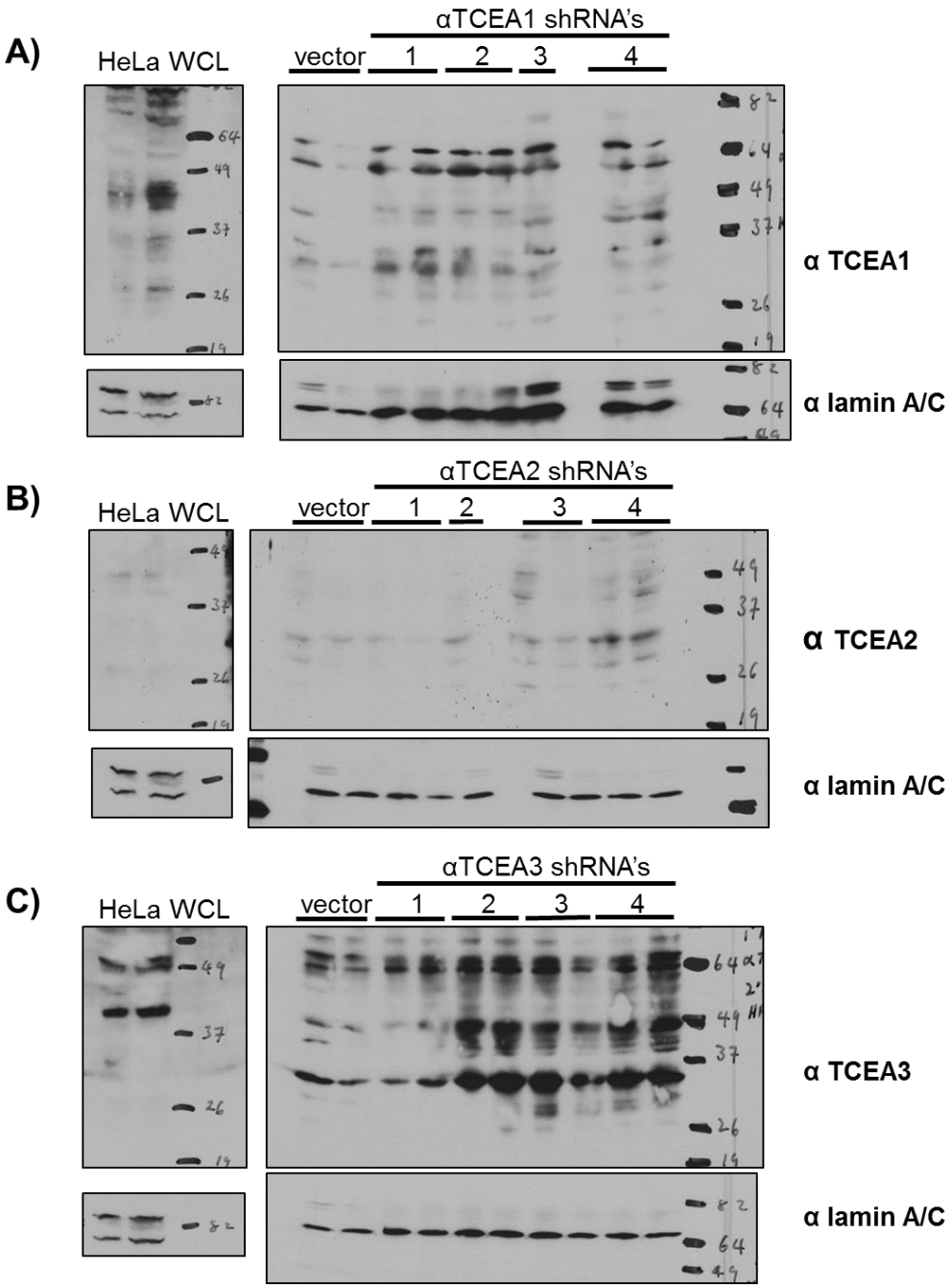

Figure 4-10: Multiple proteins reacted with anti-TFIIS antibodies in Western blot analysis.
HeLa cells were mock transfected or transfected with 2 µg of pSuperior derived constructs expressing shRNA targeting different TFIIS isoforms (TCEA1-3) for 48 hours. Whole cells lysates were prepared at times indicated and fractionated on 10% SDS-polyacrylamide gels and probed with either anti-TCEA1, anti-TCEA2, or anti-TCEA3 primary antibody in Western blot analysis. Lamin A/C served as loading control in each experiment.

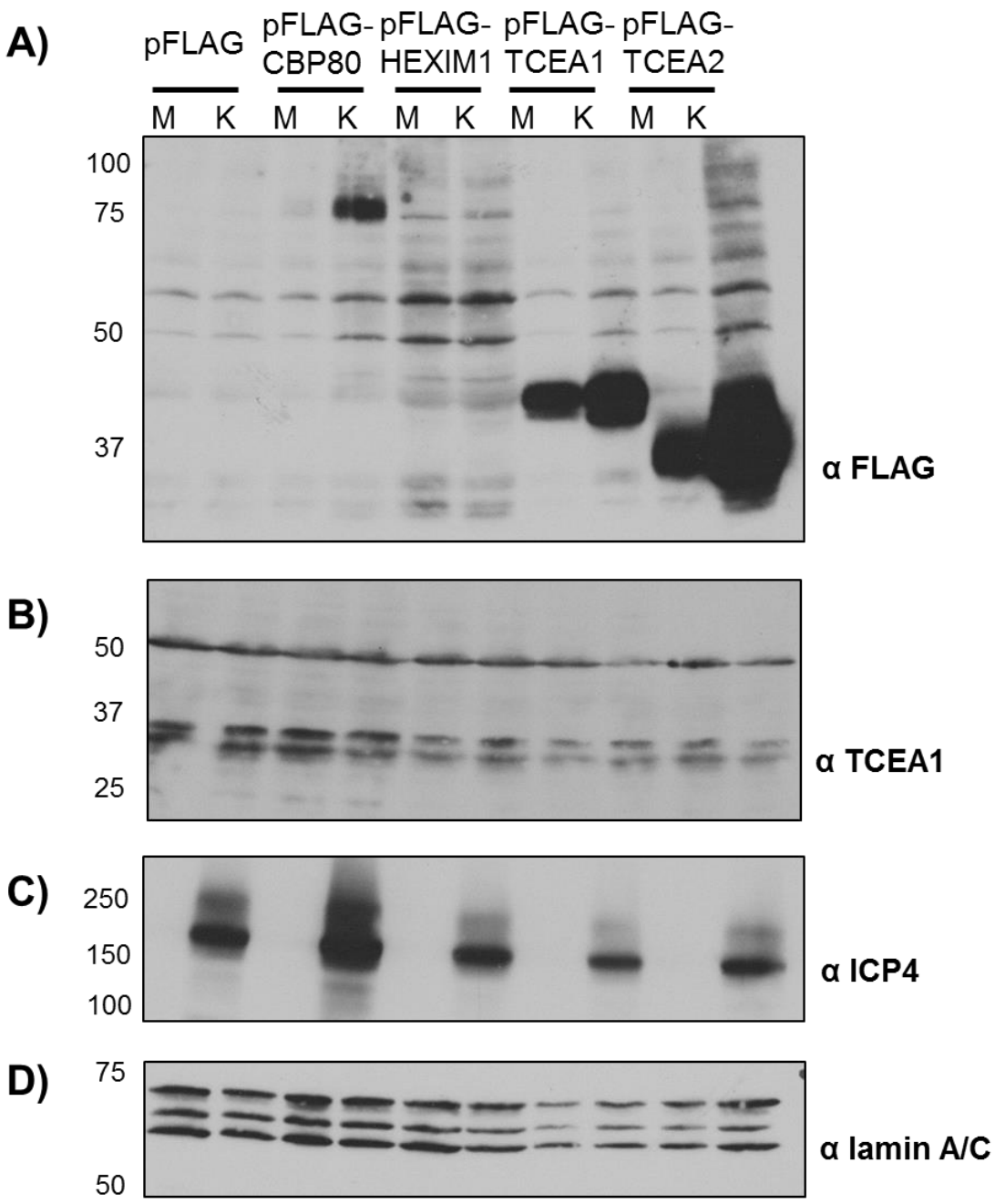

Figure 4-11: Anti-TCEA1 antibody cross-reacted nonspecifically.
HeLa cells overexpressing FLAG-tagged proteins were mock infected (M) or infected with WT HSV-1 (K) at MOI of 10 for 8 hours. Whole cell lysates were prepared and fractionated on 5-15% SDS-PAGE gels and probed with **A)** anti-FLAG and **B)** anti-TCEA1 primary antibodies in Western blot analysis. **C)** ICP4 served as infection control and **D)** lamin A/C served as loading control.

Discussion

Transcription and DNA repair have been known to be linked for a long time and many studies have shown that the cell repairs DNA damage on the strand being transcribed for transcriptionally active genes faster than the non-transcribed strand or on transcriptionally silent regions of the genome (52,88,104). The TC-NER pathway is not only a defense for genome stability, but also appears to protect cells from p53-mediated apoptosis by preventing persistent blockage of elongating RNAP II (52,73). While the TC-NER pathway is an important defense mechanism for the cell against DNA lesions, it is also important for the cell not to mark paused RNAP II as being arrested, which can then lead to proteasomal degradation of the polymerase as well as unfinished transcripts. The GTF TFIIS stimulates RNAP II elongation through its RNase H activity and helps to maintain proper alignment of the DNA-RNAP II-RNA complex after polymerase pausing.

In the current study, we investigated whether or not TFIIS is involved in HSV-1 transcription based on the model of colliding RNAP II complexes being cleared by proteasomal degradation when viral transcriptional activity is high. Prior to degradation, elongation stimulating factors such as TFIIS could be recruited to arrested RNAP II to attempt to restart transcription. Although preliminary evidence suggested that one of the isoforms of TFIIS might be re-localized to HSV-1 transcription compartments in the IF experiments, higher resolution confocal co-localization studies did not show consistent co-localization patterns between TFIIS and RNAP II nor between TFIIS and viral transcription-replication compartments. Functional knockdown experiments were unsuccessful as well, however, interpretation of the knockdown experiments was clouded by the lack of specificity of the three commercial antibodies that were used to detect TCEA isoforms. Several strong bands of both higher and lower molecular weight than predicted for TCEA proteins were seen on each blot so that identification of the correct band was not possible. Further, TCEA1 and TCEA2 antibodies failed to recognize FLAG-tagged TCEA1 and TCEA2 on Western blots, casting further doubt about the specificity of these antibodies. This result also brings into question all of

the co-localization studies using immunofluorescence because it is unclear which cellular proteins were being stained with these relatively nonspecific antibodies.

While these studies provided no evidence that TFIIS is involved in HSV-1 transcription, because of the importance of TC-NER in the cell, it may be worth examining other components in the pathway. Two mechanisms have been proposed for the resolution of arrested RNAP II at the arrest site to allow access to the repair components in the pathway (158). In one model, the Cockayne syndrome protein B (CSB), a SWI/SNF-like enzyme translocates the arrested RNAP II on the DNA template to allow repair components access to the DNA lesion. Cells with dysfunctional CSB proteins are severely impaired in DNA repair and are unable to recover RNA synthesis following DNA damage. If the collision model is correct, we might expect to see a higher degree of association between RNAP II and CSB during HSV-1 infection. We would not predict that CSB plays a functional role in HSV-1 transcription since the arrest of RNAP II is due to collision of transcription complexes rather than DNA damage. The alternative mechanism in which the RNAP II translocation by the action of CSB proves to be insufficient or impossible, then the polymerase is removed by proteolysis (91,129). In this pathway, the CSA protein, an E3 ubiquitin ligase, polyubiquitinates RNAP II to mark the polymerase for degradation. The COP9 signalsome complex (CSN) has been found to interact with the CSA-Cullin4A complex to inhibit the E3 ubiquitin ligase activity of CSA (77). Because degradation of stalled elongating RNAP II appears to be beneficial for productive HSV-1 infection, inhibition of CSA E3 ubiquitin ligase activity either by a CSA knockout or overexpression of CSN components might also negatively impact viral yield. An overexpression of CSA in HSV-1 infected cells could also prove to be interesting. Though the RNAP II collision model proposes that the removal of stalled RNAP II by the proteasome is necessary to resolve arrested transcription complexes, there must be a minimum level of RNAP II required to sustain the high level of viral transcription in HSV-1 infected cells. Would an increase in CSA activity tip the balance against the virus by accelerating proteolysis of RNAP II?

Materials and Methods

Cells, viral strains, and virus infection

HeLa cells were grown on minimal essential medium (MEM) containing 10% newborn calf serum. Rabbit skin fibroblasts (RSF) and Vero cells were grown on minimal essential medium supplemented with 8% fetal calf serum and 4% donor calf serum. HSV-1 wild-type (WT) strain KOS was described previously. HeLa cells were infected with WT HSV-1 KOS as indicated at a multiplicity of infection (MOI) of 10 and were incubated at 37°C for the times indicated in the figure legends.

shRNA expression vector construction, transfection and puromycin selection

pSuperior (OligoEngine) based shRNA expression plasmids TFIIS isoforms were constructed by insertions of target-specific sequences according to manufacturer's protocol. The insertion sequences were designed using the siDESIGN Center tool (GE Dharmcon). For puromycin selection experiments, plasmid DNA was transfected into cells using Lipofectamine 2000 reagent (Invitrogen) according to the manufacturer's protocol for 24 hours, then incubated in MEM supplemented with puromycin selective agent at concentrations indicated in figures. Cells were either stained with crystal violet or DAPI to facilitate imaging using a Zeiss Axiovert 200M microscope. Cell counts were estimated using Volocity software (Perkin Elmer). Experiments were performed in triplicate and at least three fields were counted for each. For transfection/infection experiments, plasmid DNA was transfected into cells for 24 hours, then infected with WT HSV-1 KOS for 8 hours.

Western blot analysis

HeLa cells were transfected and then infected as indicated in the figure legends. At the times indicated, cells were washed with cold phosphate-buffered saline (PBS) and harvested in cold PBS supplemented with protease inhibitors (4 mM Pefabloc® and 0.1 mg/ml leupectin). Cells were pelleted by centrifugation at 5,000 RPM for 3 minutes at 4°C and resuspended in low-salt lysis buffer (10 mM Tris-HCl, pH 7.5, 3 mM $CaCl_2$, 2 mM $MgCl_2$, 0.5% NP-40) for 5 minutes then lysed by syringe passages. NaCl was

added to each sample to final concentration of 500 mM. Whole cell lysates (WCL) were quantified for total protein content in triplicate by Bradford assays (Coomassie Plus, Thermo Scientific) according to manufacturer's protocol. Sample aliquots containing 30 µg of total protein were diluted with low-salt lysis buffer to final volume of 90 µl and mixed with 6X ESS loading buffer (350 mM Tris-HCl, 600 mM DTT, 10% SDS, 30% glycerol, 0.125% bromophenol blue), as described previously. WCL were fractionated on 5-15% gradient sodium dodecyl sulfate polyacrylamide gels (SDS-PAGE) and transferred to nitrocellulose membranes. Membranes were probed as described previously. Primary antibodies used for immuno-blotting were as follows: mouse monoclonal anti-TCEA1 (Abcam) at 1:500; rabbit polyclonal anti-TCEA2 (Abcam) at 1:500; mouse monoclonal anti-TCEA3 (Abnova) at 1:2,000; mouse monoclonal anti-FLAG epitope M2 (Sigma- Aldrich) at 1:1,000; rabbit polyclonal anti-Lamin A/C (Cell Signaling Technology) at 1:2,000; mouse monoclonal anti-ICP4 (P1101; Virusys) at 1:5,000.

Immunofluorescence confocal microscopy

HeLa cells grown on glass cover slips were infected as described in the figure legends. Cells were either untreated or were incubated with MEM supplemented with 20 µg/ml α-amanitin as indicated in the figure legends. Cells were fixed with 3.7% formaldehyde at the times indicated and immunofluorescent staining was performed as described previously. Cells were stained with anti-TCEA1 (Abcam) at 1:50; anti-TCEA2 (Abnova) at 1:50; anti-TCEA3 (Abnova) at 1:100; anti-RNAP II antibody ARNA3 (EMD Millipore) at 1:50; anti-ICP4 (P1101) at 1:500. Alexa Fluor® conjugated anti-mouse IgG subtype specific secondary antibodies were used to recognize primary antibodies as described in figures. Z-stacks were captured in 1.0 µm optical slices with 0.5 µm overlapping in between slices using a Zeiss LSM510 confocal microscope with a 63X oil immersion objective. Z-stacks were de-convoluted and analyzed for co-localized pixels in the Volocity software.

RNA extraction, cDNA synthesis, and quantitative PCR

HeLa cells were infected as described in the figures and total RNA was extracted at the times indicated using the TRIzol® reagent (Life Technologies) according to the manufacturer's protocol. Total RNA was quantified using a NanoDrop® ND-1000 spectrophotometer (Thermo Scientific) prior to reverse transcription. 1 µg of total RNA was reverse transcribed into cDNA using the iScript™ cDNA synthesis kit (Bio-Rad) according to manufacturer's protocol. qPCR analysis was performed using 2 µl of cDNA template DNA, 2 pmole each of the forward and reverse primer, and 10 µl of the 2X iQ™ SYBR® Green Supermix (Bio-Rad Laboratories) on a Bio-Rad MyiQ real-time PCR detection system. Serially diluted known quantities of pCMV-3tag-TCEA1 or pCMV-3tag-TCEA2 plasmid served as standard curves to quantify TCEA1 and TCEA2 transcript levels respectively. Three independent experiments were analyzed by qPCR in triplicates. PCR primer sequences can be found in Table 4-1.

Table 4-1: TCEA1/2 qPCR primers

Gene	Segment	Primers	
		Forward	Reverse
TCEA1	Proximal CDS	5’ CTATTCGCAAGCAGAGTACAGATG 3’	5’ CAAGGTCTTTCTCAGTTGATGGC 3’
	Distal CDS	5’ AAAGAAGCCATCAGAGAGCATCAG 3’	5’ TGTCATTGGTTCATCAGCACTACG 3’
TCEA2	Proximal CDS	5’ GGATGTCTGTCAACGCCCTTC 3’	5’ CCCGCTCCCTGGCTTTGG 3’
	Distal CDS	5’ GCGGCGGAATGTGCTGTG 3’	5’ TCTGGTGCTCTCGGATGGC 3’

Chapter 5
The Collision Model of RNAP II in HSV-1 infection

The studies detailed in this thesis began with the observations of an intermediately phosphorylated RNAP II in HSV-1 infected cells by the Rice laboratory and work done by our own lab revealing that elongating RNAP II is degraded at late times in HSV-1 infection. Work from the Rice lab have subsequently discovered another mechanism by which the serine-2 elongating form of RNAP II is decreased through the action of a HSV-1 protein ICP22, although the details have not yet been elucidated. Other groups also have reported results that might implicate viral kinases U_L13 and U_S3 in affecting the phosphorylation state of RNAP II, but to date, phosphorylation sites on RNAP II CTD specific to HSV-1 infected cells have not been identified. Nevertheless, it is attractive to think that perhaps the virus modifies RNAP II differently from its host cell and this somehow tilts in favor of the expression of viral genes. It seems unusual and puzzling that HSV-1 would induce a degradation of the polymerase that it requires for its own gene expression at a time of highly active viral gene expression. Furthermore, we can observe the degradation of elongating RNAP II starting at about six hours post infection, before the completion of viral replication cycle at around sixteen hours post infection in cell culture models. Dai-Ju *et al*. prevented RNAP II degradation with proteasome inhibitors and found that it had a negative effect on the yield of viral progeny and on late protein levels. These results led to the proposal of the collision model that is central to this thesis.

The collision model proposes that the combination of a compact genome with many nested ORFs and highly active transcription could lead to collisions of RNAP II complexes that are transcribing the HSV-1 genome. These collisions if left unresolved, can lead to RNAP IIs becoming arrested on the viral genome and could trigger proteasomal degradation to clear the stalled complexes. At the start of the infection, only five IE genes are actively transcribed and levels of RNAP II remain similar to uninfected cells. At about five hours post infection, viral DNA synthesis begins and early gene expression is starting to peak while

late gene transcription begins. These events coincide with the appearance of the intermediately phosphorylated RNAP II described by the Rice lab and the first noticeable decrease of elongating RNAP II in cells infected with WT HSV-1. As infection progresses, DNA synthesis continues and by eight hours post infection, the entire HSV-1 genome is actively transcribed. By this time, the phospho-serine 2 form of RNAP II is significantly decreased as measured by by Western blot analysis. Overall, the amount of activity on the HSV-1 genome appears to have an inverse relationship with the level of elongating RNAP II in infected cells, and indeed, inhibiting viral transcription did prevent RNAP II degradation.

The intermediately phosphorylated RNAP II first described by the Rice lab could well be at least partially responsible for a dwindling population of phospho-serine-2 RNAP II. The sites of phosphorylation of this intermediate form have not been elucidated. The HSV-1 kinase U_L13 has been shown by the Rice group to be required, along with ICP22 for the detection of the intermediate form. It has also been shown by the Blaho group that this form is not apparent in all cell types. The intermediate form is more apparent in Vero cells compared to HeLa cells and HEL cells. Further, deletion of ICP22, which results in the disappearance of the intermediate form does not have a significant effect on HSV-1 transcription in primate cell lines, although there is a host range effect with ICP22 deletion mutants replicating poorly in hamster cell lines.

Because there is a pronounced decrease in the serine-2 phosphorylated form of RNAP II during HSV-I infection, Rice and his colleagues postulated that this form might not be required during infection for viral transcription. To test the notion that HSV-1 transcription elongation might not require RNAP II phosphorylated at serine 2 residues, we tested the effects on HSV-1 transcription of inhibiting CDK9, the cellular kinase that is responsible for this modification. In experiments detailed in Chapter 2, we found that inhibiting CDK9 kinase activity through small molecules DRB and flavopiridol strongly affected HSV-1 nascent RNA synthesis and mRNA accumulation in a negative way. Overexpression of HEXIM1, an endogenous CDK9 negative regulator, or expression of CDK9 harboring a kinase-dead mutation, had

similar effects. Not surprisingly, inhibition of CDK9 reduced viral progeny yields by almost 100-fold. Our results strongly suggest that CDK9 kinase activity, and therefore phosphorylation of serine 2 residues on RNAP II CTD is required in HSV-1 transcription as it is in its host cell. Instead of a novel form of RNAP II induced by HSV-1, the intermediately phosphorylated RNAP II perhaps results from the combination of proteasomal degradation of elongating RNAP II and heightened cycling of RNAP II between hyperphosphorylated forms during initiation and elongation and hypophosphorylated forms for pre-initiation in infected cells.

To truly substantiate the collision model in HSV-1 infected cells, it is important to determine if RNAP II complexes are stalled on the viral genome at times when transcription is highly active. We attempted ChIP-qPCR analysis of two gene clusters in the viral genome in Chapter 3. The optimization experiment results showed promising efficiency for four of the anti-RNAP II antibodies, but the actual experimental results were inconsistent and there was a high signal to noise ratio. The 4H8 antibody was the only antibody that gave somewhat consistent results, but only the Early UL39/40 gene cluster results matched their expected expression profile. The Late UL44 gene cluster did not show a RNAP II occupancy map expected of its expression profile and the quality of the data was questionable. We have failed find direct evidence that transcribing RNAP II complexes collide at late times in HSV-1 infected cells. A more comprehensive approach of RNA-seq analysis might be more fruitful in the future.

The collision model of elongating RNAP II in HSV-1 infected cells may have similarities to transcription-coupled DNA repair. DNA repair has been long been known to be coupled with transcription, and actively transcribing genes are repaired faster than silent ones. Although it has been shown to stimulate RNAP II elongation, the GTF TFIIS has been recently been suggested to be one of the “sensors” in the transcription-coupled DNA repair pathway. We explored the potential involvement of TFIIS in HSV-1 transcription in Chapter 4. Preliminary results showed that one of the TFIIS isoforms relocalized to the nuclei of HSV-1 infected cells and suggested that TFIIS might colocalize with viral transcription-replication

compartments. Higher resolution confocal analysis however, found inconsistent co-localization patterns between TFIIS and RNAP II and the confocal results did not support the preliminary studies that suggested that TFIIS co-localized with viral transcription-replication compartments. When attempting to perform functional analysis by knocking down TFIIS, we discovered that the antibodies we were using lack the specificities claimed by the manufacturers. This of course, nullified our initial results. At this time, we do not have any data supporting the notion that TFIIS functions as a sensor protein as it does in transcription-coupled DNA repair, during HSV-1 infection.

In summary, this thesis investigated aspects of the collision model of elongating RNAP II during HSV-1 lytic infection. We provided support that viral transcription required RNAP II CTD phosphorylation at serine 2 residues by CDK9 (Chapter 2), attempted to assess RNAP II occupancy on the viral genome during lytic infection (Chapter 3), and explored possible involvement of TFIIS, a host cell component of the transcription-coupled DNA repair pathway (Chapter 4). While we could not draw definitive conclusions from the ChIP-qPCR analysis, we were able to generate ChIP results that matched the expected expression profile of an Early viral gene, even at late times in infection when RNAP II levels are low. With refinement of the protocol and expanded genome coverage, better insight might be gained on RNAP II occupancy on the HSV-1 genome. An unexpected result from the experiment was that viral DNA appeared to replicate at a faster pace than viral transcription in this experiment. This finding is preliminary and would benefit from the proposed expansion in scope. The results on TFIIS in HSV-1 infected cells might have been an artifact of the nonspecific antibodies that were used. It is still possible that the collision model is linked to the transcription-coupled DNA repair pathway and exploration of other components in the pathway could prove to be a worthwhile endeavor in the future.

Reference List

1. **Ahn, S. H., M. Kim, and S. Buratowski**. 2004. Phosphorylation of serine 2 within the RNA polymerase II C-terminal domain couples transcription and 3' end processing. Mol.Cell **13**:67-76. doi:S1097276503004921 [pii].

2. **Akoulitchev, S., T. P. Makela, R. A. Weinberg, and D. Reinberg**. 1995. Requirement for TFIIH kinase activity in transcription by RNA polymerase II. Nature **377**:557-560. doi:10.1038/377557a0 [doi].

3. **Akoulitchev, S. and D. Reinberg**. 1998. The molecular mechanism of mitotic inhibition of TFIIH is mediated by phosphorylation of CDK7. Genes Dev. **12**:3541-3550.

4. **Allison, L. A., J. K. Wong, V. D. Fitzpatrick, M. Moyle, and C. J. Ingles**. 1988. The C-terminal domain of the largest subunit of RNA polymerase II of Saccharomyces cerevisiae, Drosophila melanogaster, and mammals: a conserved structure with an essential function. Mol.Cell Biol. **8**:321-329.

5. **Anindya, R., O. Aygun, and J. Q. Svejstrup**. 2007. Damage-induced ubiquitylation of human RNA polymerase II by the ubiquitin ligase Nedd4, but not Cockayne syndrome proteins or BRCA1. Mol.Cell **28**:386-397. doi:S1097-2765(07)00671-5 [pii];10.1016/j.molcel.2007.10.008 [doi].

6. **Archambault, J., F. Lacroute, A. Ruet, and J. D. Friesen**. 1992. Genetic interaction between transcription elongation factor TFIIS and RNA polymerase II. Mol.Cell Biol. **12**:4142-4152.

7. **Aso, T., J. W. Conaway, and R. C. Conaway**. 1995. The RNA polymerase II elongation complex. FASEB J. **9**:1419-1428.

8. **Awrey, D. E., N. Shimasaki, C. Koth, R. Weilbaecher, V. Olmsted, S. Kazanis, X. Shan, J. Arellano, C. H. Arrowsmith, C. M. Kane, and A. M. Edwards**. 1998. Yeast transcript elongation factor (TFIIS), structure and function. II: RNA polymerase binding, transcript cleavage, and read-through. J Biol.Chem. **273**:22595-22605.

9. **Baradaran, K., C. E. Dabrowski, and P. A. Schaffer**. 1994. Transcriptional analysis of the region of the herpes simplex virus type 1 genome containing the UL8, UL9, and UL10 genes and identification of a novel delayed-early gene product, OBPC. J.Virol. **68**:4251-4261.

10. **Barboric, M. and B. M. Peterlin**. 2005. A new paradigm in eukaryotic biology: HIV Tat and the control of transcriptional elongation. PLoS.Biol. **3**:e76. doi:10.1371/journal.pbio.0030076 [doi].

11. **Bastian, T. W. and S. A. Rice**. 2009. Identification of sequences in herpes simplex virus type 1 ICP22 that influence RNA polymerase II modification and viral late gene expression. J.Virol. **83**:128-139. doi:JVI.01954-08 [pii];10.1128/JVI.01954-08 [doi].

12. **Bataille, A. R., C. Jeronimo, P. E. Jacques, L. Laramee, M. E. Fortin, A. Forest, M. Bergeron, S. D. Hanes, and F. Robert**. 2012. A universal RNA polymerase II CTD cycle is orchestrated by complex interplays between kinase, phosphatase, and isomerase enzymes along genes. Mol.Cell **45**:158-170. doi:S1097-2765(11)00951-8 [pii];10.1016/j.molcel.2011.11.024 [doi].

13. **Batterson, W., D. Furlong, and B. Roizman**. 1983. Molecular genetics of herpes simplex virus. VIII. further characterization of a temperature-sensitive mutant defective in release of viral DNA and in other stages of the viral reproductive cycle. J.Virol. **45**:397-407.

14. **Baumli, S., J. A. Endicott, and L. N. Johnson**. 2010. Halogen bonds form the basis for selective P-TEFb inhibition by DRB. Chem.Biol. **17**:931-936. doi:S1074-5521(10)00312-1 [pii];10.1016/j.chembiol.2010.07.012 [doi].

15. **Baumli, S., G. Lolli, E. D. Lowe, S. Troiani, L. Rusconi, A. N. Bullock, J. E. Debreczeni, S. Knapp, and L. N. Johnson**. 2008. The structure of P-TEFb (CDK9/cyclin T1), its complex with flavopiridol and regulation by phosphorylation. EMBO J. **27**:1907-1918. doi:emboj2008121 [pii];10.1038/emboj.2008.121 [doi].

16. **Bentley, D.** 1999. Coupling RNA polymerase II transcription with pre-mRNA processing. Curr.Opin.Cell Biol. **11**:347-351. doi:S0955-0674(99)80048-9 [pii];10.1016/S0955-0674(99)80048-9 [doi].

17. **Bentley, D. L.** 2005. Rules of engagement: co-transcriptional recruitment of pre-mRNA processing factors. Curr.Opin.Cell Biol. **17**:251-256. doi:S0955-0674(05)00048-7 [pii];10.1016/j.ceb.2005.04.006 [doi].

18. **Bigalke, J. M., S. A. Dames, W. Blankenfeldt, S. Grzesiek, and M. Geyer**. 2011. Structure and dynamics of a stabilized coiled-coil domain in the P-TEFb regulator Hexim1. J.Mol.Biol. **414**:639-653. doi:S0022-2836(11)01146-6 [pii];10.1016/j.jmb.2011.10.022 [doi].

19. **Biglione, S., S. A. Byers, J. P. Price, V. T. Nguyen, O. Bensaude, D. H. Price, and W. Maury**. 2007. Inhibition of HIV-1 replication by P-TEFb inhibitors DRB, seliciclib and flavopiridol correlates with release of free P-TEFb from the large, inactive form of the complex. Retrovirology. **4**:47. doi:1742-4690-4-47 [pii];10.1186/1742-4690-4-47 [doi].

20. **Boutell, C. and R. D. Everett**. 2013. Regulation of alphaherpesvirus infections by the ICP0 family of proteins. J.Gen.Virol. **94**:465-481. doi:vir.0.048900-0 [pii];10.1099/vir.0.048900-0 [doi].

21. **Brannan, K. and D. L. Bentley**. 2012. Control of Transcriptional Elongation by RNA Polymerase II: A Retrospective. Genet.Res.Int. **2012**:170173. doi:10.1155/2012/170173 [doi].

22. **Bres, V., S. M. Yoh, and K. A. Jones**. 2008. The multi-tasking P-TEFb complex. Curr.Opin.Cell Biol. **20**:334-340. doi:S0955-0674(08)00080-X [pii];10.1016/j.ceb.2008.04.008 [doi].

23. **Brody, Y., N. Neufeld, N. Bieberstein, S. Z. Causse, E. M. Bohnlein, K. M. Neugebauer, X. Darzacq, and Y. Shav-Tal**. 2011. The in vivo kinetics of RNA polymerase II elongation during co-transcriptional splicing. PLoS.Biol. **9**:e1000573. doi:10.1371/journal.pbio.1000573 [doi].

24. **Buratowski, S. and P. A. Sharp**. 1990. Transcription initiation complexes and upstream activation with RNA polymerase II lacking the C-terminal domain of the largest subunit. Mol.Cell Biol. **10**:5562-5564.

25. **Chapman, R. D., M. Heidemann, T. K. Albert, R. Mailhammer, A. Flatley, M. Meisterernst, E. Kremmer, and D. Eick**. 2007. Transcribing RNA polymerase II is phosphorylated at CTD residue serine-7. Science **318**:1780-1782. doi:318/5857/1780 [pii];10.1126/science.1145977 [doi].

26. **Chen, H., X. Contreras, Y. Yamaguchi, H. Handa, B. M. Peterlin, and S. Guo**. 2009. Repression of RNA polymerase II elongation in vivo is critically dependent on the C-terminus of Spt5. PLoS.One. **4**:e6918. doi:10.1371/journal.pone.0006918 [doi].

27. **Chen, I. H., L. Li, L. Silva, and R. M. Sandri-Goldin**. 2005. ICP27 recruits Aly/REF but not TAP/NXF1 to herpes simplex virus type 1 transcription sites although TAP/NXF1 is required for ICP27 export. J.Virol. **79**:3949-3961. doi:79/7/3949 [pii];10.1128/JVI.79.7.3949-3961.2005 [doi].

28. **Chen, I. H., K. S. Sciabica, and R. M. Sandri-Goldin**. 2002. ICP27 interacts with the RNA export factor Aly/REF to direct herpes simplex virus type 1 intronless mRNAs to the TAP export pathway. J.Virol. **76**:12877-12889.

29. **Cho, E. J., M. S. Kobor, M. Kim, J. Greenblatt, and S. Buratowski**. 2001. Opposing effects of Ctk1 kinase and Fcp1 phosphatase at Ser 2 of the RNA polymerase II C-terminal domain. Genes Dev. **15**:3319-3329. doi:10.1101/gad.935901 [doi].

30. **Cho, H., T. K. Kim, H. Mancebo, W. S. Lane, O. Flores, and D. Reinberg**. 1999. A protein phosphatase functions to recycle RNA polymerase II. Genes Dev. **13**:1540-1552.

31. **Cho, W. K., M. K. Jang, K. Huang, C. A. Pise-Masison, and J. N. Brady**. 2010. Human T-lymphotropic virus type 1 Tax protein complexes with P-TEFb and competes for Brd4 and 7SK snRNP/HEXIM1 binding. J.Virol. **84**:12801-12809. doi:JVI.00943-10 [pii];10.1128/JVI.00943-10 [doi].

32. **Christofori, G. and W. Keller**. 1989. Poly(A) polymerase purified from HeLa cell nuclear extract is required for both cleavage and polyadenylation of pre-mRNA in vitro. Mol.Cell Biol. **9**:193-203.

33. **Cojocaru, M., C. Jeronimo, D. Forget, A. Bouchard, D. Bergeron, P. Cote, G. G. Poirier, J. Greenblatt, and B. Coulombe**. 2008. Genomic location of the human RNA polymerase II general machinery: evidence for a role of TFIIF and Rpb7 at both early and late stages of transcription. Biochem J **409**:139-147. doi:BJ20070751 [pii];10.1042/BJ20070751 [doi].

34. **Cook, W. J. and D. M. Coen**. 1996. Temporal regulation of herpes simplex virus type 1 UL24 mRNA expression via differential polyadenylation. Virology **218**:204-213. doi:S0042-6822(96)90180-4 [pii];10.1006/viro.1996.0180 [doi].

35. **Cook, W. J., K. K. Wobbe, J. Boni, and D. M. Coen**. 1996. Regulation of neighboring gene expression by the herpes simplex virus type 1 thymidine kinase gene. Virology **218**:193-203. doi:S0042-6822(96)90179-8 [pii];10.1006/viro.1996.0179 [doi].

36. **Dahmus, M. E.** 1996. Reversible phosphorylation of the C-terminal domain of RNA polymerase II. J.Biol.Chem. **271**:19009-19012.

37. **Dai-Ju, J. Q., L. Li, L. A. Johnson, and R. M. Sandri-Goldin**. 2006. ICP27 interacts with the C-terminal domain of RNA polymerase II and facilitates its recruitment to herpes simplex virus 1

transcription sites, where it undergoes proteasomal degradation during infection. J.Virol. **80**:3567-3581. doi:80/7/3567 [pii];10.1128/JVI.80.7.3567-3581.2006 [doi].

38. **Danko, C. G., N. Hah, X. Luo, A. L. Martins, L. Core, J. T. Lis, A. Siepel, and W. L. Kraus**. 2013. Signaling pathways differentially affect RNA polymerase II initiation, pausing, and elongation rate in cells. Mol.Cell **50**:212-222. doi:S1097-2765(13)00171-8 [pii];10.1016/j.molcel.2013.02.015 [doi].

39. **Darzacq, X., Y. Shav-Tal, T. de, V, Y. Brody, S. M. Shenoy, R. D. Phair, and R. H. Singer**. 2007. In vivo dynamics of RNA polymerase II transcription. Nat.Struct.Mol.Biol. **14**:796-806. doi:nsmb1280 [pii];10.1038/nsmb1280 [doi].

40. **Doyle, O., J. L. Corden, C. Murphy, and J. G. Gall**. 2002. The distribution of RNA polymerase II largest subunit (RPB1) in the Xenopus germinal vesicle. J.Struct.Biol. **140**:154-166. doi:S1047847702005476 [pii].

41. **Durand, L. O., S. J. Advani, A. P. Poon, and B. Roizman**. 2005. The carboxyl-terminal domain of RNA polymerase II is phosphorylated by a complex containing cdk9 and infected-cell protein 22 of herpes simplex virus 1. J.Virol. **79**:6757-6762. doi:79/11/6757 [pii];10.1128/JVI.79.11.6757-6762.2005 [doi].

42. **Durand, L. O. and B. Roizman**. 2008. Role of cdk9 in the optimization of expression of the genes regulated by ICP22 of herpes simplex virus 1. J.Virol. **82**:10591-10599. doi:JVI.01242-08 [pii];10.1128/JVI.01242-08 [doi].

43. **Egloff, S. and S. Murphy**. 2008. Cracking the RNA polymerase II CTD code. Trends Genet. **24**:280-288. doi:S0168-9525(08)00128-5 [pii];10.1016/j.tig.2008.03.008 [doi].

44. **Egloff, S., D. O'Reilly, R. D. Chapman, A. Taylor, K. Tanzhaus, L. Pitts, D. Eick, and S. Murphy**. 2007. Serine-7 of the RNA polymerase II CTD is specifically required for snRNA gene expression. Science **318**:1777-1779. doi:318/5857/1777 [pii];10.1126/science.1145989 [doi].

45. **Eisenberg, E. and E. Y. Levanon**. 2013. Human housekeeping genes, revisited. Trends Genet. **29**:569-574. doi:S0168-9525(13)00089-9 [pii];10.1016/j.tig.2013.05.010 [doi].

46. **Eissenberg, J. C., J. Ma, M. A. Gerber, A. Christensen, J. A. Kennison, and A. Shilatifard**. 2002. dELL is an essential RNA polymerase II elongation factor with a general role in development. Proc.Natl.Acad.Sci.U.S.A **99**:9894-9899. doi:10.1073/pnas.152193699 [doi];152193699 [pii].

47. **Everett, R. D.** 1987. The regulation of transcription of viral and cellular genes by herpesvirus immediate-early gene products (review). Anticancer Res. **7**:589-604.

48. **Feichtinger, S., T. Stamminger, R. Muller, L. Graf, B. Klebl, J. Eickhoff, and M. Marschall**. 2011. Recruitment of cyclin-dependent kinase 9 to nuclear compartments during cytomegalovirus late replication: importance of an interaction between viral pUL69 and cyclin T1. J.Gen.Virol. **92**:1519-1531. doi:vir.0.030494-0 [pii];10.1099/vir.0.030494-0 [doi].

49. **Fish, R. N. and C. M. Kane**. 2002. Promoting elongation with transcript cleavage stimulatory factors. Biochim.Biophys.Acta **1577**:287-307. doi:S0167478102004591 [pii].

50. **Fong, N. and D. L. Bentley**. 2001. Capping, splicing, and 3' processing are independently stimulated by RNA polymerase II: different functions for different segments of the CTD. Genes Dev. **15**:1783-1795. doi:10.1101/gad.889101 [doi].

51. **Fong, N., G. Bird, M. Vigneron, and D. L. Bentley**. 2003. A 10 residue motif at the C-terminus of the RNA pol II CTD is required for transcription, splicing and 3' end processing. EMBO J. **22**:4274-4282. doi:10.1093/emboj/cdg396 [doi].

52. **Fousteri, M. and L. H. Mullenders**. 2008. Transcription-coupled nucleotide excision repair in mammalian cells: molecular mechanisms and biological effects. Cell Res. **18**:73-84. doi:cr20086 [pii];10.1038/cr.2008.6 [doi].

53. **Fraser, K. A. and S. A. Rice**. 2005. Herpes simplex virus type 1 infection leads to loss of serine-2 phosphorylation on the carboxyl-terminal domain of RNA polymerase II. J.Virol. **79**:11323-11334. doi:79/17/11323 [pii];10.1128/JVI.79.17.11323-11334.2005 [doi].

54. **Fraser, K. A. and S. A. Rice**. 2007. Herpes simplex virus immediate-early protein ICP22 triggers loss of serine 2-phosphorylated RNA polymerase II. J.Virol. **81**:5091-5101. doi:JVI.00184-07 [pii];10.1128/JVI.00184-07 [doi].

55. **Fujinaga, K., D. Irwin, Y. Huang, R. Taube, T. Kurosu, and B. M. Peterlin**. 2004. Dynamics of human immunodeficiency virus transcription: P-TEFb phosphorylates RD and dissociates negative effectors from the transactivation response element. Mol.Cell Biol. **24**:787-795.

56. **Garriga, J., H. Xie, Z. Obradovic, and X. Grana**. 2010. Selective control of gene expression by CDK9 in human cells. J.Cell Physiol **222**:200-208. doi:10.1002/jcp.21938 [doi].

57. **Gillette, T. G., F. Gonzalez, A. Delahodde, S. A. Johnston, and T. Kodadek**. 2004. Physical and functional association of RNA polymerase II and the proteasome. Proc.Natl.Acad.Sci.U.S.A **101**:5904-5909. doi:10.1073/pnas.0305411101 [doi];0305411101 [pii].

58. **Glover-Cutter, K., S. Larochelle, B. Erickson, C. Zhang, K. Shokat, R. P. Fisher, and D. L. Bentley**. 2009. TFIIH-associated Cdk7 kinase functions in phosphorylation of C-terminal domain Ser7 residues, promoter-proximal pausing, and termination by RNA polymerase II. Mol.Cell Biol. **29**:5455-5464. doi:MCB.00637-09 [pii];10.1128/MCB.00637-09 [doi].

59. **Goding, C. R. and P. O'Hare**. 1989. Herpes simplex virus Vmw65-octamer binding protein interaction: a paradigm for combinatorial control of transcription. Virology **173**:363-367.

60. **Gomes, N. P., G. Bjerke, B. Llorente, S. A. Szostek, B. M. Emerson, and J. M. Espinosa**. 2006. Gene-specific requirement for P-TEFb activity and RNA polymerase II phosphorylation within the p53 transcriptional program. Genes Dev. **20**:601-612. doi:20/5/601 [pii];10.1101/gad.1398206 [doi].

61. **Grondin, B. and N. DeLuca**. 2000. Herpes simplex virus type 1 ICP4 promotes transcription preinitiation complex formation by enhancing the binding of TFIID to DNA. J.Virol. **74**:11504-11510.

62. **Gu, B., D. Eick, and O. Bensaude**. 2013. CTD serine-2 plays a critical role in splicing and termination factor recruitment to RNA polymerase II in vivo. Nucleic Acids Res. **41**:1591-1603. doi:gks1327 [pii];10.1093/nar/gks1327 [doi].

63. **Gu, W. and D. Reines**. 1995. Identification of a decay in transcription potential that results in elongation factor dependence of RNA polymerase II. J.Biol.Chem. **270**:11238-11244.

64. **Guo, L., W. J. Wu, L. D. Liu, L. C. Wang, Y. Zhang, L. Q. Wu, Y. Guan, and Q. H. Li**. 2012. Herpes simplex virus 1 ICP22 inhibits the transcription of viral gene promoters by binding to and blocking the recruitment of P-TEFb. PLoS.One. **7**:e45749. doi:10.1371/journal.pone.0045749 [doi];PONE-D-12-17065 [pii].

65. **Hagglund, R. and B. Roizman**. 2004. Role of ICP0 in the strategy of conquest of the host cell by herpes simplex virus 1. J.Virol. **78**:2169-2178.

66. **Haines, N. M., Y. I. Kim, A. J. Smith, and N. J. Savery**. 2014. Stalled transcription complexes promote DNA repair at a distance. Proc.Natl.Acad.Sci.U.S.A **111**:4037-4042. doi:1322350111 [pii];10.1073/pnas.1322350111 [doi].

67. **Harreman, M., M. Taschner, S. Sigurdsson, R. Anindya, J. Reid, B. Somesh, S. E. Kong, C. A. Banks, R. C. Conaway, J. W. Conaway, and J. Q. Svejstrup**. 2009. Distinct ubiquitin ligases act sequentially for RNA polymerase II polyubiquitylation. Proc.Natl.Acad.Sci.U.S.A **106**:20705-20710. doi:0907052106 [pii];10.1073/pnas.0907052106 [doi].

68. **Hartzog, G. A., T. Wada, H. Handa, and F. Winston**. 1998. Evidence that Spt4, Spt5, and Spt6 control transcription elongation by RNA polymerase II in Saccharomyces cerevisiae. Genes Dev. **12**:357-369.

69. **Hayes, S. and P. O'Hare**. 1993. Mapping of a major surface-exposed site in herpes simplex virus protein Vmw65 to a region of direct interaction in a transcription complex assembly. J.Virol. **67**:852-862.

70. **Heidemann, M., C. Hintermair, K. Voss, and D. Eick**. 2013. Dynamic phosphorylation patterns of RNA polymerase II CTD during transcription. Biochim.Biophys.Acta **1829**:55-62. doi:S1874-9399(12)00156-3 [pii];10.1016/j.bbagrm.2012.08.013 [doi].

71. **Herold, B. C., R. J. Visalli, N. Susmarski, C. R. Brandt, and P. G. Spear**. 1994. Glycoprotein C-independent binding of herpes simplex virus to cells requires cell surface heparan sulphate and glycoprotein B. J.Gen.Virol. **75 (Pt 6)**:1211-1222.

72. **Hsin, J. P. and J. L. Manley**. 2012. The RNA polymerase II CTD coordinates transcription and RNA processing. Genes Dev. **26**:2119-2137. doi:26/19/2119 [pii];10.1101/gad.200303.112 [doi].

73. **Hubbard, K., J. Catalano, R. K. Puri, and A. Gnatt**. 2008. Knockdown of TFIIS by RNA silencing inhibits cancer cell proliferation and induces apoptosis. BMC.Cancer **8**:133. doi:1471-2407-8-133 [pii];10.1186/1471-2407-8-133 [doi].

74. **Ishibashi, T., M. Dangkulwanich, Y. Coello, T. A. Lionberger, L. Lubkowska, A. S. Ponticelli, M. Kashlev, and C. Bustamante**. 2014. Transcription factors IIS and IIF enhance transcription

efficiency by differentially modifying RNA polymerase pausing dynamics. Proc.Natl.Acad.Sci.U.S.A **111**:3419-3424. doi:1401611111 [pii];10.1073/pnas.1401611111 [doi].

75. **Johnson, L. A., L. Li, and R. M. Sandri-Goldin**. 2009. The cellular RNA export receptor TAP/NXF1 is required for ICP27-mediated export of herpes simplex virus 1 RNA, but the TREX complex adaptor protein Aly/REF appears to be dispensable. J.Virol. **83**:6335-6346. doi:JVI.00375-09 [pii];10.1128/JVI.00375-09 [doi].

76. **Johnson, L. A. and R. M. Sandri-Goldin**. 2009. Efficient nuclear export of herpes simplex virus 1 transcripts requires both RNA binding by ICP27 and ICP27 interaction with TAP/NXF1. J.Virol. **83**:1184-1192. doi:JVI.02010-08 [pii];10.1128/JVI.02010-08 [doi].

77. **Kamiuchi, S., M. Saijo, E. Citterio, J. M. de, J. H. Hoeijmakers, and K. Tanaka**. 2002. Translocation of Cockayne syndrome group A protein to the nuclear matrix: possible relevance to transcription-coupled DNA repair. Proc.Natl.Acad.Sci.U.S.A **99**:201-206. doi:10.1073/pnas.012473199 [doi];99/1/201 [pii].

78. **Kanai, A., T. Kuzuhara, K. Sekimizu, and S. Natori**. 1991. Heterogeneity and tissue-specific expression of eukaryotic transcription factor S-II-related protein mRNA. J Biochem **109**:674-677.

79. **Kapasi, A. J., C. L. Clark, K. Tran, and D. H. Spector**. 2009. Recruitment of cdk9 to the immediate-early viral transcriptosomes during human cytomegalovirus infection requires efficient binding to cyclin T1, a threshold level of IE2 86, and active transcription. J.Virol. **83**:5904-5917. doi:JVI.02651-08 [pii];10.1128/JVI.02651-08 [doi].

80. **Kapasi, A. J. and D. H. Spector**. 2008. Inhibition of the cyclin-dependent kinases at the beginning of human cytomegalovirus infection specifically alters the levels and localization of the RNA polymerase II carboxyl-terminal domain kinases cdk9 and cdk7 at the viral transcriptosome. J.Virol. **82**:394-407. doi:JVI.01681-07 [pii];10.1128/JVI.01681-07 [doi].

81. **Kettenberger, H., K. J. Armache, and P. Cramer**. 2003. Architecture of the RNA polymerase II-TFIIS complex and implications for mRNA cleavage. Cell **114**:347-357. doi:S0092867403005981 [pii].

82. **Kim, H., B. Erickson, W. Luo, D. Seward, J. H. Graber, D. D. Pollock, P. C. Megee, and D. L. Bentley**. 2010. Gene-specific RNA polymerase II phosphorylation and the CTD code. Nat.Struct.Mol.Biol. **17**:1279-1286. doi:nsmb.1913 [pii];10.1038/nsmb.1913 [doi].

83. **Kim, J., M. Guermah, and R. G. Roeder**. 2010. The human PAF1 complex acts in chromatin transcription elongation both independently and cooperatively with SII/TFIIS. Cell **140**:491-503. doi:S0092-8674(09)01636-5 [pii];10.1016/j.cell.2009.12.050 [doi].

84. **Kim, M., H. Suh, E. J. Cho, and S. Buratowski**. 2009. Phosphorylation of the yeast Rpb1 C-terminal domain at serines 2, 5, and 7. J.Biol.Chem. **284**:26421-26426. doi:M109.028993 [pii];10.1074/jbc.M109.028993 [doi].

85. **Knipe, D. M., D. Senechek, S. A. Rice, and J. L. Smith**. 1987. Stages in the nuclear association of the herpes simplex virus transcriptional activator protein ICP4. J.Virol. **61**:276-284.

86. **Komarnitsky, P., E. J. Cho, and S. Buratowski**. 2000. Different phosphorylated forms of RNA polymerase II and associated mRNA processing factors during transcription. Genes Dev. **14**:2452-2460.

87. **Kwak, H. and J. T. Lis**. 2013. Control of transcriptional elongation. Annu.Rev.Genet. **47**:483-508. doi:10.1146/annurev-genet-110711-155440 [doi].

88. **Laine, J. P. and J. M. Egly**. 2006. When transcription and repair meet: a complex system. Trends Genet. **22**:430-436. doi:S0168-9525(06)00174-0 [pii];10.1016/j.tig.2006.06.006 [doi].

89. **Laquerre, S., R. Argnani, D. B. Anderson, S. Zucchini, R. Manservigi, and J. C. Glorioso**. 1998. Heparan sulfate proteoglycan binding by herpes simplex virus type 1 glycoproteins B and C, which differ in their contributions to virus attachment, penetration, and cell-to-cell spread. J.Virol. **72**:6119-6130.

90. **Larsen, E., K. Kwon, F. Coin, J. M. Egly, and A. Klungland**. 2004. Transcription activities at 8-oxoG lesions in DNA. DNA Repair (Amst) **3**:1457-1468. doi:10.1016/j.dnarep.2004.06.008 [doi];S1568786404001831 [pii].

91. **Lee, K. B., D. Wang, S. J. Lippard, and P. A. Sharp**. 2002. Transcription-coupled and DNA damage-dependent ubiquitination of RNA polymerase II in vitro. Proc.Natl.Acad.Sci.U.S.A **99**:4239-4244. doi:10.1073/pnas.072068399 [doi];072068399 [pii].

92. **Li, L., L. A. Johnson, J. Q. Dai-Ju, and R. M. Sandri-Goldin**. 2008. Hsc70 focus formation at the periphery of HSV-1 transcription sites requires ICP27. PLoS.One. **3**:e1491. doi:10.1371/journal.pone.0001491 [doi].

93. **Lian, Z., A. Karpikov, J. Lian, M. C. Mahajan, S. Hartman, M. Gerstein, M. Snyder, and S. M. Weissman**. 2008. A genomic analysis of RNA polymerase II modification and chromatin architecture related to 3' end RNA polyadenylation. Genome Res. **18**:1224-1237. doi:gr.075804.107 [pii];10.1101/gr.075804.107 [doi].

94. **Long, M. C., V. Leong, P. A. Schaffer, C. A. Spencer, and S. A. Rice**. 1999. ICP22 and the UL13 protein kinase are both required for herpes simplex virus-induced modification of the large subunit of RNA polymerase II. J.Virol. **73**:5593-5604.

95. **Mancebo, H. S., G. Lee, J. Flygare, J. Tomassini, P. Luu, Y. Zhu, J. Peng, C. Blau, D. Hazuda, D. Price, and O. Flores**. 1997. P-TEFb kinase is required for HIV Tat transcriptional activation in vivo and in vitro. Genes Dev. **11**:2633-2644.

96. **Mandel, C. R., S. Kaneko, H. Zhang, D. Gebauer, V. Vethantham, J. L. Manley, and L. Tong**. 2006. Polyadenylation factor CPSF-73 is the pre-mRNA 3'-end-processing endonuclease. Nature **444**:953-956. doi:nature05363 [pii];10.1038/nature05363 [doi].

97. **Marshall, N. F., J. Peng, Z. Xie, and D. H. Price**. 1996. Control of RNA polymerase II elongation potential by a novel carboxyl-terminal domain kinase. J.Biol.Chem. **271**:27176-27183.

98. **Marshall, N. F. and D. H. Price**. 1992. Control of formation of two distinct classes of RNA polymerase II elongation complexes. Mol.Cell Biol. **12**:2078-2090.

99. **Marshall, N. F. and D. H. Price**. 1995. Purification of P-TEFb, a transcription factor required for the transition into productive elongation. J.Biol.Chem. **270**:12335-12338.

100. **Mayer, A., M. Lidschreiber, M. Siebert, K. Leike, J. Soding, and P. Cramer**. 2010. Uniform transitions of the general RNA polymerase II transcription complex. Nat.Struct.Mol.Biol. **17**:1272-1278. doi:nsmb.1903 [pii];10.1038/nsmb.1903 [doi].

101. **McCracken, S., N. Fong, E. Rosonina, K. Yankulov, G. Brothers, D. Siderovski, A. Hessel, S. Foster, S. Shuman, and D. L. Bentley**. 1997. 5'-Capping enzymes are targeted to pre-mRNA by binding to the phosphorylated carboxy-terminal domain of RNA polymerase II. Genes Dev. **11**:3306-3318.

102. **McCracken, S., N. Fong, K. Yankulov, S. Ballantyne, G. Pan, J. Greenblatt, S. D. Patterson, M. Wickens, and D. L. Bentley**. 1997. The C-terminal domain of RNA polymerase II couples mRNA processing to transcription. Nature **385**:357-361. doi:10.1038/385357a0 [doi].

103. **McCracken, S., E. Rosonina, N. Fong, M. Sikes, A. Beyer, K. O'Hare, S. Shuman, and D. Bentley**. 1998. Role of RNA polymerase II carboxy-terminal domain in coordinating transcription with RNA processing. Cold Spring Harb.Symp.Quant.Biol. **63**:301-309.

104. **Mellon, I., V. A. Bohr, C. A. Smith, and P. C. Hanawalt**. 1986. Preferential DNA repair of an active gene in human cells. Proc.Natl.Acad.Sci.U.S.A **83**:8878-8882.

105. **Mellon, I. and P. C. Hanawalt**. 1989. Induction of the Escherichia coli lactose operon selectively increases repair of its transcribed DNA strand. Nature **342**:95-98. doi:10.1038/342095a0 [doi].

106. **Mellon, I., G. Spivak, and P. C. Hanawalt**. 1987. Selective removal of transcription-blocking DNA damage from the transcribed strand of the mammalian DHFR gene. Cell **51**:241-249. doi:0092-8674(87)90151-6 [pii].

107. **Michels, A. A., A. Fraldi, Q. Li, T. E. Adamson, F. Bonnet, V. T. Nguyen, S. C. Sedore, J. P. Price, D. H. Price, L. Lania, and O. Bensaude**. 2004. Binding of the 7SK snRNA turns the HEXIM1 protein into a P-TEFb (CDK9/cyclin T) inhibitor. EMBO J. **23**:2608-2619. doi:10.1038/sj.emboj.7600275 [doi];7600275 [pii].

108. **Mone, M. J., M. Volker, O. Nikaido, L. H. Mullenders, A. A. van Zeeland, P. J. Verschure, E. M. Manders, and D. R. van**. 2001. Local UV-induced DNA damage in cell nuclei results in local transcription inhibition. EMBO Rep. **2**:1013-1017. doi:10.1093/embo-reports/kve224 [doi];2/11/1013 [pii].

109. **Muniz, L., S. Egloff, B. Ughy, B. E. Jady, and T. Kiss**. 2010. Controlling cellular P-TEFb activity by the HIV-1 transcriptional transactivator Tat. PLoS.Pathog. **6**:e1001152. doi:10.1371/journal.ppat.1001152 [doi].

110. **Muse, G. W., D. A. Gilchrist, S. Nechaev, R. Shah, J. S. Parker, S. F. Grissom, J. Zeitlinger, and K. Adelman**. 2007. RNA polymerase is poised for activation across the genome. Nat.Genet. **39**:1507-1511. doi:ng.2007.21 [pii];10.1038/ng.2007.21 [doi].

111. **Nakanishi, Y., K. Sekimizu, H. Tamura, and S. Natori**. 1981. Purification of a new protein stimulating RNA polymerase II from Ehrlich ascites tumor cells: comparison with proteins purified before. J Biochem **90**:805-814.

112. **Natori, S., K. Takeuchi, and D. Mizuno**. 1973. DNA-dependent RNA polymerase from Ehrlich ascites tumor cells. 3. Ribonuclease H and elongating activity of stimulatory factor S-II. J.Biochem. **74**:1177-1182.

113. **Natori, S., K. Takeuchi, K. Takeuchi, and D. Mizuno**. 1973. DNA dependent RNA polymerase from Ehrlich ascites tumor cells. II. Factors stimulating the activity of RNA polymerase II. J Biochem **73**:879-888.

114. **Nechaev, S. and K. Adelman**. 2011. Pol II waiting in the starting gates: Regulating the transition from transcription initiation into productive elongation. Biochim.Biophys.Acta **1809**:34-45. doi:S1874-9399(10)00139-2 [pii];10.1016/j.bbagrm.2010.11.001 [doi].

115. **Nechooshtan, G., M. Elgrably-Weiss, and S. Altuvia**. 2014. Changes in transcriptional pausing modify the folding dynamics of the pH-responsive RNA element. Nucleic Acids Res. **42**:622-630. doi:gkt868 [pii];10.1093/nar/gkt868 [doi].

116. **Nonet, M., D. Sweetser, and R. A. Young**. 1987. Functional redundancy and structural polymorphism in the large subunit of RNA polymerase II. Cell **50**:909-915. doi:0092-8674(87)90517-4 [pii].

117. **Nowak, D. E., B. Tian, and A. R. Brasier**. 2005. Two-step cross-linking method for identification of NF-kappaB gene network by chromatin immunoprecipitation. Biotechniques **39**:715-725. doi:000112014 [pii].

118. **Ouchida, R., M. Kusuhara, N. Shimizu, T. Hisada, Y. Makino, C. Morimoto, H. Handa, F. Ohsuzu, and H. Tanaka**. 2003. Suppression of NF-kappaB-dependent gene expression by a hexamethylene bisacetamide-inducible protein HEXIM1 in human vascular smooth muscle cells. Genes Cells **8**:95-107. doi:618 [pii].

119. **Palangat, M., J. A. Grass, M. F. Langelier, B. Coulombe, and R. Landick**. 2011. The RPB2 flap loop of human RNA polymerase II is dispensable for transcription initiation and elongation. Mol.Cell Biol. **31**:3312-3325. doi:MCB.05318-11 [pii];10.1128/MCB.05318-11 [doi].

120. **Palermo, R. D., H. M. Webb, and M. J. West**. 2011. RNA polymerase II stalling promotes nucleosome occlusion and pTEFb recruitment to drive immortalization by Epstein-Barr virus. PLoS.Pathog. **7**:e1002334. doi:10.1371/journal.ppat.1002334 [doi];PPATHOGENS-D-11-01046 [pii].

121. **Patturajan, M., R. J. Schulte, B. M. Sefton, R. Berezney, M. Vincent, O. Bensaude, S. L. Warren, and J. L. Corden**. 1998. Growth-related changes in phosphorylation of yeast RNA polymerase II. J.Biol.Chem. **273**:4689-4694.

122. **Peterlin, B. M., J. E. Brogie, and D. H. Price**. 2012. 7SK snRNA: a noncoding RNA that plays a major role in regulating eukaryotic transcription. Wiley.Interdiscip.Rev.RNA. **3**:92-103. doi:10.1002/wrna.106 [doi].

123. **Peterlin, B. M. and D. H. Price**. 2006. Controlling the elongation phase of transcription with P-TEFb. Mol.Cell **23**:297-305. doi:S1097-2765(06)00429-1 [pii];10.1016/j.molcel.2006.06.014 [doi].

124. **Phatnani, H. P. and A. L. Greenleaf**. 2006. Phosphorylation and functions of the RNA polymerase II CTD. Genes Dev. **20**:2922-2936. doi:20/21/2922 [pii];10.1101/gad.1477006 [doi].

125. **Prather, D. M., E. Larschan, and F. Winston**. 2005. Evidence that the elongation factor TFIIS plays a role in transcription initiation at GAL1 in Saccharomyces cerevisiae. Mol.Cell Biol. **25**:2650-2659. doi:25/7/2650 [pii];10.1128/MCB.25.7.2650-2659.2005 [doi].

126. **Price, D. H.** 2000. P-TEFb, a cyclin-dependent kinase controlling elongation by RNA polymerase II. Mol.Cell Biol. **20**:2629-2634.

127. **Rajcani, J., V. Andrea, and R. Ingeborg**. 2004. Peculiarities of herpes simplex virus (HSV) transcription: an overview. Virus Genes **28**:293-310. doi:5269258 [pii].

128. **Rajcani, J. and V. Durmanova**. 2000. Early expression of herpes simplex virus (HSV) proteins and reactivation of latent infection. Folia Microbiol.(Praha) **45**:7-28.

129. **Ratner, J. N., B. Balasubramanian, J. Corden, S. L. Warren, and D. B. Bregman**. 1998. Ultraviolet radiation-induced ubiquitination and proteasomal degradation of the large subunit of RNA polymerase II. Implications for transcription-coupled DNA repair. J.Biol.Chem. **273**:5184-5189.

130. **Reines, D., R. C. Conaway, and J. W. Conaway**. 1999. Mechanism and regulation of transcriptional elongation by RNA polymerase II. Curr.Opin.Cell Biol. **11**:342-346. doi:S0955-0674(99)80047-7 [pii];10.1016/S0955-0674(99)80047-7 [doi].

131. **Reines, D., P. Ghanouni, W. Gu, J. Mote, Jr., and W. Powell**. 1993. Transcription elongation by RNA polymerase II: mechanism of SII activation. Cell Mol.Biol.Res. **39**:331-338.

132. **Renner, D. B., Y. Yamaguchi, T. Wada, H. Handa, and D. H. Price**. 2001. A highly purified RNA polymerase II elongation control system. J.Biol.Chem. **276**:42601-42609. doi:10.1074/jbc.M104967200 [doi];M104967200 [pii].

133. **Rice, S. A., M. C. Long, V. Lam, P. A. Schaffer, and C. A. Spencer**. 1995. Herpes simplex virus immediate-early protein ICP22 is required for viral modification of host RNA polymerase II and establishment of the normal viral transcription program. J.Virol. **69**:5550-5559.

134. **Rice, S. A., M. C. Long, V. Lam, and C. A. Spencer**. 1994. RNA polymerase II is aberrantly phosphorylated and localized to viral replication compartments following herpes simplex virus infection. J.Virol. **68**:988-1001.

135. **Rodriguez, C. R., E. J. Cho, M. C. Keogh, C. L. Moore, A. L. Greenleaf, and S. Buratowski**. 2000. Kin28, the TFIIH-associated carboxy-terminal domain kinase, facilitates the recruitment of mRNA processing machinery to RNA polymerase II. Mol.Cell Biol. **20**:104-112.

136. **Roizman, B.** 1996. The function of herpes simplex virus genes: a primer for genetic engineering of novel vectors. Proc.Natl.Acad.Sci.U.S.A **93**:11307-11312.

137. **Roizman, B.** 1999. HSV gene functions: what have we learned that could be generally applicable to its near and distant cousins? Acta Virol. **43**:75-80.

138. **Rondon, A. G., M. Gallardo, M. Garcia-Rubio, and A. Aguilera**. 2004. Molecular evidence indicating that the yeast PAF complex is required for transcription elongation. EMBO Rep. **5**:47-53. doi:10.1038/sj.embor.7400045 [doi];7400045 [pii].

139. **Salerno, D., M. G. Hasham, R. Marshall, J. Garriga, A. Y. Tsygankov, and X. Grana**. 2007. Direct inhibition of CDK9 blocks HIV-1 replication without preventing T-cell activation in primary human peripheral blood lymphocytes. Gene **405**:65-78. doi:S0378-1119(07)00480-5 [pii];10.1016/j.gene.2007.09.010 [doi].

140. **Sandri-Goldin, R. M.** 1998. ICP27 mediates HSV RNA export by shuttling through a leucine-rich nuclear export signal and binding viral intronless RNAs through an RGG motif. Genes Dev. **12**:868-879.

141. **Sandri-Goldin, R. M.** 2011. The many roles of the highly interactive HSV protein ICP27, a key regulator of infection. Future.Microbiol. **6**:1261-1277. doi:10.2217/fmb.11.119 [doi].

142. **Sawadogo, M. and A. Sentenac**. 1990. RNA polymerase B (II) and general transcription factors. Annu.Rev.Biochem. **59**:711-754. doi:10.1146/annurev.bi.59.070190.003431 [doi].

143. **Schweikhard, V., C. Meng, K. Murakami, C. D. Kaplan, R. D. Kornberg, and S. M. Block**. 2014. Transcription factors TFIIF and TFIIS promote transcript elongation by RNA polymerase II by synergistic and independent mechanisms. Proc.Natl.Acad.Sci.U.S.A **111**:6642-6647. doi:1405181111 [pii];10.1073/pnas.1405181111 [doi].

144. **Selth, L. A., S. Sigurdsson, and J. Q. Svejstrup**. 2010. Transcript Elongation by RNA Polymerase II. Annu.Rev.Biochem. **79**:271-293. doi:10.1146/annurev.biochem.78.062807.091425 [doi].

145. **Shi, Y., D. C. Di Giammartino, D. Taylor, A. Sarkeshik, W. J. Rice, J. R. Yates, III, J. Frank, and J. L. Manley**. 2009. Molecular architecture of the human pre-mRNA 3' processing complex. Mol.Cell **33**:365-376. doi:S1097-2765(09)00025-2 [pii];10.1016/j.molcel.2008.12.028 [doi].

146. **Shieh, M. T., D. WuDunn, R. I. Montgomery, J. D. Esko, and P. G. Spear**. 1992. Cell surface receptors for herpes simplex virus are heparan sulfate proteoglycans. J.Cell Biol. **116**:1273-1281.

147. **Shilatifard, A.** 1998. Factors regulating the transcriptional elongation activity of RNA polymerase II. FASEB J. **12**:1437-1446.

148. **Shilatifard, A., J. W. Conaway, and R. C. Conaway**. 1997. Mechanism and regulation of transcriptional elongation and termination by RNA polymerase II. Curr.Opin.Genet.Dev. **7**:199-204. doi:S0959-437X(97)80129-3 [pii].

149. **Sims, R. J., III, R. Belotserkovskaya, and D. Reinberg**. 2004. Elongation by RNA polymerase II: the short and long of it. Genes Dev. **18**:2437-2468. doi:18/20/2437 [pii];10.1101/gad.1235904 [doi].

150. **Singh, J. and E. K. Wagner**. 1993. Transcriptional analysis of the herpes simplex virus type 1 region containing the TRL/UL junction. Virology **196**:220-231. doi:S0042-6822(83)71470-4 [pii];10.1006/viro.1993.1470 [doi].

151. **Smith, I. L., M. A. Hardwicke, and R. M. Sandri-Goldin**. 1992. Evidence that the herpes simplex virus immediate early protein ICP27 acts post-transcriptionally during infection to regulate gene expression. Virology **186**:74-86.

152. **Somesh, B. P., J. Reid, W. F. Liu, T. M. Sogaard, H. Erdjument-Bromage, P. Tempst, and J. Q. Svejstrup**. 2005. Multiple mechanisms confining RNA polymerase II ubiquitylation to polymerases undergoing transcriptional arrest. Cell **121**:913-923. doi:S0092-8674(05)00353-3 [pii];10.1016/j.cell.2005.04.010 [doi].

153. **Souki, S. K., P. D. Gershon, and R. M. Sandri-Goldin**. 2009. Arginine methylation of the ICP27 RGG box regulates ICP27 export and is required for efficient herpes simplex virus 1 replication. J.Virol. **83**:5309-5320. doi:JVI.00238-09 [pii];10.1128/JVI.00238-09 [doi].

154. **Souki, S. K. and R. M. Sandri-Goldin**. 2009. Arginine methylation of the ICP27 RGG box regulates the functional interactions of ICP27 with SRPK1 and Aly/REF during herpes simplex virus 1 infection. J.Virol. **83**:8970-8975. doi:JVI.00801-09 [pii];10.1128/JVI.00801-09 [doi].

155. **Spencer, C. A., M. E. Dahmus, and S. A. Rice**. 1997. Repression of host RNA polymerase II transcription by herpes simplex virus type 1. J.Virol. **71**:2031-2040.

156. **Stingley, S. W., J. J. Ramirez, S. A. Aguilar, K. Simmen, R. M. Sandri-Goldin, P. Ghazal, and E. K. Wagner**. 2000. Global analysis of herpes simplex virus type 1 transcription using an oligonucleotide-based DNA microarray. J.Virol. **74**:9916-9927.

157. **Sun, A., G. V. Devi-Rao, M. K. Rice, L. W. Gary, D. C. Bloom, R. M. Sandri-Goldin, P. Ghazal, and E. K. Wagner**. 2004. Immediate-early expression of the herpes simplex virus type 1 ICP27 transcript is not critical for efficient replication in vitro or in vivo. J.Virol. **78**:10470-10478. doi:10.1128/JVI.78.19.10470-10478.2004 [doi];78/19/10470 [pii].

158. **Svejstrup, J. Q.** 2003. Rescue of arrested RNA polymerase II complexes. J.Cell Sci. **116**:447-451.

159. **Svejstrup, J. Q.** 2007. Contending with transcriptional arrest during RNAPII transcript elongation. Trends Biochem.Sci. **32**:165-171. doi:S0968-0004(07)00053-9 [pii];10.1016/j.tibs.2007.02.005 [doi].

160. **Swanson, M. S. and F. Winston**. 1992. SPT4, SPT5 and SPT6 interactions: effects on transcription and viability in Saccharomyces cerevisiae. Genetics **132**:325-336.

161. **Takagi, Y., J. W. Conaway, and R. C. Conaway**. 1995. A novel activity associated with RNA polymerase II elongation factor SIII. SIII directs promoter-independent transcription initiation by RNA polymerase II in the absence of initiation factors. J.Biol.Chem. **270**:24300-24305.

162. **Tamrakar, S., A. J. Kapasi, and D. H. Spector**. 2005. Human cytomegalovirus infection induces specific hyperphosphorylation of the carboxyl-terminal domain of the large subunit of RNA polymerase II that is associated with changes in the abundance, activity, and localization of cdk9

and cdk7. J.Virol. **79**:15477-15493. doi:79/24/15477 [pii];10.1128/JVI.79.24.15477-15493.2005 [doi].

163. **Taylor, T. J., E. E. McNamee, C. Day, and D. M. Knipe**. 2003. Herpes simplex virus replication compartments can form by coalescence of smaller compartments. Virology **309**:232-247. doi:S0042682203001077 [pii].

164. **Toth, Z., K. F. Brulois, L. Y. Wong, H. R. Lee, B. Chung, and J. U. Jung**. 2012. Negative elongation factor-mediated suppression of RNA polymerase II elongation of Kaposi's sarcoma-associated herpesvirus lytic gene expression. J.Virol. **86**:9696-9707. doi:JVI.01012-12 [pii];10.1128/JVI.01012-12 [doi].

165. **Uptain, S. M., C. M. Kane, and M. J. Chamberlin**. 1997. Basic mechanisms of transcript elongation and its regulation. Annu.Rev.Biochem. **66**:117-172. doi:10.1146/annurev.biochem.66.1.117 [doi].

166. **van, d. B., V, E. Citterio, D. Hoogstraten, A. Zotter, J. M. Egly, W. A. van Cappellen, J. H. Hoeijmakers, A. B. Houtsmuller, and W. Vermeulen**. 2004. DNA damage stabilizes interaction of CSB with the transcription elongation machinery. J.Cell Biol. **166**:27-36. doi:10.1083/jcb.200401056 [doi];jcb.200401056 [pii].

167. **Viswanathan, A. and P. W. Doetsch**. 1998. Effects of nonbulky DNA base damages on Escherichia coli RNA polymerase-mediated elongation and promoter clearance. J.Biol.Chem. **273**:21276-21281.

168. **Wada, T., T. Takagi, Y. Yamaguchi, A. Ferdous, T. Imai, S. Hirose, S. Sugimoto, K. Yano, G. A. Hartzog, F. Winston, S. Buratowski, and H. Handa**. 1998. DSIF, a novel transcription elongation factor that regulates RNA polymerase II processivity, is composed of human Spt4 and Spt5 homologs. Genes Dev. **12**:343-356.

169. **Watson, S., S. Mercier, C. Bye, J. Wilkinson, A. L. Cunningham, and A. N. Harman**. 2007. Determination of suitable housekeeping genes for normalisation of quantitative real time PCR analysis of cells infected with human immunodeficiency virus and herpes viruses. Virol.J. **4**:130. doi:1743-422X-4-130 [pii];10.1186/1743-422X-4-130 [doi].

170. **Weir, J. P.** 2001. Regulation of herpes simplex virus gene expression. Gene **271**:117-130. doi:S0378111901005121 [pii].

171. **Wenzel, S., B. M. Martins, P. Rosch, and B. M. Wohrl**. 2010. Crystal structure of the human transcription elongation factor DSIF hSpt4 subunit in complex with the hSpt5 dimerization interface. Biochem.J. **425**:373-380. doi:BJ20091422 [pii];10.1042/BJ20091422 [doi].

172. **Wery, M., E. Shematorova, D. B. Van, J. Vandenhaute, P. Thuriaux, and M. Van, V**. 2004. Members of the SAGA and Mediator complexes are partners of the transcription elongation factor TFIIS. EMBO J **23**:4232-4242. doi:10.1038/sj.emboj.7600326 [doi];7600326 [pii].

173. **West, S., N. Gromak, and N. J. Proudfoot**. 2004. Human 5' --> 3' exonuclease Xrn2 promotes transcription termination at co-transcriptional cleavage sites. Nature **432**:522-525. doi:nature03035 [pii];10.1038/nature03035 [doi].

174. **Wilson, M. D., M. Harreman, and J. Q. Svejstrup**. 2013. Ubiquitylation and degradation of elongating RNA polymerase II: the last resort. Biochim.Biophys.Acta **1829**:151-157. doi:S1874-9399(12)00145-9 [pii];10.1016/j.bbagrm.2012.08.002 [doi].

175. **Wu, C. H., Y. Yamaguchi, L. R. Benjamin, M. Horvat-Gordon, J. Washinsky, E. Enerly, J. Larsson, A. Lambertsson, H. Handa, and D. Gilmour**. 2003. NELF and DSIF cause promoter proximal pausing on the hsp70 promoter in Drosophila. Genes Dev. **17**:1402-1414. doi:10.1101/gad.1091403 [doi];17/11/1402 [pii].

176. **Yamada, T., Y. Yamaguchi, N. Inukai, S. Okamoto, T. Mura, and H. Handa**. 2006. P-TEFb-mediated phosphorylation of hSpt5 C-terminal repeats is critical for processive transcription elongation. Mol.Cell **21**:227-237. doi:S1097-2765(05)01812-5 [pii];10.1016/j.molcel.2005.11.024 [doi].

177. **Yamaguchi, Y., H. Shibata, and H. Handa**. 2013. Transcription elongation factors DSIF and NELF: promoter-proximal pausing and beyond. Biochim.Biophys.Acta **1829**:98-104. doi:S1874-9399(12)00205-2 [pii];10.1016/j.bbagrm.2012.11.007 [doi].

178. **Yamaguchi, Y., T. Takagi, T. Wada, K. Yano, A. Furuya, S. Sugimoto, J. Hasegawa, and H. Handa**. 1999. NELF, a multisubunit complex containing RD, cooperates with DSIF to repress RNA polymerase II elongation. Cell **97**:41-51. doi:S0092-8674(00)80713-8 [pii].

179. **Yan, Q., R. J. Moreland, J. W. Conaway, and R. C. Conaway**. 1999. Dual roles for transcription factor IIF in promoter escape by RNA polymerase II. J.Biol.Chem. **274**:35668-35675.

180. **Yeo, M., P. S. Lin, M. E. Dahmus, and G. N. Gill**. 2003. A novel RNA polymerase II C-terminal domain phosphatase that preferentially dephosphorylates serine 5. J.Biol.Chem. **278**:26078-26085. doi:10.1074/jbc.M301791200 [doi];M301791200 [pii].

181. **Yik, J. H., R. Chen, R. Nishimura, J. L. Jennings, A. J. Link, and Q. Zhou**. 2003. Inhibition of P-TEFb (CDK9/Cyclin T) kinase and RNA polymerase II transcription by the coordinated actions of HEXIM1 and 7SK snRNA. Mol.Cell **12**:971-982. doi:S1097276503003885 [pii].

182. **Zawel, L., K. P. Kumar, and D. Reinberg**. 1995. Recycling of the general transcription factors during RNA polymerase II transcription. Genes Dev. **9**:1479-1490.

183. **Zehring, W. A., J. M. Lee, J. R. Weeks, R. S. Jokerst, and A. L. Greenleaf**. 1988. The C-terminal repeat domain of RNA polymerase II largest subunit is essential in vivo but is not required for accurate transcription initiation in vitro. Proc.Natl.Acad.Sci.U.S.A **85**:3698-3702.

184. **Zhang, Y., Y. Kim, N. Genoud, J. Gao, J. W. Kelly, S. L. Pfaff, G. N. Gill, J. E. Dixon, and J. P. Noel**. 2006. Determinants for dephosphorylation of the RNA polymerase II C-terminal domain by Scp1. Mol.Cell **24**:759-770. doi:S1097-2765(06)00733-7 [pii];10.1016/j.molcel.2006.10.027 [doi].

185. **Zhou, C. and D. M. Knipe**. 2002. Association of herpes simplex virus type 1 ICP8 and ICP27 proteins with cellular RNA polymerase II holoenzyme. J.Virol. **76**:5893-5904.

186. **Zhou, M., M. A. Halanski, M. F. Radonovich, F. Kashanchi, J. Peng, D. H. Price, and J. N. Brady**. 2000. Tat modifies the activity of CDK9 to phosphorylate serine 5 of the RNA polymerase II

carboxyl-terminal domain during human immunodeficiency virus type 1 transcription. Mol.Cell Biol. **20**:5077-5086.